THE ROLE OF EUTROPHICATION AND SEDIMENT PHOSPHORUS SATURATION IN THE FORMATION OF HARMFUL CYANOBACTERIAL BLOOMS

A Thesis
Submitted to the Graduate Faculty
of the
North Dakota State University
of Agriculture and Applied Science

By

Taylor Young

In Partial Fulfillment of the Requirements
for the Degree of
MASTER OF SCIENCE

Major Program:
Natural Resource Management

October 2020

Fargo, North Dakota

North Dakota State University
Graduate School

Title

THE ROLE OF EUTROPHICATION AND SEDIMENT PHOSPHORUS SATURATION IN THE FORMATION OF HARMFUL CYANOBACTERIAL BLOOMS

By

Taylor Young

The Supervisory Committee certifies that this ***disquisition*** complies with North Dakota State University's regulations and meets the accepted standards for the degree of

MASTER OF SCIENCE

SUPERVISORY COMMITTEE:

Christina Hargiss
Chair

Jack Norland

Aaron Daigh

Jon Sweetman

Approved:

11/16/2020
Date

Edward DeKeyser
Department Chair

ABSTRACT

Harmful cyanobacterial blooms have been a growing concern as global climate change and eutrophication of lakes, rivers, and oceans continually push conditions to favor cyanobacteria over other phytoplankton. Two studies were conducted assessing the impacts of hyper-eutrophication on phytoplankton communities, and phosphorous saturation in the sediments. Excess nutrients available to phytoplankton resulted in dominant cyanobacteria, and predictability of growth, by nutrient limitation, becoming drastically diminished. Sediments were observed to be fully phosphorus saturated, preventing the sequestration of excess phosphorus, and providing a consistent source of phosphorus throughout each season. Extreme saturation of nutrients reduces the predictability of systems and perpetuates the cycles of nutrient release, fueled by the growth and decay of harmful cyanobacterial blooms.

ACKNOWLEDGMENTS

I would like to thank my graduate committee: Christina, Jack, Aaron, and Jon for the time and considerable help that went into this project and thesis. I would also like to thank the staff at Des Lacs and Lostwood National Wildlife Refuges for their time and commitment to getting this project started and helping keep it running smoothly. A special thanks to Laurie Richardson and Chad Zorn for getting through the mountain of paperwork and the logistics involved with the project. To Jason Melin for literally helping to keep the boat afloat and all the other mechanical help. Also, a special thanks to Nick Johnson for all the time spent on the project.

I would also like to thank Joe Nett, Mike Ell, Aaron Larson and the rest of the North Dakota Department of Environmental Quality for being the expertise at the start and funding and processing the very many samples from this project. A thanks to the Fish and Wildlife Service for the financial support, without which this project would not have been possible. A sincere thank you to all involved.

Taylor Young

TABLE OF CONTENTS

LIST OF TABLES

LIST OF FIGURES

LIST OF ABBREVIATIONS

BV .....Cyanobacterial Biovolume

CHY-*a*.....Chlorophyll-*a*

DLNWR.....Des Lacs National Wildlife Refuge

DN .....Dissolved Nitrogen

DP .....Dissolved Phosphorus

DRP .....Dissolved Reactive Phosphorus

ELISA.....Enzyme Linked Immunosorbent Assay

GDD.....Growing Degree Days

HCBs .....Harmful Cyanobacterial Blooms.

IC.....Inorganic Carbon

N.....Nitrogen

N_2.....Atmospheric Nitrogen

NMS.....Nonmetric Multi-Dimensional Scaling

OC.....Organic Carbon

P.....Phosphorus

PERMANOVA.....Permutational Multivariate Analysis of Variance

SD.....Secchi Disk Transparency

TC.....Total Carbon

TP.....Total Phosphorus

US.....United States

CHAPTER 1. LITERATURE REVIEW

The impacts of harmful cyanobacterial blooms (HCBs) are on the rise. Anthropocentric nutrient loading and climate change drive conditions that favor cyanobacteria over other phytoplankton in the world's increasingly eutrophic lakes, rivers, and oceans. (Paerl, Hall, & Calandrino, 2011). HCBs are not a new occurrence and reports of blooms and resulting livestock poisonings date back as early as 1878 (Francis, 1878; Veal et al., 2017). More recently, the number of blooms continue to escalate with increasing focus on the factors driving HCBs (Dodds et al., 2009; Harke et al., 2016; O'Neil, Davis, Burford, & Gobbler, 2012). Hundreds of lakes have been assessed in relation to HCBs in the Americas, Europe and Asia (Dolman et al., 2012; Graham, Jones, Jones, Downing, & Clevenger, 2004; Wang et al., 2018), but the many factors that control HCBs continue to be deliberated.

Cyanobacteria are a large and diverse group of phytoplankton capable of producing harmful compounds called cyanotoxins (Merel et al., 2013). These toxins are broadly delineated into three categories with hepatotoxins targeting the liver, dermatoxins causing skin irritation, and neurotoxins targeting the nervous system (Bishop, Anet, & Gorham, 1959; Harke et al., 2016). The production of these cyanotoxins have been linked to specific genes (Kurmayer & Christiansen, 2009); however, some strains appear to be able to regulate this gene expression based on environmental conditions (Merel et al., 2013). The best strategy for preventing the production of cyanotoxins is to prevent large blooms of cyanobacteria from occurring (Downing, Watson, & McCauley 2001; Paerl et al., 2011).

Anthropogenic loading of nutrients, primarily nitrogen (N) and phosphorus (P), are considered the largest contributors to HCBs (O'Neil et al., 2012), and are estimated to cost the United States approximately 2.2 billion dollars annually (Dodds et al., 2009). The large economic

impacts, caused by HCBs, result in considerable pressure to better understand the effects of nutrient loading on HCBs. Past studies suggest that P is the primary limiting nutrient in large blooms (Schindler, 1974; Schindler, 1977). This belief led to P being the primary focus for extensive legislative controls regulating P releases into the environment (Harke et al., 2016). More recent studies have suggested that the management of N may play an equal or greater role in the management of HCB's in some systems (Chaffin & Bridgeman, 2013; Dolman et al., 2012; O'Neil et al., 2012; Scott & McCarthy, 2010).

Eutrophication of lakes is not the only reason for an increase in HCBs. Increasing temperatures induced by global climate change affect phytoplankton communities (Huisman et al., 2018; Paerl & Huisman, 2009; Paul, 2008). Seasonal temperature changes tend to result in community shifts that start with diatoms at cooler temperatures, then shifting to green algae, and eventually cyanobacteria, which become the most dominant at the highest temperatures (Reynolds, 1997; Yang et al., 2017). Additionally, in a study by Davis, Berry, Boyer, and Gobler (2009), it was shown that the growth rate for toxic strains of *Microcystis* significantly outweighed the growth of nontoxic strains at higher temperatures. The dominance of cyanobacteria and toxic strains of cyanobacteria at higher temperatures is likely to result in more frequent and severe HCBs if global temperature trends continue.

1.1. Anthropogenic Nutrient Loading

Cyanobacteria are poor competitors for N and P in nutrient replete lakes, but dominate community structures under eutrophic conditions (Graham et al., 2004). Natural nutrient releases, like P from apatite, are generally slow and not likely to contribute to eutrophication (Paytan & McLaughlin, 2007). Therefore, the reliance on eutrophic conditions emphasizes that the increasing frequency of HCBs is closely tied to anthropogenic nutrient loading and land use.

The effects of anthropogenic nutrient loading are exemplified by Hobbs and Wong (2019), where sediment cores were taken from a lake in Washington and used to evaluate the effects of land use on phytoplankton. Before the land around the lake became a park in 1969, farming was the primary land use beginning in the early 1900's. Sediments from before 1900 were used to represent historic levels of algal productivity. Analysis showed algal productivity increasing in conjunction with farming activity, then returning to historic levels within ten years of the park's establishment (Hobbs & Wong, 2019). This study represents how strongly localized land use can enhance algal production or inhibit production with mindful practices.

Efforts to reduce P released into systems have helped to return a number of lakes to oligotrophic states. A study by Jeppesen et al. (2005) reviewed 35 case studies where P reduction was the primary effort in reducing states of eutrophication in the studied systems. Here it was shown that typically after 10 to 15 years, internal loading was reduced enough to result in lower amounts of total phosphorus (TP), and consequently a reduction in the amount of total phytoplankton biomass. They found that in deeper lakes, community structures shifted towards chrysophytes and dinophytes, while cyanobacteria abundance was reduced. In shallower lakes however, diatoms and chrysophytes became more dominant, but there was little difference in cyanobacteria abundance (Jeppesen et al., 2005).

A review by Ni, Yuan, and Liu (2020), has suggested that the singular focus on TP may not be effective in reducing the effects of P in aquatic ecosystems. Dissolved reactive phosphorus (DRP), though a relatively small constituent of TP, may have a greater impact on algal growth. DRP is more biologically available to algae and may be more mobile. The review suggests that agricultural conservation practices aimed at reducing losses of TP may be ineffective or even enhance the loss of DRP (Ni et al., 2020). This shows that further considerations must be made in the efforts to reduce P released into aquatic ecosystems.

1.2. Adsorption and Desorption of Phosphorus in Sediments

The sediments in aquatic ecosystems act as a reservoir for P, and suspended particles in water columns have a strong affinity for dissolved phosphorus (Lebo, 1991; Wu, Jin, Gao, Xu, & Chen, 2019). The rates at which P is adsorbed and desorbed is dependent on sediment particle size, with an exponential increase in adsorption with decreasing particle size. (Walter & Morse, 1984; Zhang & Huang, 2007). Aerobic conditions typically favor adsorption of P, while anaerobic conditions typically favor desorption (Hietanen & Lukkari, 2007).

The process of P adsorption onto sediments involves the transition of soluble forms of P to less soluble forms bound to cations, primarily with Al^{3+}, Fe^{3+}, and Ca^{2+} (Shrestha & Lin, 1996). In acidic sediments, $Al^{3+}$and Fe^{3+} rapidly precipitate phosphates, and in basic sediments, Ca^{2+} more rapidly precipitate phosphates (Hepher, 1958, Shrestha & Lin, 1996). Different sediment types can also affect P adsorption rates. In a study by Shrestha and Lin (1996), sediments comprised of sand, subsurface farm soil, and commercial bentonite were mixed at varying ratios and tested for P saturation capacity. In this study, treatments with higher clay content showed markedly higher P saturation capacity. This is likely due to the larger surface area associated with finer clay particles (Shrestha & Lin, 1996).

Shrestha and Lin (1996) also examined the ratios of loosely bound P, Al-P, Fe-P and Ca-P. It was shown that in the cases where bentonite was added to soil to increase clay content, Al-P and Ca-P increased appreciably with the treatment, but Fe-P decreased with increasing bentonite content (Shrestha & Lin, 1996). This shows that the types of available cations must be considered in conjunction with the soil types of sediments, not only the particle size.

Even small amounts of fine particles can greatly increase the total surface area in sediments. As shown by Walter and Morse (1984), where they examined the dissolution of carbonates in sediments by dividing sediment particles by size, greater than and less than 62 microns. The smaller

particle group accounted for only 16 percent of the total weight of the sample; however, the smaller particle group accounted for an adsorption rate ten times higher than all particles greater than 62-microns (Walter & Morse 1984, Zhang & Huang, 2007). It can be inferred that P adsorption and desorption would react similarly to varying particle size.

Phosphorus exchange across the sediment–water interface, via adsorption and desorption, plays a crucial role in governing the availability of water-soluble P (Froelich, 1988). Suspension of sediment particles into the water column increases the surface area available for P exchange; with smaller particles being more likely to be resuspended due to wave action and reside in the water column for larger periods of time (Wang & Li, 2010). Thus, greater amounts of fine particles are likely to increase adsorption and desorption of P into and out of the water column.

A study by Komatsu, Fukushima, and Harasawa (2007) developed a model to predict the long-term effects of global climate change on lakes and the algal blooms they produce. Their model suggested that surface and hypolimnion temperatures are likely to rise significantly. This will likely deepen the thermocline, increasing oxygen demand for aerobic decomposition, and in turn promoting increased releases of P into the water column (Komatsu et al., 2007). Aerobic conditions typically favor P adsorption, while anaerobic conditions typically favor desorption (Hietanen & Lukkari, 2007; Lasater & Haggard, 2017).

Sediments can play a large role in promoting or potentially inhibiting bloom formation by either sequestering or releasing P and other nutrients into the water column (Zhu et al., 2012). The degradation of blooms can also impact this sediment-water column relationship. Zhu et al. (2012) demonstrated this in a study of Lake Taihu, China. They observed that decaying blooms could effectively remove nutrients from the sediment by creating areas of hypoxia as the algae decays. These areas of hypoxia facilitate the rapid release of nutrients like ammonia and phosphorous, which then in turn fuel further bloom formation (Zhu et al., 2012) (Figure 1.1).

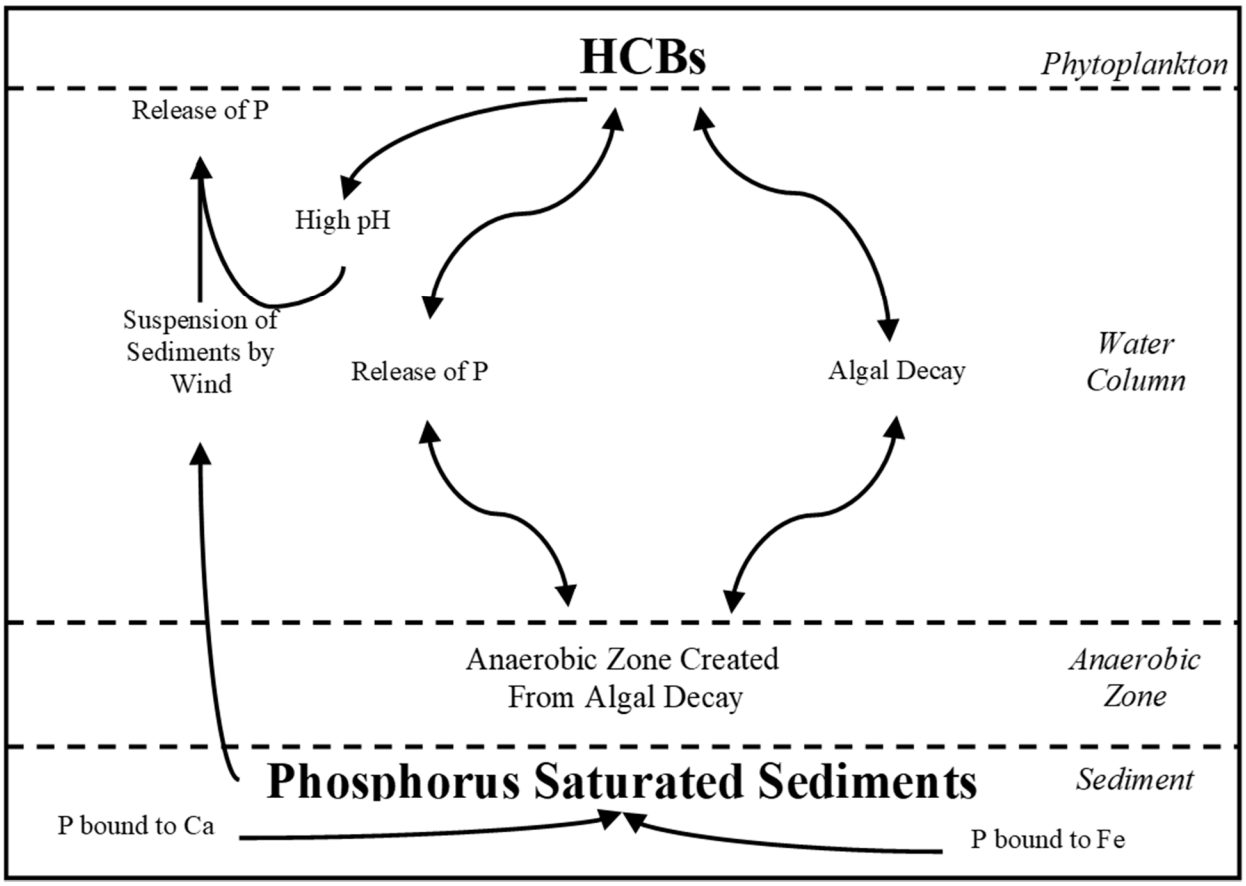

Figure 1.1. Diagram showing the interactions between HCBs, the water column, and sediments in eutrophic P saturated systems.

1.3. Nitrogen

Recent studies have shown that N can be as or more limiting to phytoplankton growth than P in aquatic ecosystems (Chaffin & Bridgeman, 2013; Dolman et al., 2012; O'Neil et al., 2012; Scott & McCarthy, 2010). These studies examine how seasonal changes can play a large role in nutrient limitation. They have also challenged some of the stronger arguments against N limitation, including the theory that N cannot limit aquatic systems because many cyanobacteria are capable of fixing atmospheric N (N_2) (Scott & McCarthy, 2010).

Nitrogen fixation is an energy consuming process, and while cyanobacteria may be able to supplement N demands in the biofilm layer over the course of a few weeks, they would not be capable of fixing N at an ecosystem level (Scott & McCarthy, 2010). Additionally, a study by

Dolman et al. (2012) looked in depth at nine taxa of cyanobacteria, six able to fix N_2 and three that are unable. They found that there was no set pattern or differentiation between N^2 fixing and non-N_2 fixing taxa. As an example, *C. raciborskii*, a N_2 fixing taxa, showed its highest relative abundance in a N enriched environment. While *P. agardhii*, a non- N_2 fixing taxa, showed its highest abundance in relatively P enriched waters. Additionally, they showed that in a P saturated lake, a saturation point was reached between total P and cyanobacteria biovolume, while there was no saturating relationship between N and biovolume (Dolman et al. 2012). These results indicate that P is not the single answer regarding what limits cyanobacteria growth, and these limits may be determined more at a genus and species level rather than for cyanobacteria as a whole.

Another factor, when considering nutrient limitation, are changes to lakes brought on by seasonal variation. In a study by Søndergaard, Lauridsen, Johansson, & Jeppesen (2017), 817 Danish lakes were evaluated for N and P concentrations. The study showed that in shallow holomictic lakes, N levels became lower as the summer progressed, while P levels remained consistent or even increased (Søndergaard et al. 2017). This can partially be attributed to higher temperatures, which lead to higher rates of denitrification as the summer progresses (Saunders & Kalff, 2001).

This concept is further reinforced in a study by Dolman, Mischke, and Wiedner (2016), where 369 German lakes were assessed. It was found that in both stratified and polymictic lakes, N limitation increased as the summer progressed, peaking between July and September. In stratified lakes, P limitation occurred in 60 to 70 percent of the lakes between April and May, then declined to 40 to 50 percent between August and October. In polymictic lakes, P limitation occurred in 60 to 70 percent of lakes in April, then fell to 10 to 20 percent between July and September. Nitrogen limitation increased to 50 to 60 percent between June and September (Dolman et al., 2016). These studies show that nutrient limitation can be a dynamic element changing throughout the season.

The warmer temperatures that coincide with the later summer months not only result in loss of N from a system due to denitrification; but warmer temperatures may also result in a release of N into the water column from the decomposition of organic matter (Wetzel, 2001). Furthermore, cyanobacteria tend to favor biologically reduced forms of N (ammonium) over oxidized forms like nitrite and nitrate (Chaffin & Bridgeman, 2013; Paerl, Gardner, McCarthy, Peierls, & Wilhelm, 2014; Paerl & Huisman, 2009; Paerl et al., 2015). This infers that large late summer blooms may be fueled by large releases of ammonium from organic matter as temperatures rise.

1.4. Cyanobacteria Competitive Advantages

In addition to dominating in higher temperatures, cyanobacteria have physiological traits that give them a competitive advantage over other phytoplankton. Some cyanobacteria, like *Microcystis,* can regulate their buoyancy by forming and collapsing intracellular gas vesicles (Walsby. Hayes, Boje, & Stal, 1997). This allow cyanobacteria to migrate throughout the water column depending on their needs.

Large blooms coincide with high rates of photosynthesis and consequently high CO_2 demands (Paerl & Ustach, 1982; Paerl et al., 2011). This can result in pH levels above 9, which can result in free CO_2 representing less than one percent of total dissolved inorganic carbon (Paerl et al., 2011; Paerl & Ustach, 1982). Buoyant cyanobacteria gain a large competitive advantage over phytoplankton lower in the water column as they are better able to directly intercept free CO_2 in the atmosphere (Paerl & Ustach, 1982; Visser et al., 2016). Dense bloom formation can also result in intensive shading; creating an environment where light then becomes a limiting factor to growth. This is another situation where buoyancy control can be a distinct advantage.

In addition to being able to compete for resources at the surface, vertical migration allows for competition near the nutrient rich sediments. *Microcystis* has a high capacity to take advantage of this, being able to sequester P both intracellularly and on its external surfaces (Carr & Whitton, 1982;

Saxton, Arnold, Bourbonniere, McKay, & Wilhelm 2012). This competitive advantage for both light and nutrients helps buoyant cyanobacteria gain a significant advantage over other phytoplankton.

1.5. Cyanobacteria and the Production of Cyanotoxins

The dynamics that govern the production of cyanobacterial biomass, and the subsequent cyanotoxins they produce, are still debated and are likely specific to each individual location where cyanobacteria are produced (Reichwaldt & Ghadouani, 2012; Sinang, Reichwaldt, & Ghadouani, 2015; Waajen, Faassen, & Lürling, 2014). Production of cyanotoxins has been shown to be highly variable even within lake systems (Sitoki, Kurmayer, & Rott, 2012), with production being linked to specific gene expressions, which can vary by strain (Pineda-Mendoza, Zúñiga, & Martínez-Jerónimo, 2015). Local physical, chemical, and biological conditions are thought to be the dominant factors contributing to regulation of these genes, though there is little agreement on the extent to which each factor contributes to toxin production (Paerl et al., 2011; Paerl & Oten, 2013; Sinang et al., 2015). This implies that general assumptions may not be accurate in predicting the potential for blooms to become toxic, and that each specific site must be assessed individually.

There are several different toxins produced by cyanobacteria with microcystin, anatoxin-a, and cylindrospermopsin being among the most common globally (Harke et al., 2016). Among these three, microcstins are the most widespread and are primarily produced by the genera *Microcystis*, *Planktothrix*, and *Dolichospermum* (Buratti et al., 2017). Microcystin has been the most widely studied, yet the reasons for its production are still unknown, and theories for its purpose range from grazing defense and acclimation to ultraviolet light to intracellular communications (Harke et al., 2016).

1.6. References

Bishop, C. T., Anet E. F., & Gorham P.R. (1959). Isolation and identification of the fast-death factor in *Microcystis aeruginosa* NRC-1. *Canadian Journal of Biochemistry and Physiology, 37(3)*, 453–471.

Buratti, F. M., Manganelli, M., Vichi, S., Stefanelli, M., Scardala, S., Testai, E., & Funari, E. (2017). Cyanotoxins: producing organisms, occurrence, toxicity, mechanism of action and human

health toxicological risk evaluation. *Archives of Toxicology*, *91*(3), 1049–1130. https://doi.org/10.1007/s00204-016-1913-6

Carr N. G., & Whitton B. A. (1982). *The biology of Cyanobacteria*. Blackwell Scientific Publications.

Chaffin, J. D., & Bridgeman, T. B. (2013). Organic and inorganic nitrogen utilization by nitrogen-stressed cyanobacteria during bloom conditions. *Journal of Applied Phycology*, *26*(1), 299–309. https://doi.org/10.1007/s10811-013-0118-0

Davis, T. W., Berry, D. L., Boyer, G. L., & Gobler, C. J. (2009). The effects of temperature and nutrients on the growth and dynamics of toxic and non-toxic strains of Microcystis during cyanobacteria blooms. *Harmful Algae*, *8*(5), 715–725. https://doi.org/10.1016/j.hal.2009.02.004

Dodds, W. K., Bouska, W. W., Eitzmann, J. L., Pilger, T. J., Pitts, K. L., Riley, A. J., … Thornbrugh, D. J. (2009). Eutrophication of U.S. freshwaters: Analysis of potential economic damages. *Environmental Science and Technology*, *43*(1), 12–19. https://doi.org/10.1021/es801217q

Dolman, A. M., Rücker, J., Pick, F. R., Fastner, J., Rohrlack, T., Mischke, U., & Wiedner, C. (2012). Cyanobacteria and cyanotoxins: The influence of nitrogen versus phosphorus. *PLoS ONE*, *7*(6). https://doi.org/10.1371/journal.pone.0038757

Dolman, A. M., Mischke, U., & Wiedner, C. (2016). Lake-type-specific seasonal patterns of nutrient limitation in German lakes, with target nitrogen and phosphorus concentrations for good ecological status. *Freshwater Biology*, *61*(4), 444–456. https://doi.org/10.1111/fwb.12718

Downing, J. A., Watson, S. B., & McCauley, E. (2001). Predicting cyanobacteria dominance in lakes. *Canadian Journal of Fisheries and Aquatic Sciences*, *58*(10), 1905–1908. https://doi.org/10.1139/f01-143

Francis, G. (1878). Poisonous Australian lake. *Nature*, *18*(444), 11–12. https://doi.org/10.1038/018011d0

Froelich, P. N. (1988). Kinetic control of dissolved phosphate in natural rivers and estuaries: A primer on the phosphate buffer mechanism. *Limnology and Oceanography*, *33(4 part 2)*, 649–668. https://doi.org/10.4319/lo.1988.33.4_part_2.0649

Graham, J. L., Jones, J. R., Jones, S. B., Downing, J. A., & Clevenger, T. E. (2004). Environmental factors influencing microcystin distribution and concentration in the Midwestern United States. *Water Research*, *38*(20), 4395–4404. https://doi.org/10.1016/j.watres.2004.08.004

Harke, M. J., Steffen, M. M., Gobler, C. J., Otten, T. G., Wilhelm, S. W., Wood, S. A., & Paerl, H. W. (2016). A review of the global ecology, genomics, and biogeography of the toxic cyanobacterium, *Microcystis* spp. *Harmful Algae*, *54*, 4–20. https://doi.org/10.1016/j.hal.2015.12.007

Hepher, B. (1958). On the dynamics of phosphorus added to fishponds in Israel1. *Limnology and Oceanography*, *3*(1), 84–100. https://doi.org/10.4319/lo.1958.3.1.0084

Hietanen, S., & Lukkari, K. (2007). Effects of short-term anoxia on benthic denitrification, nutrient fluxes and phosphorus forms in coastal Baltic sediment. *Aquatic Microbial Ecology*, *49*, 293–302. https://doi.org/10.3354/ame01146

Hobbs, W., & Wong, S. (2019). The prevalence of cyanobacteria: A historical perspective from lake sediment (Environmental assessment program, Washington State Department of Ecology, Publication No. 19-03-011). Retrieved from https://fortress.wa.gov/ecy/publications/SummaryPages/1903011.html

Huisman, J., Codd, G. A., Paerl, H. W., Ibelings, B. W., Verspagen, J. M. H., & Visser, P. M. (2018). Cyanobacterial blooms. *Nature Reviews Microbiology*, *16*(8), 471–483. https://doi.org/10.1038/s41579-018-0040-1

Jeppesen, E., Sondergaard, M., Jensen, J. P., Havens, K. E., Anneville, O., Carvalho, L., … Winder, M. (2005). Lake responses to reduced nutrient loading - an analysis of contemporary long-term data from 35 case studies. *Freshwater Biology*, *50*(10), 1747–1771. https://doi.org/10.1111/j.1365-2427.2005.01415.x

Komatsu, E., Fukushima, T., & Harasawa, H. (2007). A modeling approach to forecast the effect of long-term climate change on lake water quality. *Ecological Modelling*, *209*(2-4), 351–366. https://doi.org/10.1016/j.ecolmodel.2007.07.021

Kurmayer, R., & Christiansen, G. (2009). The genetic basis of toxin production in cyanobacteria. *Freshwater Reviews*, *2*(1), 31–50. https://doi.org/10.1608/frj-2.1.2

Lasater, A. L., & Haggard, B. E. (2017). Sediment phosphorus flux at Lake Tenkiller, Oklahoma: How important are internal sources? *Agricultural and Environmental Letters*, *2*(1), 1-5. https://doi.org/10.2134/ael2017.06.0017

Lebo, M. E. (1991). Particle-bound phosphorus along an urbanized coastal plain estuary. *Marine Chemistry*, *34*(3-4), 225–246. https://doi.org/10.1016/0304-4203(91)90005-h

Merel, S., Walker, D., Chicana, R., Snyder, S., Baurès, E., & Thomas, O. (2013). State of knowledge and concerns on cyanobacterial blooms and cyanotoxins. *Environment International*, *59*, 303–327. https://doi.org/10.1016/j.envint.2013.06.013

Ni, X., Yuan, Y., & Liu, W. (2020). Impact factors and mechanisms of dissolved reactive phosphorus (DRP) losses from agricultural fields: A review and synthesis study in the Lake Erie basin. *Science of The Total Environment*, *714*, 136624. https://doi.org/10.1016/j.scitotenv.2020.136624

O'Neil, J., Davis, T., Burford, M., & Gobler, C. (2012). The rise of harmful cyanobacteria blooms: The potential roles of eutrophication and climate change. *Harmful Algae*, *14*, 313–334. https://doi.org/10.1016/j.hal.2011.10.027

Paerl, H. W., Gardner, W. S., McCarthy, M. J., Peierls, B. L., & Wilhelm, S. W. (2014). Algal blooms: Noteworthy nitrogen. *Science*, *346*(6206), 175–175. https://doi.org/10.1126/science.346.6206.175-a

Paerl, H. W., Hall, N. S., & Calandrino, E. S. (2011). Controlling harmful cyanobacterial blooms in a world experiencing anthropogenic and climatic-induced change. *Science of The Total Environment*, *409*(10), 1739–1745. https://doi.org/10.1016/j.scitotenv.2011.02.001

Paerl, H. W., & Huisman, J. (2009). Climate change: a catalyst for global expansion of harmful cyanobacterial blooms. *Environmental Microbiology Reports*, *1*(1), 27–37. https://doi.org/10.1111/j.1758-2229.2008.00004.x

Paerl, H. W., & Otten, T. G. (2013). Harmful Cyanobacterial Blooms: Causes, Consequences, and Controls. *Microbial Ecology*, *65*(4), 995–1010. https://doi.org/10.1007/s00248-012-0159-y

Paerl, H. W., & Ustach, J. F. (1982). Blue-green algal scums: An explanation for their occurrence during freshwater blooms[1]. *Limnology and Oceanography*, *27*(2), 212–217. https://doi.org/10.4319/lo.1982.27.2.0212

Paerl, H. W., Xu, H., Hall, N. S., Rossignol, K. L., Joyner, A. R., Zhu, G., & Qin, B. (2015). Nutrient limitation dynamics examined on a multi-annual scale in Lake Taihu, China: implications for controlling eutrophication and harmful algal blooms. *Journal of Freshwater Ecology*, *30*(1), 5–24. https://doi.org/10.1080/02705060.2014.994047

Paul, V. J. (2008). Global warming and cyanobacterial harmful algal blooms. *Advances in Experimental Medicine and Biology Cyanobacterial Harmful Algal Blooms: State of the Science and Research Needs*, 239–257. https://doi.org/10.1007/978-0-387-75865-7_11

Paytan, A., & Mclaughlin, K. (2007). The Oceanic Phosphorus Cycle. *ChemInform*, *38*(20). https://doi.org/10.1002/chin.200720268

Pineda-Mendoza, R. M., Zúñiga, G., & Martínez-Jerónimo, F. (2015). Microcystin production in *Microcystis aeruginosa*: effect of type of strain, environmental factors, nutrient concentrations, and N:P ratio on mcyA gene expression. *Aquatic Ecology*, *50*(1), 103–119. https://doi.org/10.1007/s10452-015-9559-7

Reichwaldt, E. S., & Ghadouani, A. (2012). Effects of rainfall patterns on toxic cyanobacterial blooms in a changing climate: Between simplistic scenarios and complex dynamics. *Water Research*, *46*(5), 1372–1393. https://doi.org/10.1016/j.watres.2011.11.052

Reynolds, C. S. (1997). Successional development, energetics and diversity in planktonic communities. *Biodiversity*, 167–202. https://doi.org/10.1007/978-1-4612-1906-4_11

Saunders, D., & Kalff, J. (2001). Denitrification rates in the sediments of Lake Memphremagog, Canada–USA. *Water Research*, *35*(8), 1897–1904. https://doi.org/10.1016/s0043-1354(00)00479-6

Saxton, M. A., Arnold, R. J., Bourbonniere, R. A., McKay, R. M. L., & Wilhelm, S. W. (2012). Plasticity of total and intracellular phosphorus quotas in *Microcystis aeruginosa* cultures and Lake Erie algal assemblages. *Frontiers in Microbiology*, *3*. https://doi.org/10.3389/fmicb.2012.00003

Schindler, D. W. (1974). Eutrophication and recovery in experimental lakes: Implications for lake management. *Science*, *184*(4139), 897–899. https://doi.org/10.1126/science.184.4139.897

Schindler, D. W. (1977). Evolution of phosphorus limitation in lakes. *Science*, *195*(4275), 260–262. https://doi.org/10.1126/science.195.4275.260

Scott, J. T., & McCarthy, M. J. (2010). Nitrogen fixation may not balance the nitrogen pool in lakes over timescales relevant to eutrophication management. *Limnology and Oceanography*, *55*(3), 1265–1270. https://doi.org/10.4319/lo.2010.55.3.1265

Shrestha, M. K., & Lin, C. (1996). Determination of phosphorus saturation level in relation to clay content in formulated pond muds. *Aquacultural Engineering*, *15*(6), 441–459. https://doi.org/10.1016/s0144-8609(96)01007-2

Sinang, S. C., Reichwaldt, E. S., & Ghadouani, A. (2015). Local nutrient regimes determine site-specific environmental triggers of cyanobacterial and microcystin variability in urban lakes. *Hydrology and Earth System Sciences*, *19*(5), 2179–2195. https://doi.org/10.5194/hess-19-2179-2015

Sitoki, L., Kurmayer, R., & Rott, E. (2012). Spatial variation of phytoplankton composition, biovolume, and resulting microcystin concentrations in the Nyanza Gulf (Lake Victoria, Kenya). *Hydrobiologia*, *691*(1), 109–122. https://doi.org/10.1007/s10750-012-1062-8

Søndergaard, M., Lauridsen, T. L., Johansson, L. S., & Jeppesen, E. (2017). Nitrogen or phosphorus limitation in lakes and its impact on phytoplankton biomass and submerged macrophyte cover. *Hydrobiologia*, *795*(1), 35–48. https://doi.org/10.1007/s10750-017-3110-x

Veal, C. J., Neelamraju, C., Wolff, T., Watkinson, A., Shillito, D., & Canning, A. (2017). Managing cyanobacterial toxin risks to recreational users: a case study of inland lakes in South East Queensland. *Water Supply*, *18*(5), 1719–1726. https://doi.org/10.2166/ws.2017.233

Visser, P. M., Verspagen, J. M., Sandrini, G., Stal, L. J., Matthijs, H. C., Davis, T. W., … Huisman, J. (2016). How rising CO2 and global warming may stimulate harmful cyanobacterial blooms. *Harmful Algae*, *54*, 145–159. https://doi.org/10.1016/j.hal.2015.12.006

Waajen, G. W. A. M., Faassen, E. J., & Lürling, M. (2014). Eutrophic urban ponds suffer from cyanobacterial blooms: Dutch examples. *Environmental Science and Pollution Research*, *21*(16), 9983–9994. https://doi.org/10.1007/s11356-014-2948-y

Walsby, A. E., Hayes, P. K., Boje, R., & Stal, L. J. (1997). The selective advantage of buoyancy provided by gas vesicles for planktonic cyanobacteria in the Baltic Sea. *New Phytologist*, *136*(3), 407–417. https://doi.org/10.1046/j.1469-8137.1997.00754.x

Walter, L. M., & Morse, J. W. (1984). Reactive surface area of skeletal carbonates during dissolution: Effect of grain size. *Journal of Sedimentary Research*, *54*(4), 1081–1090. https://doi.org/10.1306/212f8562-2b24-11d7-8648000102c1865d

Wang, Q., & Li, Y. (2010). Phosphorus adsorption and desorption behavior on sediments of different origins. *Journal of Soils and Sediments*, *10*(6), 1159–1173. https://doi.org/10.1007/s11368-010-0211-9

Wang, M., Shi, W., Chen, Q., Zhang, J., Yi, Q., & Hu, L. (2018). Effects of nutrient temporal variations on toxic genotype and microcystin concentration in two eutrophic lakes. *Ecotoxicology and Environmental Safety*, *166*, 192–199. https://doi.org/10.1016/j.ecoenv.2018.09.095

Wetzel, R. G. (2015). *Limnology: Lake and river ecosystems*. Academic Press, an imprint of Elsevier.

Wu, B., Jin, H., Gao, S., Xu, J., & Chen, J. (2019). Nutrient budgets and recent decadal variations in a highly eutrophic estuary: Hangzhou Bay, China. *Journal of Coastal Research*, *36*(1), 63. https://doi.org/10.2112/jcoastres-d-18-00071.1

Yang, J., Tang, H., Zhang, X., Zhu, X., Huang, Y., & Yang, Z. (2017). High temperature and pH favor *Microcystis aeruginosa* to outcompete *Scenedesmus obliquus*. *Environmental Science and Pollution Research*, *25*(5), 4794–4802. https://doi.org/10.1007/s11356-017-0887-0

Zhang, J. Z., & Huang, X. L. (2007). Relative importance of solid-phase phosphorus and iron on the sorption behavior of sediments. *Environmental Science & Technology*, *41*(8), 2789–2795. https://doi.org/10.1021/es061836q

Zhu, M., Zhu, G., Zhao, L., Yao, X., Zhang, Y., Gao, G., & Qin, B. (2012). Influence of algal bloom degradation on nutrient release at the sediment–water interface in Lake Taihu, China. *Environmental Science and Pollution Research*, *20*(3), 1803–1811. https://doi.org/10.1007/s11356-012-1084-9

CHAPTER 2. THE EFFECTS OF EUTROPHICATION ON THE PREDICTABILITY OF HARMFUL CYANOBACTERIAL BLOOMS

2.1. Abstract

Fueled by increasing temperatures and anthropogenic loading of nutrients, harmful cyanobacterial blooms (HCBs) are increasing across the globe, impacting both coastal and inland water systems. This study assessed the impacts of eutrophication of HCBs on a large freshwater riverine system, that for management purposes, forms distinct lakes within the system. Nutrient and chlorophyll levels were monitored over the course of four sampling seasons, and phytoplankton community assemblages were surveyed over two seasons. Analysis of the data showed that conditions remained consistently eutrophic to hypereutrophic throughout each season. Unlike typical lakes, that see a seasonal transition of phytoplankton groups and cyanobacteria dominated assemblages throughout each season. Additionally, the lack of correlation between nutrients and HCB growth suggests that growth was not nutrient limited. Authors propose that under excessive eutrophication a critical threshold is surpassed where nutrients are no longer a prominent limiting factor of phytoplankton growth. Under these conditions, cyanobacteria thrive, and predictions of both phytoplankton growth and composition become unfeasible. This study is useful to researchers, scientists and managers globally looking to manage HCBs and hypereutrophic systems.

2.2. Introduction

Cyanobacteria are a large and diverse group of phytoplankton capable of producing harmful compounds called cyanotoxins (Merel et al., 2013). The impacts of harmful cyanobacterial blooms (HCBs) are on the rise with their impacts affecting communities globally (Harke et al., 2016). Anthropogenic nutrient loading and climate change drive conditions to favor cyanobacteria over other phytoplankton in the world's increasingly eutrophic lakes, rivers, and oceans (Paerl, Hall, &

Calandrino, 2011). Harmful cyanobacterial blooms are not a new occurrence, as reports of blooms and resulting livestock poisonings date back as early as 1878 (Francis, 1878; Veal et al., 2017). However, in recent years, the number of blooms has continued to escalate (Dodds et al., 2009; Harke et al., 2016; O'Neil, Davis, Burford, & Gobler, 2012). Hundreds of lakes have been assessed in relation to HCBs in the Americas, Europe and Asia (Dolman et al., 2012; Graham, Jones, Jones, Downing, & Clevenger, 2004; Wang et al., 2018), yet the many factors that control HCBs continue to be deliberated.

Anthropogenic loading of nutrients, primarily nitrogen (N) and phosphorus (P), are considered the largest contributors to HCBs (O'Neil et al., 2012), and are estimated to cost the United States approximately 2.2 billion dollars annually (Dodds et al., 2009). Past studies suggest that P is the primary limiting nutrient in large blooms (Schindler, 1974; Schindler, 1977). This belief led to P being the primary focus for extensive legislative controls regulating P releases into the environment (Harke et al., 2016). More recent studies have suggested that the management of N may play an equal or greater role in the management of HCB's in some systems (Chaffin & Bridgeman, 2013; Dolman et al., 2012; O'Neil et al., 2012; Scott & McCarthy, 2010).

While P has traditionally been limited in natural systems (Paytan & McLaughlin, 2007), anthropogenic nutrient enrichment has allowed P to eclipse N in some systems, which may favor atmospheric nitrogen fixing cyanobacteria (Paerl & Otten, 2013). More recently, the loading of N by the application of N fertilizers, stormwater runoff, wastewater treatment plants, and atmospheric deposition has become more common and may be compounding issues with systems that already have high P loading (Paerl & Otten, 2013). As systems become increasingly saturated by nutrients, there may come a point where major blooms are less limited or even not limited by nutrients. In a study by Søndergaard, Lauridsen, Johansson, and Jeppesen (2017), 817 Danish lakes were evaluated for N and P concentrations. Søndergaard et al. (2017) found strong correlations to chlorophyll

between both N and P when concentrations of N and P were relatively low, but were unable to find strong correlations at higher concentrations. A study by Xu, Paerl, Qin, Zhu, and Gaoa (2009) characterized P and N limitations at various thresholds and found growth was seasonally dependent with ambient P being limited in the spring and N being limited in the summer and fall. Additionally, they found growth responded proportionately to additions of P ranging from 14 to 214 $\mu g/L^{-1}$, and N was no longer limiting after reaching 800 $\mu g/L^{-1}$ N (Xu et al., 2009). These results suggest that nutrient limitations are seasonally dependent and limitation of one nutrient may be dependent on the abundance of the other. Information in these studies is useful, but more information is needed on identifying limitations of P and N at high concentrations in relation to HCB's.

Eutrophication of lakes is not the only driving force behind the recent increase in HCBs. Physical properties like increasing temperatures, induced by global climate change, affect phytoplankton communities (Huisman et al., 2018; Paerl & Huisman, 2009; Paul, 2008). Seasonal temperature changes tend to result in community shifts that start with diatoms at cooler temperatures, then shifting to green algae, and eventually cyanobacteria, which become the most dominant at the highest temperatures (Reynolds, 1997; Yang et al., 2017).

Studies observing the dynamics controlling HCBs have covered extensive geographic ranges, but have limited seasonal representation within individual systems (Kosten et al., 2011), or have represented entire seasonal conditions with only brief two to three-week sampling periods (Wu, Jin, Gao, Xu, & Chen, 2019). Additionally, studies to date have generally looked at limitations of N and P at low concentrations, but not shown correlations as nutrient concentrations increase (Søndergaard et al. 2017; Xu et al. 2009). It is the goal of this study to: 1) identify limitations to phytoplankton growth at high nutrient concentrations in a natural system; and 2) assess seasonal phytoplankton community patterns at high nutrient concentrations. This information is useful in the

advancement of best management practices to control HCB's, and for the development of models predicting trends in lake eutrophication and HCBs.

2.3. Methods and Materials

2.3.1. Study area

The study took place at Des Lacs National Wildlife Refuge (DLNWR), which borders the Canadian Province of Saskatchewan and lies approximately 145 kilometers west of the United States (US) state of Montana, and surrounds 45 kilometers of the Des Lacs River (Figure 2.1). The Des Lacs River feeds into the Souris River and is part of a 62,000 square-kilometer basin spanning parts of the US and Canada (Kolars, Vicchia, & Galloway, 2019). The Des Lacs River, and the valley that surrounds it, was originally carved by the sudden and rapid release of water from the glacial Lake Regina (Boettger, 1986). Presently, the river is sustained primarily by ephemeral streams fueled by spring melt and runoff, with little water entering the system from the headwaters. These ephemeral streams have led to the formation of a multitude of coulees that span the length of the Des Lacs Valley. The outwash from several major coulees form the natural dams that define the Upper, Middle, and Lower Des Lacs Lakes (Des Lacs National Wildlife Refuge, 1999) (Figure 2.1).

The Upper, Middle and Lower Des Lacs Lakes comprise approximately 2,029 hectares of open water, and another 283 hectares of marsh (Des Lacs National Wildlife Refuge, 1999). Water movement primarily occurs during the spring melt and can be magnified by spring precipitation. This is the only time of the year that sees regular flushing of water out of the system. During this time, a low flow of water travels south, eventually reaching the Souris River. Small scale flushing occurs during the spring melt, after which the system remains relatively stagnant. Large precipitation events can result in a short-term flow that can travel either northward or southward depending on what part of the system receives precipitation.

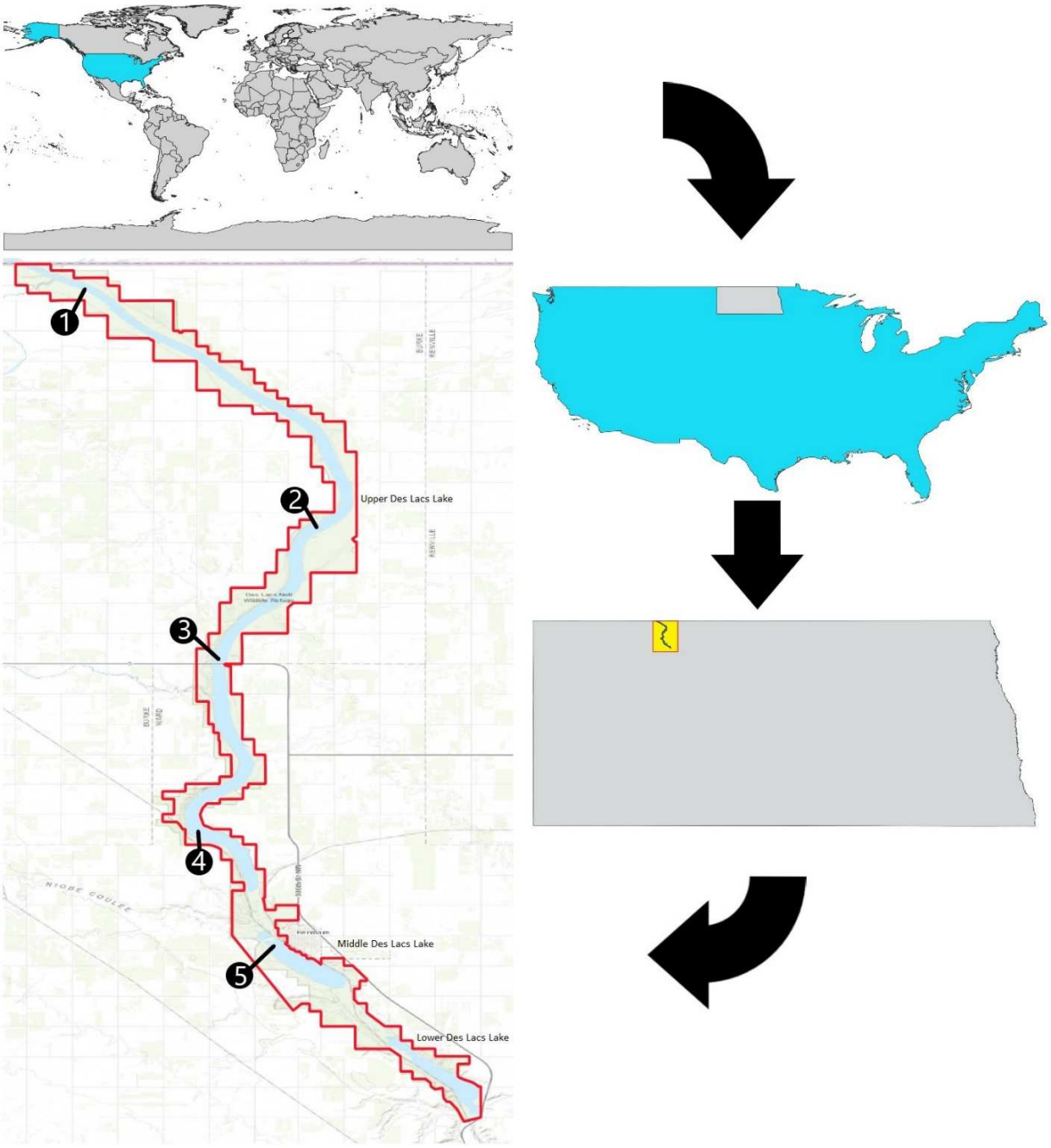

Figure 2.1. Map showing North Dakota, USA, and the location of the Des Lacs National Wildlife Refuge (red) and sites sampled as part of the study (1-5).

In an effort to manage DLNWR for increased waterfowl productivity, eight water control structures were built creating distinct marshlands and reinforcing the formation of the Upper, Middle, and Lower Des Lacs Lakes. These water control structures, in conjunction with low flows and sediment deposition from ephemeral streams, contribute to the system being relatively shallow.

The deepest site is 3.5 m deep during the spring, but averages 3 m through the majority of the growing season. The shallowest site is 1.2 m in the spring, but averages around 0.8 m throughout the growing season.

Five sites were selected for sampling within the Upper and Middle Des Lacs Lakes (Figure 2.1). From north to south, the sites have been labeled one through five, and are located at 48°59'24.1"N 102°11'33.4"W, 48°52'25.2"N 102°04'16.8"W, 48°48'37.2"N 102°07'11.7"W, 48°43'37.8"N 102°07'49.4"W, and 48°40'19.6"N 102°05'37.0"W, respectively (Figure 2.1). Each site was selected to represent spatially isolated bodies of water. Isolation was determined by distance from other sites or water control structures acting as physical barriers.

The DLNWR is home to a series of impounded lakes and wetlands that have seen annual HCBs. An earlier survey on DLNWR by the North Dakota Department of Environmental Quality (NDDEQ) found that during 1997 and 1998, the lakes could already be classified as hypereutrophic (Wax, 2006). The ranges for P and N were 110 to 385 $\mu g/L^{-1}$ and 1,790 to 3,827 $\mu g/L^{-1}$, respectively, and indicated a system that was predominantly N limited (Wax, 2006). The thresholds for eutrophication in freshwater systems for P and N are 20 to 100 $\mu g/L^{-1}$ and 500 to 1,000 $\mu g/L^{-1}$, respectively (Lin et al., 2008), putting this system far beyond the thresholds for eutrophication.

2.3.2. Water sampling

Water sampling was conducted weekly at all five sites from May to October 2016 to 2019. On each sampling date, in situ measurements were made for temperature, conductivity, and pH using a YSI PRODSS sonde (Yellow Springs, Ohio, USA). Additionally, a secchi disk was used to measure secchi disk transparency (SD) on site. Samples for lab analysis were collected at all sites using a Wildco 1.2 L Kemmerer sampler (Yulee, Florida, USA) according to NDDEQ protocol (North Dakota Department of Environmental Quality, 2020). Samples were preserved and placed

on ice before shipping to the NDDEQ lab in Bismarck, North Dakota, USA, where they were analyzed for ammonia, nitrate+nitrite, total nitrogen, and total phosphorus.

Chlorophyll-*a* (CHY-*a*) was sampled using a two-meter-long, six cm diameter, PVC column sampler. Samples were collected from the surface down to two meters, or to just above sediment if water depth was less than two meters. Samples were mixed in a Wildco 8 L churn splitter (Yulee, Florida, USA) and 50-1,000 mL of water was filtered through a 0.65 μm Whatman glass fiber filters (GE Healthcare Life Sciences, Marlborough, Massachusetts, USA). Filters were stored in sealed plastic tubes, wrapped in aluminum foil, and kept on ice until they could be shipped to the NDDEQ lab for analysis.

In 2019, an additional sample was collected each week at sites one, two, four and five to be analyzed for dissolved phosphorus (DP) and dissolved nitrogen (DN). Site three was exempted due to its proximity to site two. Samples for DP and DN were collected with a Kemmerer sampler then filtered using a 0.45-micron filter (Geotech, Denver, Colorado, USA) with a peristaltic pump (Cole-Parmer (Model 7533-50), Vernon Hills, Illinois, USA). Samples were preserved according to NDDEQ protocol, put on ice and shipped to the NDDEQ lab for analysis.

2.3.3. Phytoplankton identification and microcystin monitoring

In 2018 and 2019, an additional 250 mL sample, from the zero to two-meter column sample was collected at each site and preserved to a one percent concentration of Lugol's solution. Samples were refrigerated and shipped to BSA Environmental Services, Inc. (Beachwood, Ohio) to be analyzed for taxonomic identification and enumeration. Samples selected for analysis in 2018 were chosen to represent times of low, medium, and high intensity of blooms throughout the growing season (Table 2.1). Samples in 2019 were selected to represent a seasonal transition at sites one, two, four and five, with extra samples selected during times of high CHY-*a* production (Table 2.2). Chlorophyll measurements were used to determine bloom intensity in 2018. Samples in 2019 were

spread out approximately every two weeks with extra samples taken where CHY-*a* and microcystin readings deviated rapidly from the previous weeks sampling. Increased sample size in 2019 was due to increased funding.

Table 2.1. List of 2018 dates, site, and corresponding chlorophyll-*a* (CHY-*a*) levels for taxonomic identification samples. Samples were selected to represent times before, during, and after the lake wide bloom. Some sites experienced site specific blooms during the growing season. Color shades represent CHY-*a* abundance from lowest to highest represented as lightest to darkest respectively.

	Chlorophyll-*a* (µg/L)			
Date	Site 1	Site 4	Site 5	Relative Trend
6/20/2018	25	312.0	93.4	Pre-Lake Wide
7/17/2018	114	75.0	75.0	Bloom
8/28/2018	221	324.0	147.0	Lake wide Bloom
9/13/2018	128	191.0	119.0	Post Lake Wide
10/9/2018	86.5	175.0	51.7	Bloom

Table 2.2. List of 2019 dates, site, and corresponding chlorophyll (CHY-*a*) levels for taxonomic identification samples. Samples were selected to represent a seasonal transition beginning with relatively limited growth in the spring to high bloom growth in the late summer, then concluding with an end of season die-off. . Color shades represent CHY-*a* abundance from lowest to highest represented as lightest to darkest respectively.

	Chlorophyll-*a* (µg/L)			
Date	Site 1	Site 2	Site 4	Site 5
5/31/2019	51.2	69.4	40	16.7
6/19/2019	50		12.5	30
7/16/2019	21.7	25	30.3	117
8/5/2019	275	157	123	257
8/21/2019	81.1	35.2	121	184
9/4/2019	196	108	102	386
9/10/2019	121	86	87.8	299
9/16/2019	164	104	52.6	221
9/23/2019	117	82.3	80.1	207
10/1/2019	139	64.1	64.6	221
10/16/2019	53.4	30.2	32	141
10/22/2019	30.8	16.6	12.3	84.6

All sites were monitored for microcystin each summer between May and October (2016-2019). Recreational (0-10 ppb) test strips (Abraxix Inc., Warminster, Pennsylvania, USA) were used when blooms were visually present from 2016 to 2018. When test strips indicated high (above 10

ppb) levels of microcystin, samples were sent to BSA Environmental Services, Inc. (Beachwood Ohio) for more accurate analysis using enzyme-linked immunosorbent assay (ELISA). In 2019, samples from sites 1, 2, 4, and 5 were taken and sent to BSA Environmental Services weekly for analysis of microcystin using the ELISA method.

2.3.4. Evaluation of eutrophication

Eutrophication levels were evaluated through the use of Carlson's Trophic State Index (TSI) (Carlson, 1977; Yang et al., 2020). The formulas for TSI use SD (TSI (SD)), TP (TP (TSI)), and CHY-*a* (TSI (CHY-a)) and are shown below:

TSI(SD)= 60 – 14.41 ln(SD)

TSI(CHY-*a*)= 9.81 ln(CHY-*a*) $[\mu \frac{g}{L}]$ + 30.6

TSI(TP)= 14.42 ln(TP) $[\mu \frac{g}{L}]$ + 4.15

A TSI has no upper or lower bounds, however, values greater than 70 indicate a hypereutrophic system, values between 70 and 50 indicate a eutrophic system, values between 50 and 30 indicate a mesotrophic system, and values less than 30 indicate an oligotrophic system.

2.3.5. Statistical analysis

Nonmetric Multi-Dimensional Scaling (NMS) was used to ordinate the algal identification data and to visually present the data. The NMS analysis used PC-ORD version 7 (MjM Software Design, Gleneden Beach, OR). Patterns in the data were found using a Bray-Curtis distance measure under these conditions: 1) 500 iterations in PC-ORD to reduce from six axes to three; 2) a significant Monte Carlo test ($p \leq 0.05$) to select axes from random; 3) stress <25; 4) instability < 0.0001; and 5) selection was halted when the next axis did not reduce stress by at least five. Pearson Correlation Coefficients between selected axes scores and algal species abundance with a value of $\geq$ 0.3 or $\leq$ -0.3 were considered interpretable.

A Permutation Multivariate Analysis of Variance (PERMANOVA) was performed on the algal species data to test if locations and months were significantly different. A Bray-Curtis distance measure was used in the PERMANOVA analysis. The analysis used PRIMER-e™ (Quest Research Limited) similar to Anderson, Gorley, and Clarke (2008). Paired comparisons from the PERMANOVA analysis did not have the p-value adjusted as suggest by Anderson et al. (2008).

The Analysis Toolpak in Microsoft Excel version 1908 (Microsoft Corporation), was used to create a correlation matrix for all tested water quality and environmental parameters. Matrices were created for each year sampling was conducted, at each site, and collectively. Total CHY-*a* and cyanobacterial biovolume (BV) were used as a rough indicator of phytoplankton growth.

2.4. Results

Weekly sampling spanning four seasons showed that both nutrient and CHY-*a* levels varied widely throughout each season (Figure 2.2). Nutrient levels consistently remained above hyper eutrophic levels, but this did not directly translate to CHY-*a* levels remaining excessively high. Chlorophyll levels were characterized by periodic spikes with a larger bloom occurring sometime between late July and mid-September. Nutrient levels were generally highest in late June and early to mid-July.

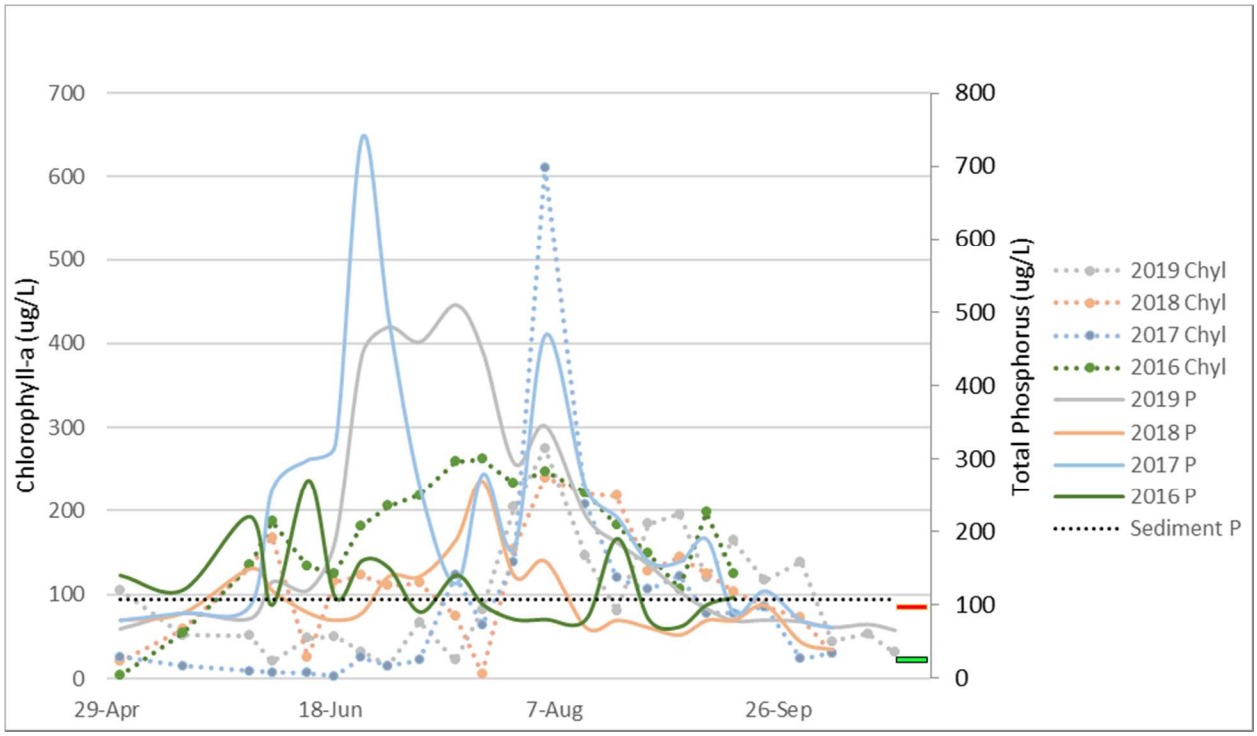

Figure 2.2. Chlorophyll and total phosphorus levels at site one between 2016 and 2019. The red and green markers indicate the boundaries between hypereutrophic (>96 µg/L), eutrophic (24 to 96 µg/L) and mesotrophic (6 to 24 µg/L) levels of phosphorus, respectively. Sediment P was measured once in 2019 at 107 µg/L.

Chlorophyll-*a* levels varied throughout the season with multiple small blooms occurring periodically. Larger bloom events generally occurred between July and September and dwarfed other blooms occurring earlier in the season. Yearly averages for CHY-*a* at each site ranged from 55.7 to 186.5 µg/L. The lowest value recorded was 3 µg/L and the highest was 611 µg/L.

Secchi disk transparency varied by site and year with substantial reductions in transparency during blooms. Transparency ranged from 0.1 to 2.1 m with the highest transparencies recorded in early summer with low transparencies (0.5 m and under) predominating throughout the remainder of the season. Transparency at site five throughout 2017 and 2019 was notably lower than sites one through four. In 2016 and 2018, SD readings were relatively low throughout the season at all sites (Table 2.3).

Table 2.3. Average secchi disk readings in meters for each site and year, including averages across sites and years.

Date	Site					
	Site 1	Site 2	Site 3	Site 4	Site 5	Average of all sites
2016	0.29	0.29	0.26	0.29	0.22	0.27
2017	0.67	0.77	0.78	0.73	0.34	0.66
2018	0.29	0.30	0.27	0.22	0.19	0.25
2019	0.48	0.82	0.75	0.92	0.28	0.65
Average all years	0.44	0.55	0.53	0.55	0.26	0.47

Phosphorus levels were inconsistent and did not have a set pattern each season. In 2018 and 2019, P levels remained relatively consistent throughout the year. The 2018 season showed the highest levels of P at the end of July, while 2019 season showed the highest levels in June and July, before gradually falling off. Despite the fluctuations of P, levels on DLNWR were always relatively high each season. Yearly averages of P among all sites ranged between 101.3 and 510.5 μg/L. The lowest reading was 40 μg/L and the highest was 1,080 μg/L (Table 2.4).

Nitrogen levels showed even greater variance throughout the season, though levels tended to be highest early in the season. Yearly N averages among all sites ranged from 1893 to 3147 μg/L. The lowest and highest readings recorded were 1410 and 7240 μg/L respectively, which were recorded at the same site during the same year (Table 2.4). Overall, 2017 and 2019 tended to be N limited (following the Redfield ratio of 16:1), with the opposite trend seen in 2016 and 2018.

Table 2.4. Showing season averages, minimum, and maximum values for phosphorus and nitrogen at each site during each year.

Phosphorus averages at all sites and all years (ug/L)						Nitrogen averages at all sites and all years (ug/L)					
Year	2016	2017	2018	2019	Average Across All Years	Year	2016	2017	2018	2019	Average Across All Years
Site 1						Site 1					
Average	126	230	108	203	167	Average	2651	3147	2419	2925	2785
Min	70	70	40	66	62	Min	1760	1410	1810	2120	1775
Max	270	740	270	510	448	Max	3760	7240	3860	4960	4955
Site2						Site2					
Average	125	211	101	205	161	Average	2520	2625	2250	3035	2608
Min	80	80	50	58	67	Min	2040	1500	1720	1990	1813
Max	230	480	330	466	377	Max	3290	5160	3810	4990	4313
Site 3						Site 3					
Average	134	205	106	241	172	Average	2713	2585	2300	2960	2639
Min	70	60	60	50	60	Min	2040	1450	1720	2060	1818
Max	300	450	220	520	373	Max	4990	5360	3220	5600	4793
Site 4						Site 4					
Average	142	203	101	299	186	Average	2731	2522	2445	2923	2655
Min	80	60	50	51	60	Min	2090	1560	1790	1880	1830
Max	260	550	170	680	415	Max	3800	5270	3120	6380	4643
Site 5						Site 5					
Average	511	333	231	388	366	Average	2461	2358	2195	1893	2227
Min	200	50	70	115	109	Min	2100	1570	1760	1540	1743
Max	1080	600	530	933	786	Max	3490	3240	2910	2230	2968
All Sites Combined						All Sites Combined					
Average	207	236	130	267	210	Average	2615	2648	2322	2747	2583
Min	100	64	54	68	72	Min	2006	1498	1760	1918	1796
Max	428	564	304	622	479	Max	3866	5254	3384	4832	4334

The lakes on DLNWR varied in N:P ratio both between years as well as throughout the year (Figure 2.3). The years 2016 and 2018 were predominately P limited, while 2017 and 2019 were predominantly N limited in sites one through four. The end of each season tended to see a large shift towards P limitation coinciding with the end of season die-off of blooms. Site five remained almost exclusively N limited every year.

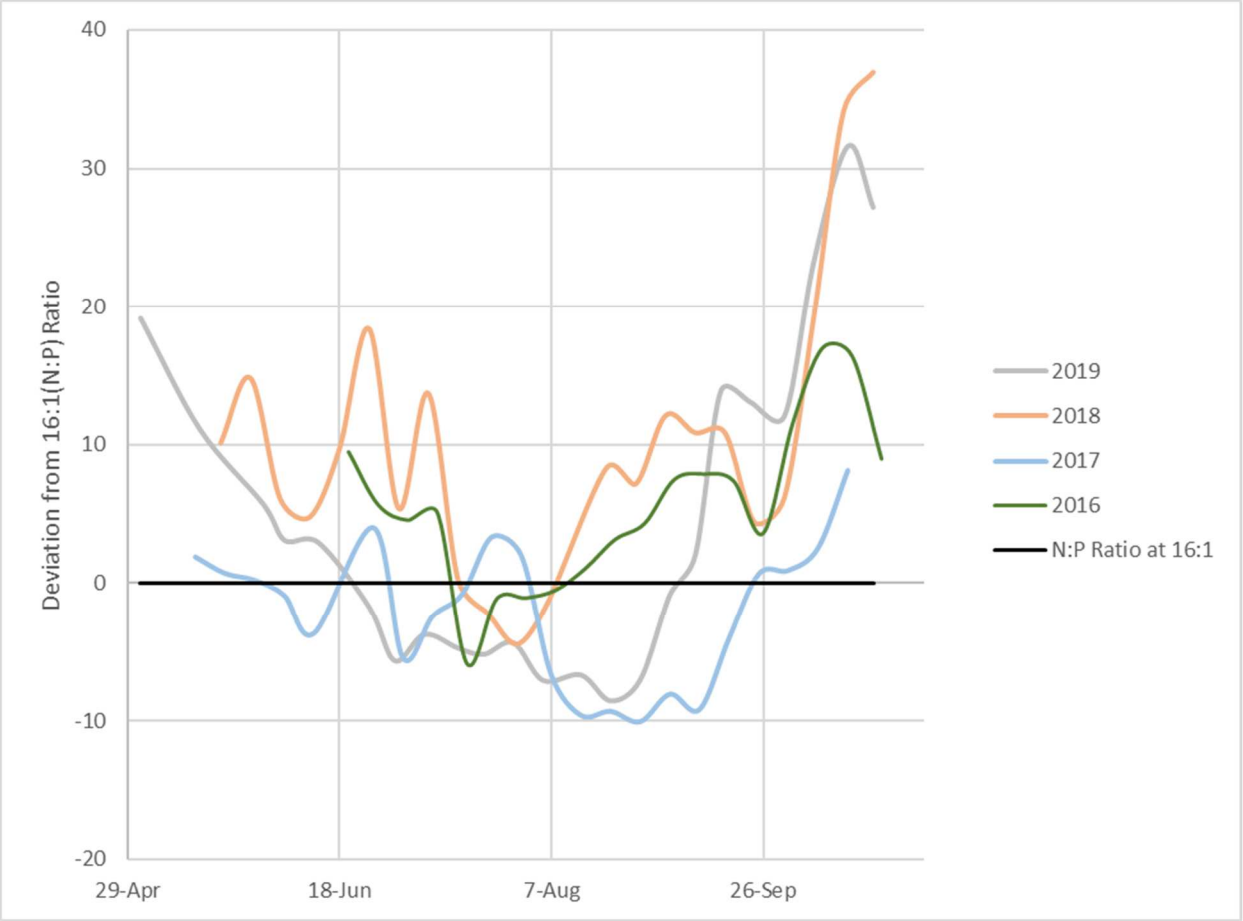

Figure 2.3. Nitrogen:Phosphorus Ratio with deviation from 16:1 for years 2016 to 2019 on Des Lacs National Wildlife Refuge. Values above the zero indicate phosphorous limitation and values below zero indicate nitrogen limitation.

In order to characterize eutrophication conditions on DLNWR, a trophic state index (TSI) (Carlson, 1977; Yang et al., 2020) was created independently using CHY-*a*, secchi depth (SD), and P readings. The TSI for all sites and parameters through all years indicated the system was consistently eutrophic to hypereutrophic throughout each season (TSI readings for the years 2016 through 2019 were 77.4. 80.4, 72.1, and 81.1 respectively). A few sampling days occurring early in the year resulted in a TSI indicating mesotrophic conditions for CHY-*a,* with a single SD reading indicating mesotrophic conditions. In example, TSI readings for CHY-*a* and SD on June 6, 2017 were 41.4 and 49.3 respectively.

The 2018 and 2019 NMS analysis found that three axes adequately explained the structure in the data (2018 stress = 4.2, instability <0.0001; 2019 stress = 7.6, instability <0.0001). The PERMANOVA results in conjunction with NMS, showed a lack of seasonal variation amongst phytoplankton genera in the 2018 season (Figures 2.4 and 2.5). In 2018, there were no significant differences ($p<0.05$) among months from June to October in phytoplankton assemblages. The 2019 season contrasted starkly with the 2018 season. Phytoplankton assemblage in 2019 showed strong seasonal variation (Figures 2.6 and 2.7). Almost all months from June to October were significantly different from each other (at $p<0.05$), with September as an exception, being not significantly different from August or October.

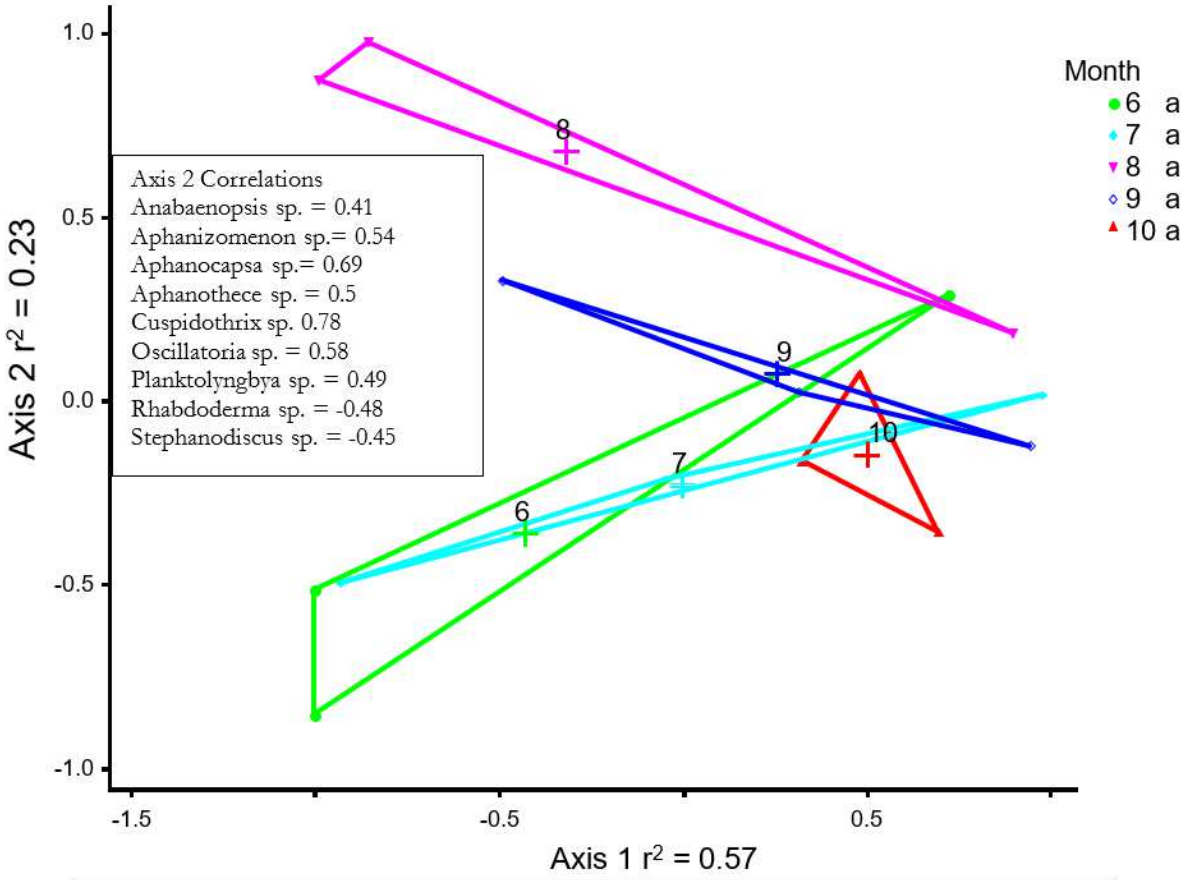

Axis1 Correlations		
Cuspidothrix sp. = -0.51	Actinastrum hantzschii = 0.63	Coelastrum sp.= 0.44
Cyclotella sp.= 0.52	Euglena sp.= 0.65	Gonium pectoral = 0.43
Monoraphidium sp.= 0.52	Peridinium sp. = 0.61	Phacus sp. = 0.42
Planktosphaeria spp. = 0.48	Planktothrix sp.= 0.8	Rhodomonas sp. = 0.45
Scenedesmus sp. = 0.62	Selenastrum sp. = 0.5	Tetraedron sp. = .0.5

Figure 2.4. NMS ordination of Axis 1 and 2 for 2018 algae samples, with convex hull polygon of the different months. Legend items followed by different letters are significantly different ($p<0.05$). The coefficient of determination between ordination distances and distances in the original n-dimensional space is shown in the axis label. Correlations between species abundance and the axis scores are shown in the boxes.

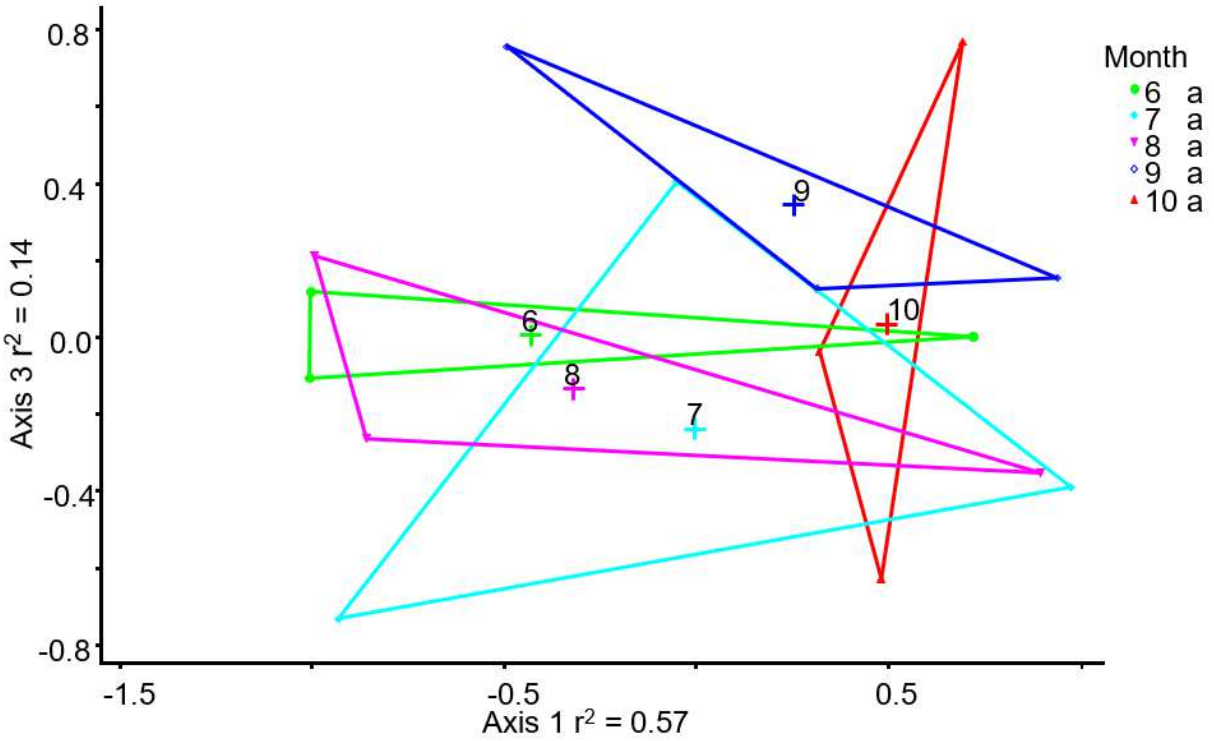

Axis1 Correlations		
Cuspidothrix sp. = -0.51	Actinastrum hantzschii = 0.63	Coelastrum sp.= 0.44
Cyclotella sp.= 0.52	Euglena sp.= 0.65	Gonium pectoral = 0.43
Monoraphidium sp.= 0.52	Peridinium sp. = 0.61	Phacus sp. = 0.42
Planktosphaeria spp. = 0.48	Planktothrix sp.= 0.8	Rhodomonas sp. = 0.45
Scenedesmus sp. = 0.62	Selenastrum sp. = 0.5	Tetraedron sp. = .0.5

Figure 2.5. NMS ordination of Axis 1 and 3 for 2018 algae samples, with convex hull polygon of the different months. Legend items followed by different letters are significantly different ($p<0.05$). The coefficient of determination between ordination distances and distances in the original n-dimensional space shown in the axis label. Correlations between species abundance and the axis scores are shown in the boxes (Axis 3 correlations are not shown because the low coefficient of determination for Axis 3).

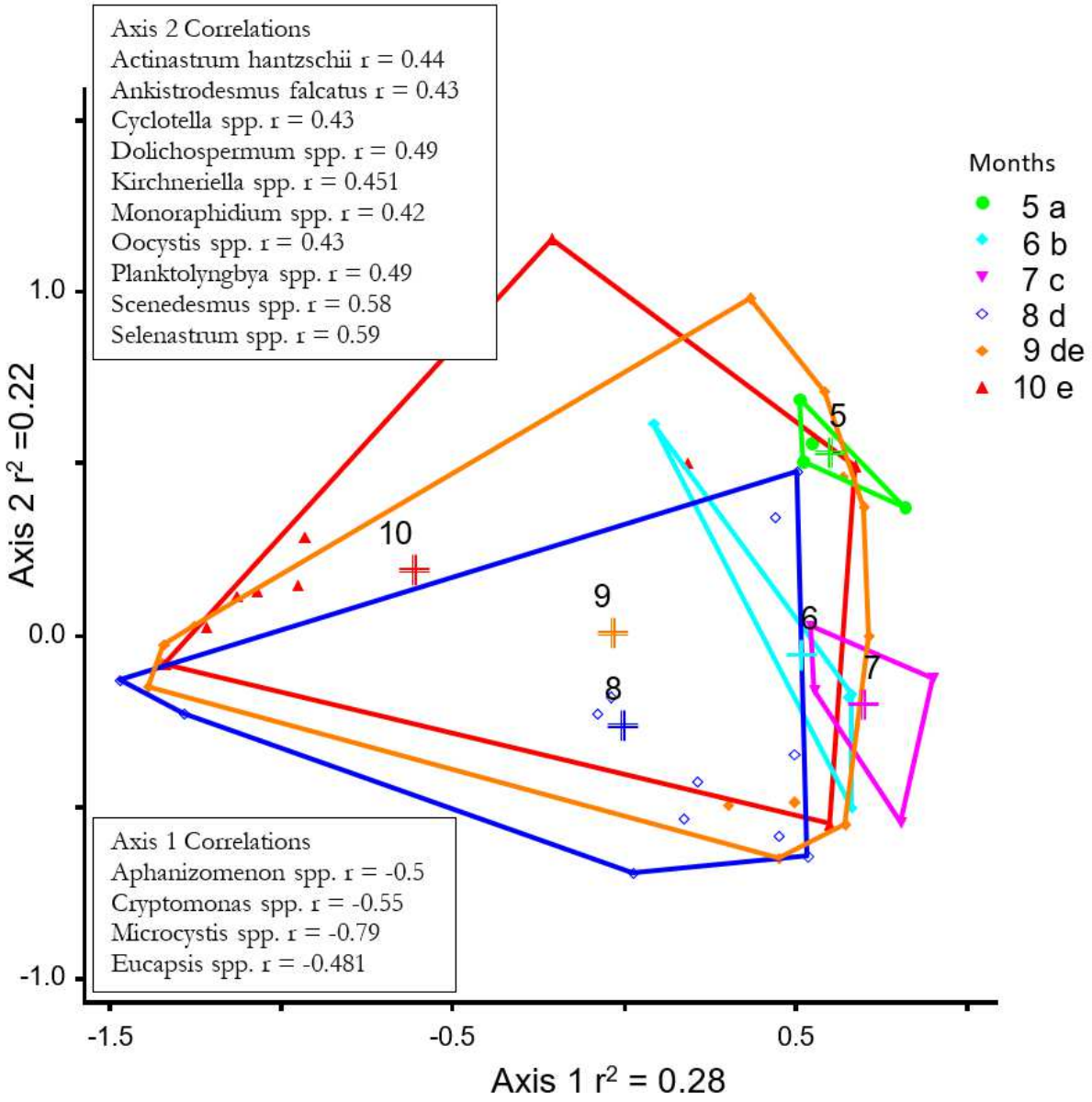

Figure 2.6. NMS ordination showing Axis 1 and 2 for 2019 algae samples with convex hull polygon of the different months. Legend items followed by different letters are significantly different at the $p<0.05$. The coefficient of determination between ordination distances and distances in the original n-dimensional space shown in the axis label. Correlations between species abundance and the axis scores are shown in the boxes.

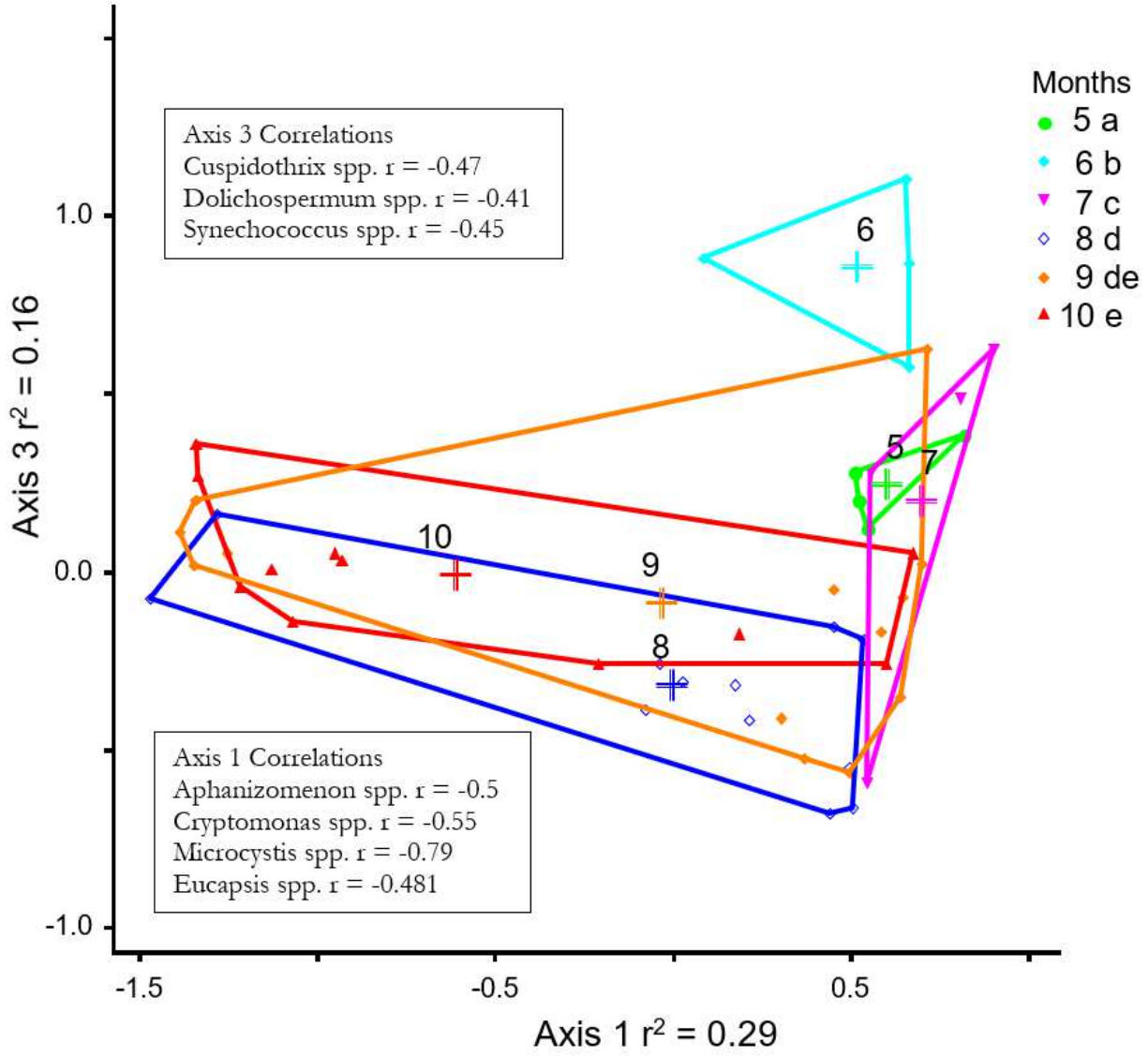

Figure 2.7. NMS ordination showing Axis 1 and 3 for 2019 algae samples with convex hull polygon of the different months. Legend items followed by different letters are significantly different at the $p<0.05$. The coefficient of determination between ordination distances and distances in the original n-dimensional space shown in the axis label. Correlations between species abundance and the axis scores are shown in the boxes.

Nonmetric Multi-Dimensional Scaling was also used to evaluate phytoplankton assemblages across sites at the genus level for both 2018 and 2019. Unlike seasonal variation, spatial variation was consistent across years. In 2018, only sites one, four, and five were sampled and sites one and four were not significantly different. Site five was significantly different from sites one and four (Figures 2.8 and 2.9). This trend continued in 2019 where sites one through four were not significantly

different from each other and site five was significantly different from sites one through four (Figures 2.10 and 2.11).

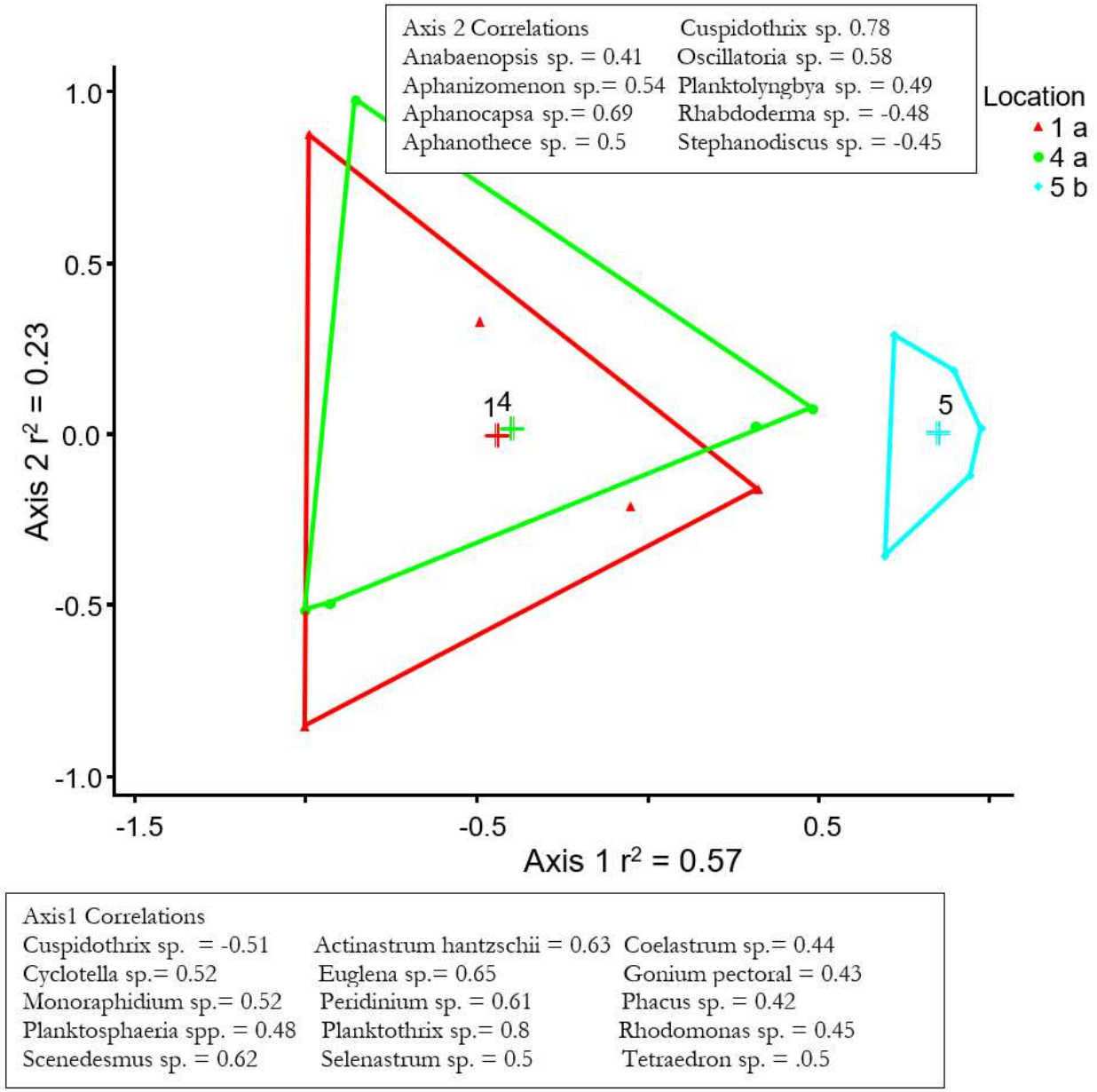

Figure 2.8. NMS ordination showing Axis 1 and 2 for 2018 algae samples with convex hull polygon of the different locations. Legend items followed by different letters are significantly different at the $p<0.05$. The coefficient of determination between ordination distances and distances in the original n-dimensional space shown in the axis label. Correlations between species abundance and the axis scores are shown in the boxes.

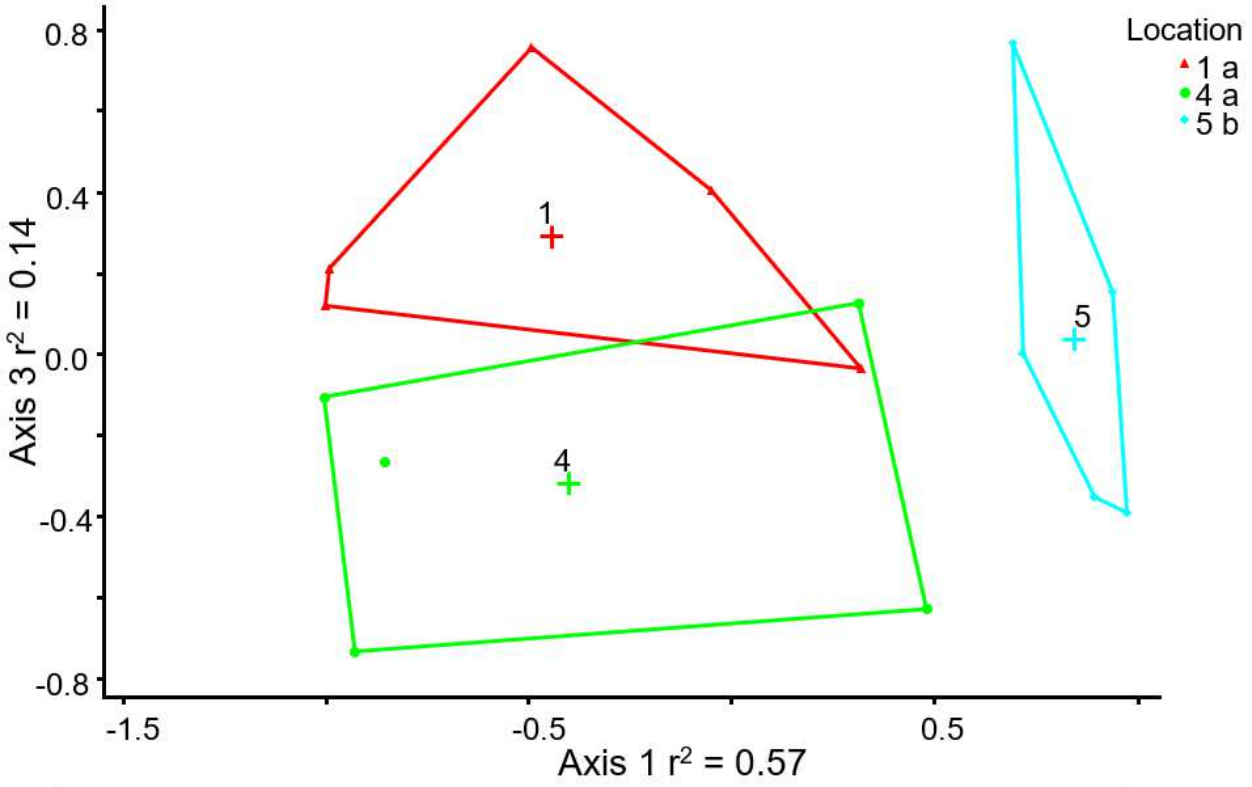

Axis1 Correlations		
Cuspidothrix sp. = -0.51	Actinastrum hantzschii = 0.63	Coelastrum sp.= 0.44
Cyclotella sp.= 0.52	Euglena sp.= 0.65	Gonium pectoral = 0.43
Monoraphidium sp.= 0.52	Peridinium sp. = 0.61	Phacus sp. = 0.42
Planktosphaeria spp. = 0.48	Planktothrix sp.= 0.8	Rhodomonas sp. = 0.45
Scenedesmus sp. = 0.62	Selenastrum sp. = 0.5	Tetraedron sp. = .0.5

Figure 2.9. NMS ordination showing Axis 1 and 3 for 2018 algae samples with convex hull polygon of the different locations. Legend items followed by different letters are significantly different at the $p<0.05$. The coefficient of determination between ordination distances and distances in the original n-dimensional space shown in the axis label. Correlations between species abundance and the axis scores are shown in the boxes (Axis 3 correlations are not shown because the low coefficient of determination for Axis 3).

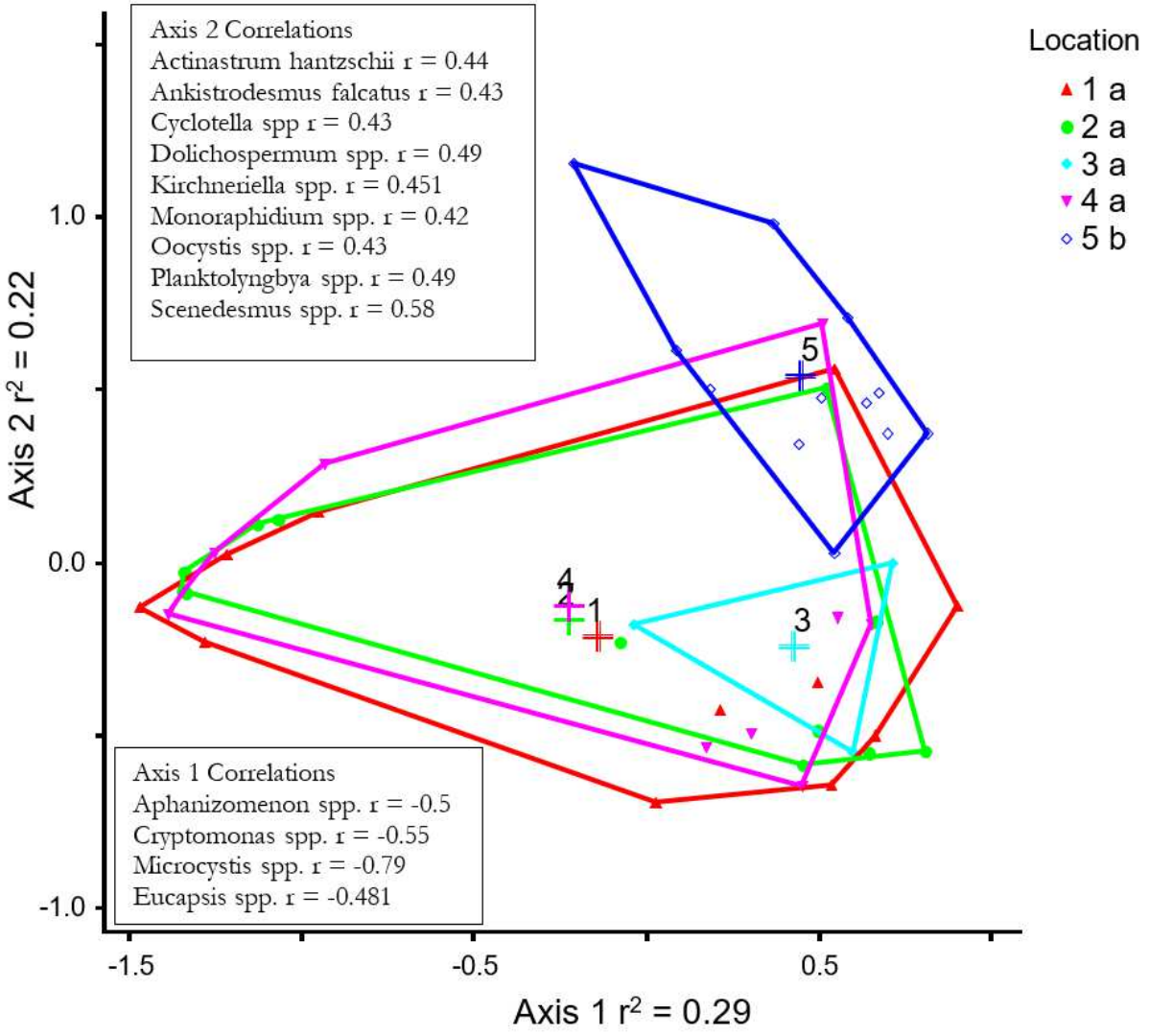

Figure 2.10. NMS ordination showing Axis 1 and 2 for 2019 algae samples with convex hull polygon of the different locations. Legend items followed by different letters are significantly different at the $p<0.05$. The coefficient of determination between ordination distances and distances in the original n-dimensional space shown in the axis label. Correlations between species abundance and the axis scores are shown in the boxes.

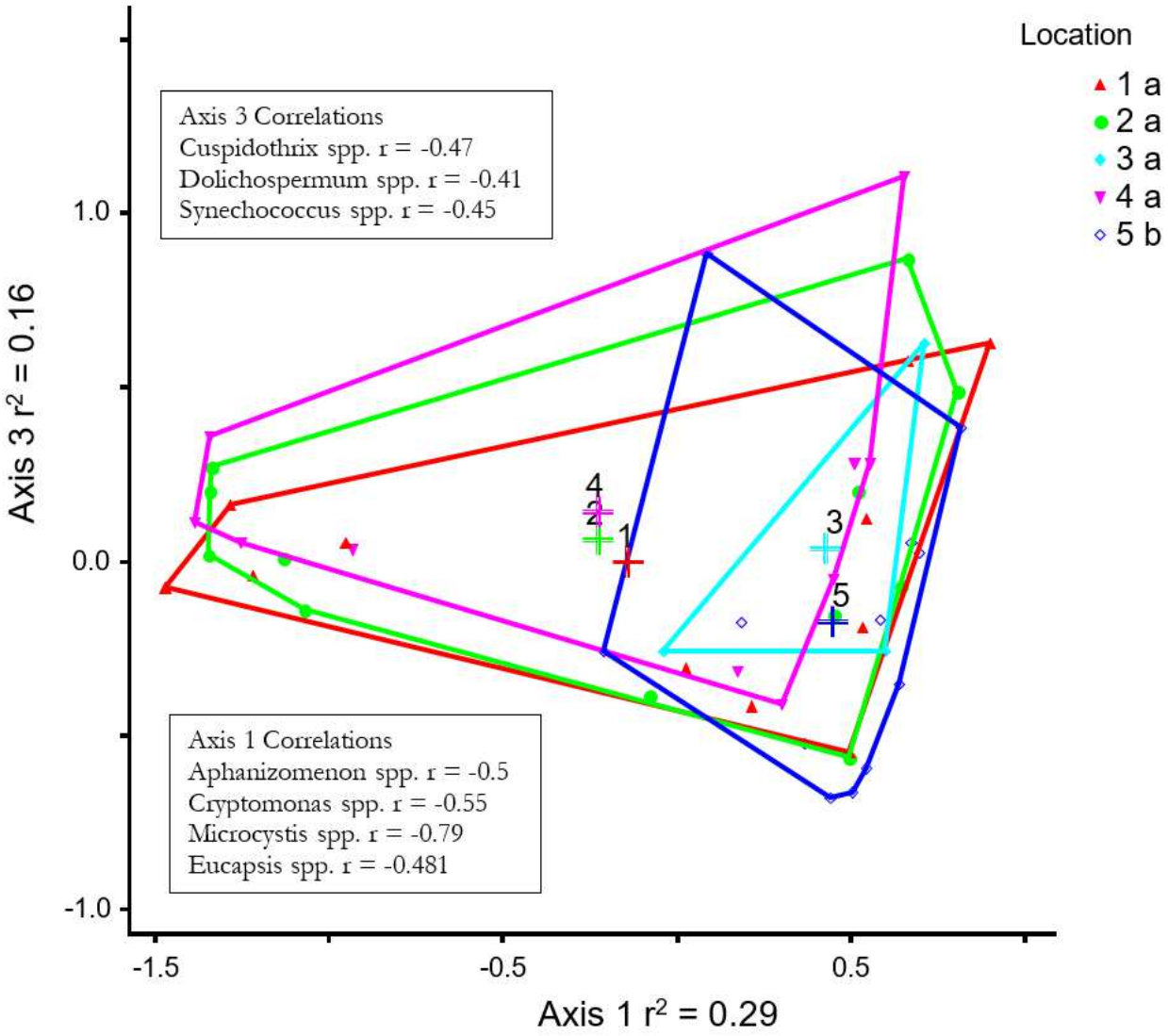

Figure 2.11. NMS ordination showing Axis 1 and 3 for 2019 algae samples with convex hull polygon of the different locations. Legend items followed by different letters are significantly different at the $p<0.05$. The coefficient of determination between ordination distances and distances in the original n-dimensional space shown in the axis label. Correlations between species abundance and the axis scores are shown in the boxes.

Phytoplankton biovolume on DLNWR in 2018 was almost entirely dominated by cyanobacteria throughout the season, contributing to as much as 99.9% of total BV in the mid to late summer when blooms were at their peak (Figure 2.12). The 2019 season showed more diversity, but was also dominated by cyanobacteria throughout most of the season. In both years, the greatest amount of diversity was in the early and later parts of the season. Chlorophyta (green algae) and

Bacillariophyta (diatoms) showed their greatest BV in the early spring, then again in the fall (Figure 2.13). Cryptophyta were present in both years, but were rarely a significant portion of the total BV. Euglenophyta and Pyrrophyta were also observed sporadically at low BV.

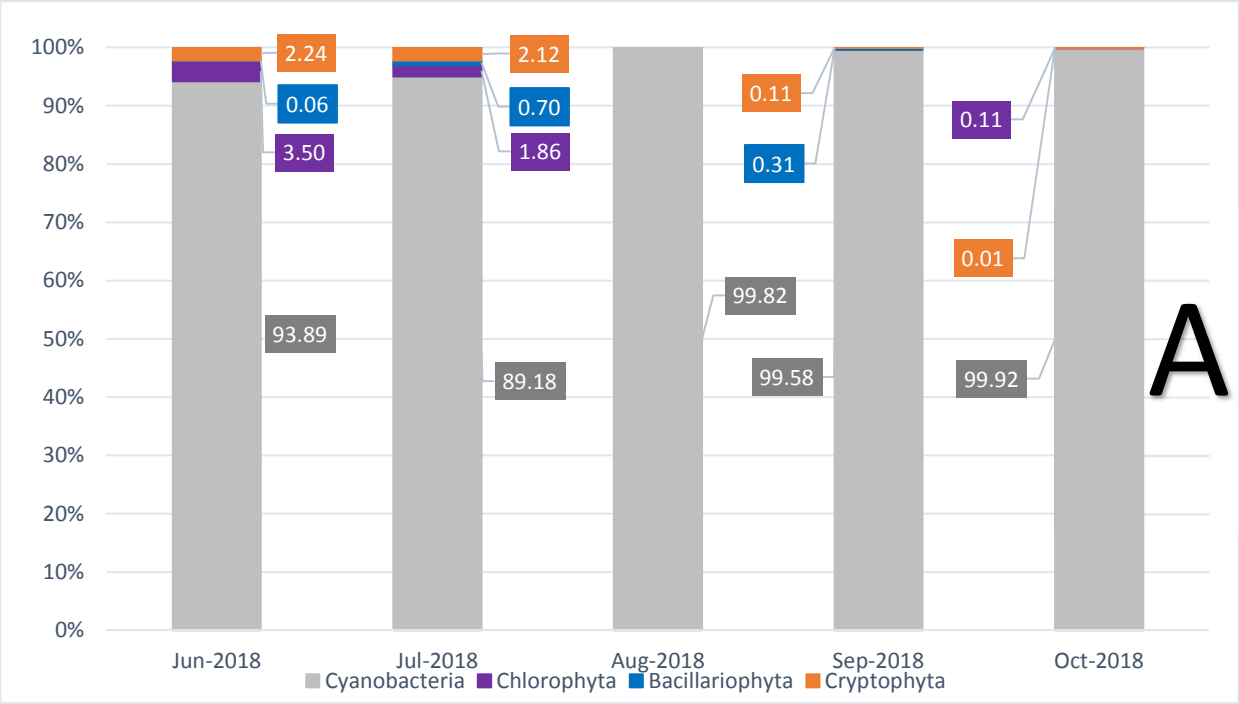

Figure 2.12. Phytoplankton identification from 2018, A represents Site 1, B Site 4, and C Site 5. Biovolume is expressed as a percentage of total biovolume for each group of phytoplankton, Euglenophyta and Pyrrophyta data excluded.

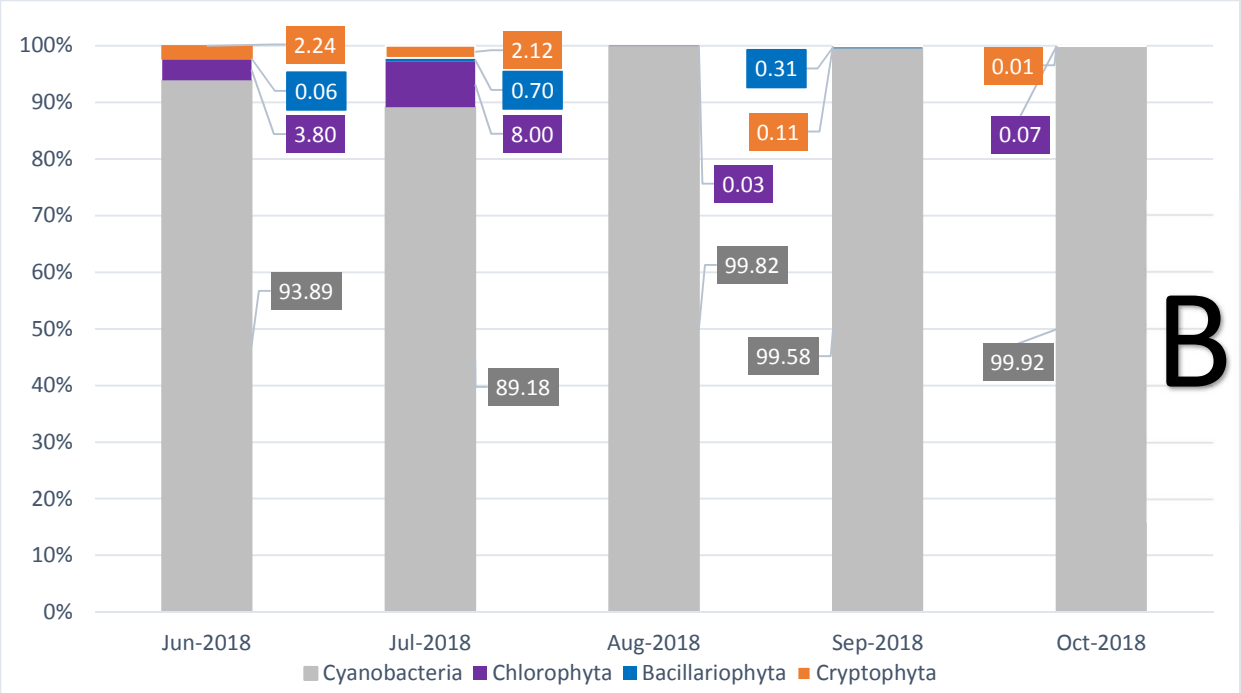

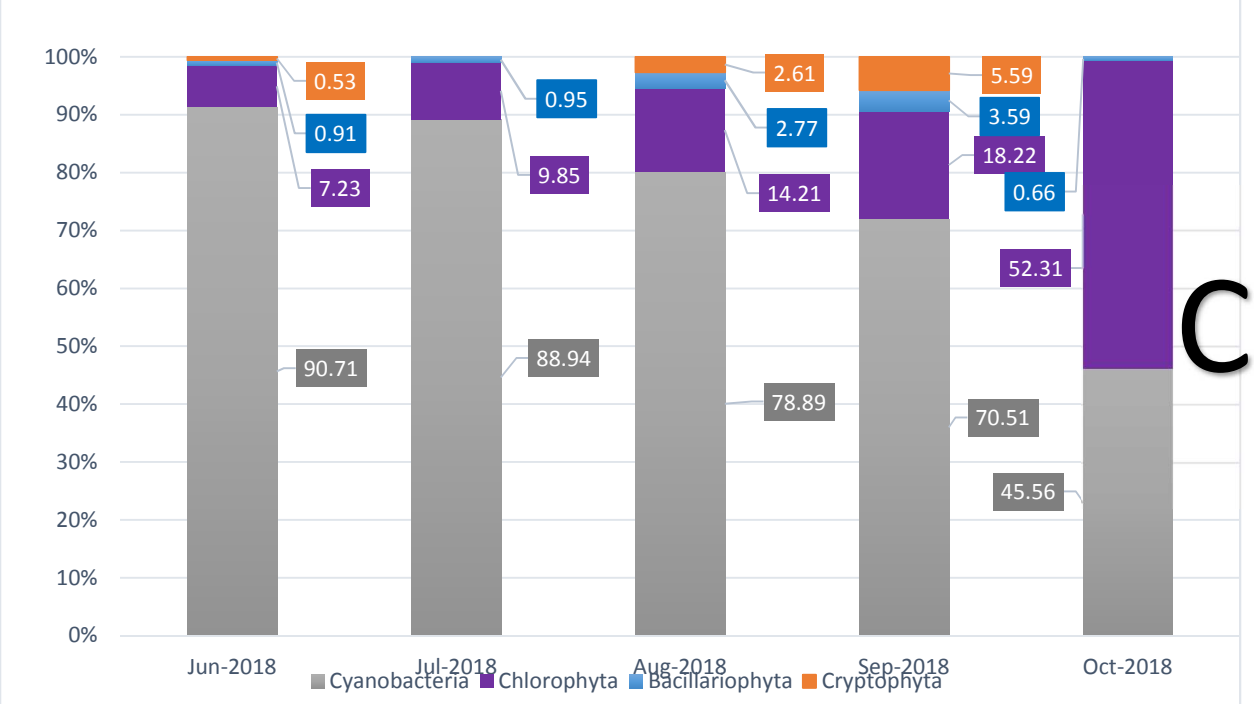

Figure 2.12. Phytoplankton identification from 2018, A represents Site 1, B Site 4, and C Site 5 (Continued). Biovolume is expressed as a percentage of total biovolume for each group of phytoplankton, Euglenophyta and Pyrrophyta data excluded.

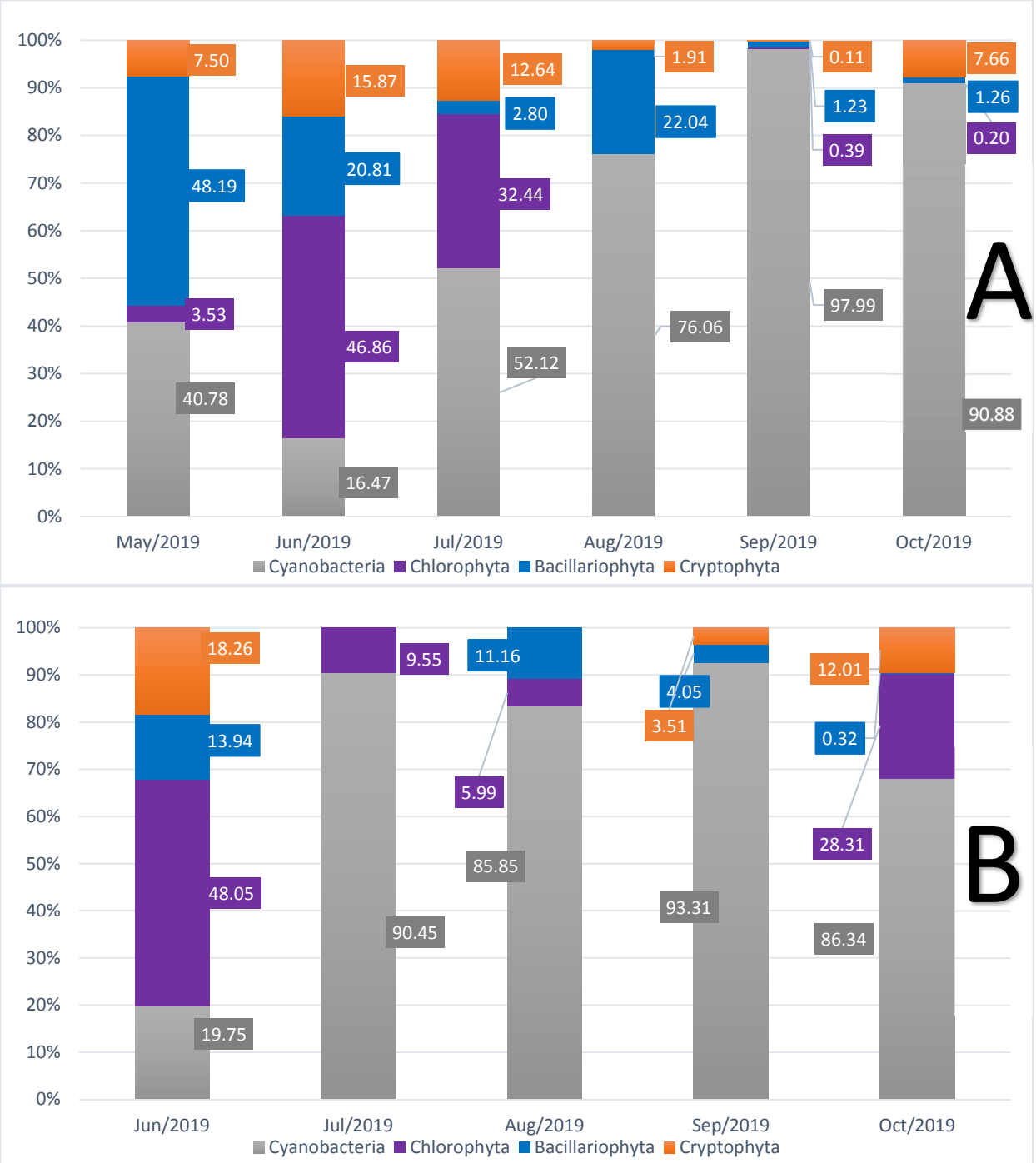

Figure 2.13. Phytoplankton identification from 2019, A represents Site 1, B Site 2, C Site 3, D Site 4, and E Site 5. Biovolume expressed as a percentage of total biovolume for each group of phytoplankton, Euglenophyta and Pyrrophyta data excluded.

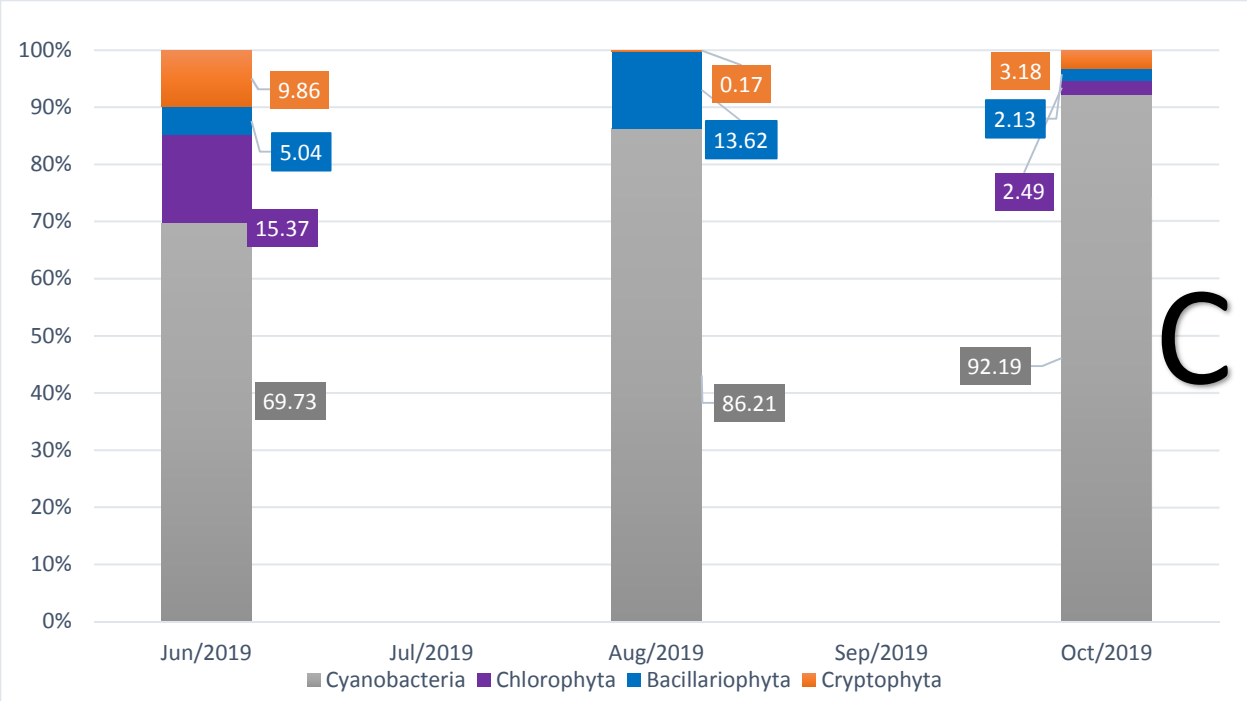

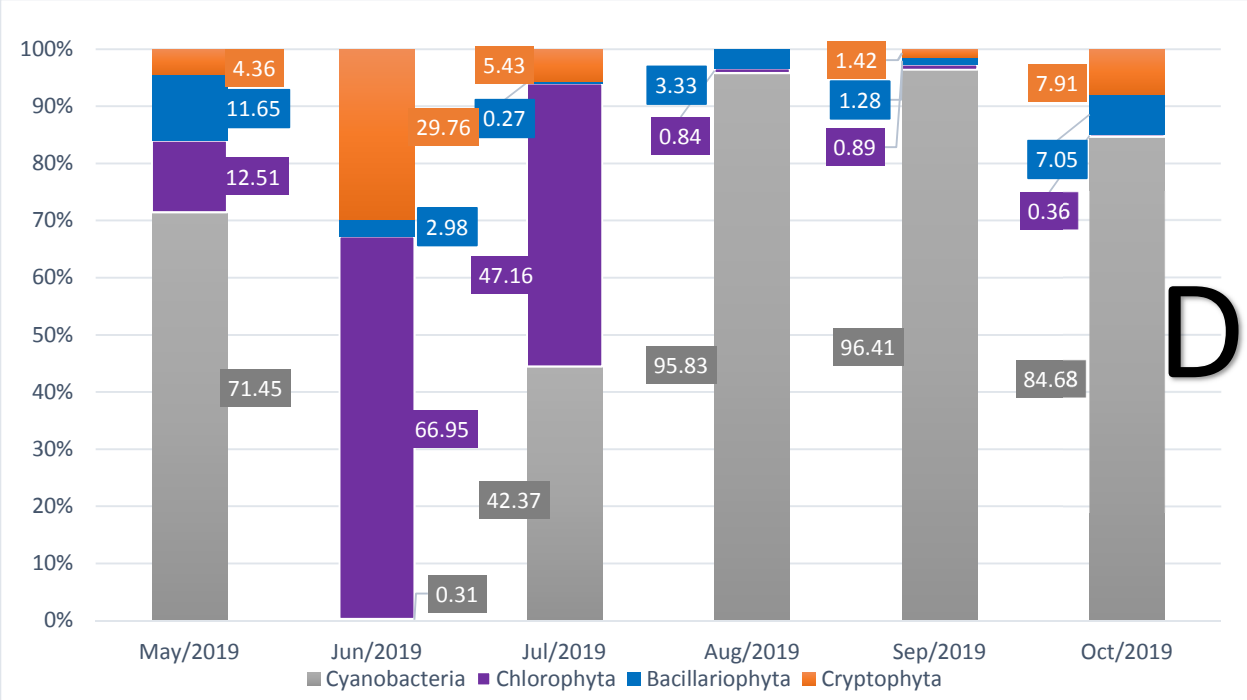

Figure 2.13. Phytoplankton identification from 2019, A represents Site 1, B Site 2, C Site 3, D Site 4, and E Site 5 (Continued). Biovolume expressed as a percentage of total biovolume for each group of phytoplankton, Euglenophyta and Pyrrophyta data excluded.

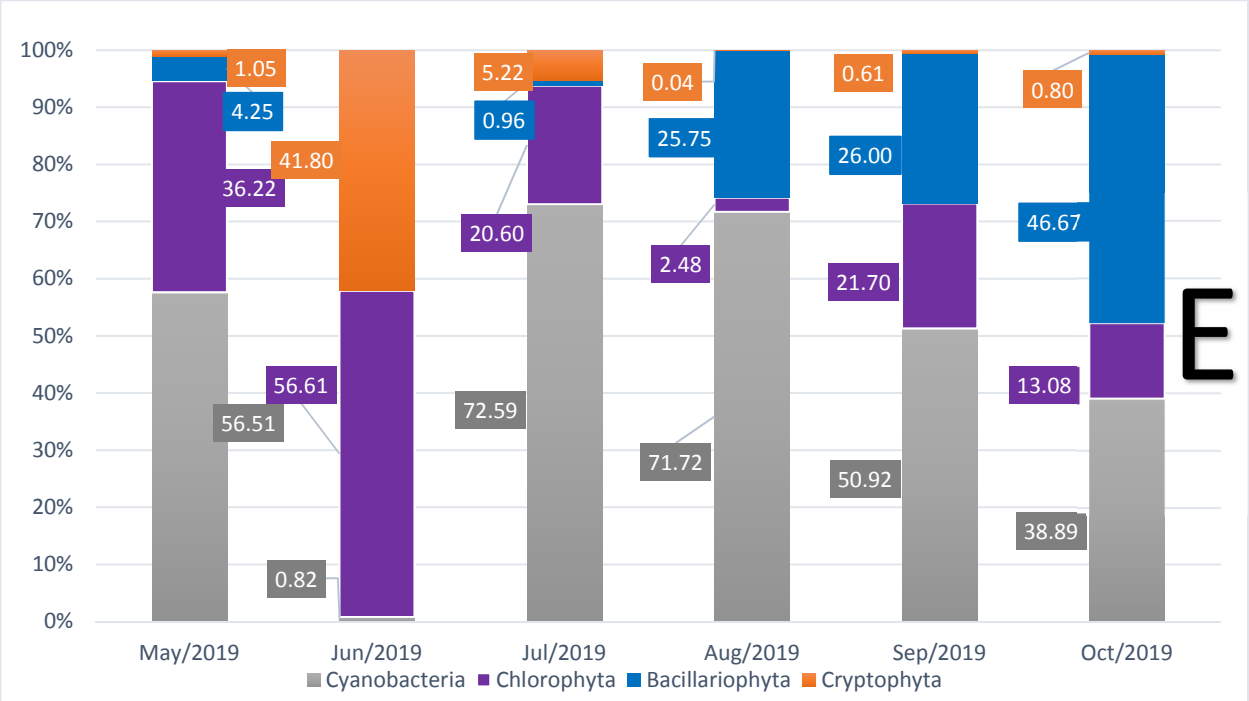

Figure 2.13. Phytoplankton identification from 2019, A represents Site 1, B Site 2, C Site 3, D Site 4, and E Site 5 (Continued). Biovolume expressed as a percentage of total biovolume for each group of phytoplankton, Euglenophyta and Pyrrophyta data excluded.

The graphic representation of biovolume samples in 2018 further exemplify what the NMS data indicated, with cyanobacteria assemblages dominating over other phytoplankton throughout the entire season. The 2019 season was a stark contrast to the 2018 season with greater seasonal variation and multiple sites showing relatively low cyanobacteria BV during periods of the season. Site one showed a transition from diatoms to green algae before being dwarfed by cyanobacteria BV. Sites two and four never supported a strong diatom community, while site five showed a large diversity with cyanobacterial never completely overshadowing other groups of phytoplankton. Only three samples were collected at site three. However, samples were collected at the start, middle and end of the season. Cyanobacteria were the dominate phylum in all three samples collected at site three.

Correlation matrices were created to identify factors driving and or limiting HCBs on DLNWR. We used CHY-*a* and BV as an indicator of phytoplankton abundance. CHY-*a* and BV

were then correlated with nutrients P, N, TP, TN and ammonia, as well as with environmental factors including water temperature and growing degree days (including 5, 10, 20, and 30-day running averages). Amongst these variables, we were unable to consistently draw any significant correlations between CHY-*a* or BV with any nutrients or environmental factors.

Strong correlations were observed sporadically, but were not observed consistently across sites or years. An example of this would be the correlation between growing degree days (GDD) values calculated from water temperatures (Table 2.5). Cumulative 30-day averages of water temperature calculated GDD resulted in moderately to strongly positive GDD values in 2019. The 2018 GDD values on the other hand, tended to be weak and/or negatively correlated with site five being the exception, showing moderate positive correlations in 2019 and strongly positive correlations in 2018.

Table 2.5. Correlation index showing correlations between growing degree days and chlorophyll-*a*. GDD is calculated from lake water temperatures that were measured by a HOBO data logger. Values include the daily value, as well as 5, 10, 20, and 30-day running averages.

Site 1												
	2019						2018					
	(1)	*(2)*	*(3)*	*(4)*	*(5)*	*(6)*	*(1)*	*(2)*	*(3)*	*(4)*	*(5)*	*(6)*
(1) GDD@0C	1.00						1.00					
(2) GDD 5-Day	1.00	1.00					1.00	1.00				
(3) GDD 10-Day	0.95	0.95	1.00				0.93	0.93	1.00			
(4) GDD 20-Day	0.96	0.96	0.96	1.00			0.92	0.92	0.97	1.00		
(5) GDD 30-Day	0.95	0.95	0.98	0.99	1.00		0.93	0.93	0.98	0.97	1.00	
(6) Chlorophyll	0.14	0.16	0.13	0.40	0.67	1.00	-0.47	-0.47	-0.49	-0.50	-0.42	1.00
Site 2												
	2019						2018					
	(1)	*(2)*	*(3)*	*(4)*	*(5)*	*(6)*	*(1)*	*(2)*	*(3)*	*(4)*	*(5)*	*(6)*
(1) GDD@0C	1.00						1.00					
(2) GDD 5-Day	0.76	1.00					1.00	1.00				
(3) GDD 10-Day	0.98	0.77	1.00				1.00	1.00	1.00			
(4) GDD 20-Day	0.87	0.60	0.90	1.00			0.99	0.99	1.00	1.00		
(5) GDD 30-Day	0.79	0.45	0.82	0.99	1.00		0.99	0.99	0.99	1.00	1.00	
(6) Chlorophyll	0.15	-0.31	0.23	0.40	0.68	1.00	-0.36	-0.36	-0.30	-0.22	0.00	1.00

Table 2.5. Correlation index showing correlations between growing degree days and chlorophyll-*a* (Continued). GDD is calculated from lake water temperatures that were measured by a HOBO data logger. Values include the daily value, as well as 5, 10, 20, and 30-day running averages.

Site 3												
	2019						2018					
	(1)	*(2)*	*(3)*	*(4)*	*(5)*	*(6)*	*(1)*	*(2)*	*(3)*	*(4)*	*(5)*	*(6)*
(1) GDD@0C	1.00						1.00					
(2) GDD 5-Day	1.00	1.00					1.00	1.00				
(3) GDD 10-Day	0.96	0.96	1.00				0.99	0.99	1.00			
(4) GDD 20-Day	0.94	0.94	0.99	1.00			0.99	0.99	1.00	1.00		
(5) GDD 30-Day	0.91	0.91	0.99	1.00	1.00		0.99	0.99	0.99	1.00	1.00	
(6) Chlorophyll	0.14	0.20	0.43	0.54	0.79	1.00	-0.34	-0.27	-0.23	-0.17	0.06	1.00
Site 4												
	2019						2018					
	(1)	*(2)*	*(3)*	*(4)*	*(5)*	*(6)*	*(1)*	*(2)*	*(3)*	*(4)*	*(5)*	*(6)*
(1) GDD@0C	1.00						1.00					
(2) GDD 5-Day	1.00	1.00					0.93	1.00				
(3) GDD 10-Day	0.97	0.97	1.00				0.99	0.94	1.00			
(4) GDD 20-Day	0.95	0.95	0.99	1.00			0.99	0.94	0.99	1.00		
(5) GDD 30-Day	0.94	0.94	0.99	0.99	1.00		0.98	0.95	0.99	1.00	1.00	
(6) Chlorophyll	0.23	0.27	0.46	0.62	0.91	1.00	-0.06	-0.20	0.08	0.23	0.41	1.00
Site 5												
	2019						2018					
	(1)	*(2)*	*(3)*	*(4)*	*(5)*	*(6)*	*(1)*	*(2)*	*(3)*	*(4)*	*(5)*	*(6)*
(1) GDD@0C	1.00						1.00					
(2) GDD 5-Day	1.00	1.00					1.00	1.00				
(3) GDD 10-Day	0.96	0.96	1.00				0.98	0.98	1.00			
(4) GDD 20-Day	0.94	0.94	0.99	1.00			0.96	0.96	0.99	1.00		
(5) GDD 30-Day	0.92	0.92	0.97	0.99	1.00		0.92	0.92	0.96	0.98	1.00	
(6) Chlorophyll	-0.18	-0.14	0.03	0.15	0.45	1.00	0.04	0.10	0.15	0.29	0.81	1.00

Correlation values calculated for nutrients in 2019 (Table 2.6) showed a wide array of values between sites. Cryptophyta BV percent showed a strikingly high correlation with TN values at site one, but had little to no correlation at other sites. Cyanobacteria had a moderate to strong correlation with CHY-*a* values at sites one, two, and four, but no correlation at site five. Cyanobacteria also had a weakly to moderately negative correlation to TP at sites one and four, but

had a moderately strong positive correlation at site five. Not all correlation matrices are shown, but no consistent patterns were observed across any calculated correlations.

Table 2.6. Correlation index for 2019 showing correlations for chlorophyll and phytoplankton biovolume (BV) with microcyctin, dissolved phosphorus (Diss P), dissolved nitrogen (Diss N), total phosphorus (TP), total nitrogen (TN), the trophic state values for chlorophyll-*a* (TSI-CHY-*a*), total phosphorus (TSI-TP) and secchi depth (TSI-SD).

2019 Nutrient Correlations													
2019 Site 1	*(1)*	*(2)*	*(3)*	*(4)*	*(5)*	*(6)*	*(7)*	*(8)*	*(9)*	*(10)*	*(11)*	*(12)*	*(13)*
(1) Microcystin	1.00												
(2) Diss P	-0.14	1.00											
(3) Diss_N	-0.37	0.90	1.00										
(4) TP	-0.17	0.98	0.87	1.00									
(5) TN	-0.39	0.81	0.90	0.83	1.00								
(6) TSI-CHY-*a*	0.82	-0.62	-0.81	-0.61	-0.83	1.00							
(7) TSI-TP	-0.37	0.94	0.81	0.96	0.53	-0.51	1.00						
(8) TSI-SD	-0.42	0.17	0.24	0.23	0.24	-0.08	0.32	1.00					
(9) CHY-*a*	0.84	-0.15	-0.41	-0.13	-0.38	0.96	-0.42	-0.08	1.00				
(10) Bacillariophyta BV %	-0.64	-0.08	-0.11	-0.05	-0.09	-0.29	0.04	0.35	-0.43	1.00			
(11) Chlorophyta BV %	-0.63	0.62	0.76	0.65	0.75	-0.57	0.71	0.75	-0.54	0.16	1.00		
(12) Cryptophyta BV %	-0.86	0.42	0.74	0.43	0.91	-0.89	0.39	0.33	-0.85	0.25	0.71	1.00	
(13) Cyanobacteria BV %	0.89	-0.41	-0.54	-0.44	-0.59	0.68	-0.51	-0.69	0.73	-0.68	-0.82	-0.77	1.00
2019 Site 2	*(1)*	*(2)*	*(3)*	*(4)*	*(5)*	*(6)*	*(7)*	*(8)*	*(9)*	*(10)*	*(11)*	*(12)*	*(13)*
(1) Microcystin	1.00												
(2) Diss_P	-0.13	1.00											
(3) Diss_N	-0.48	0.77	1.00										
(4) TP	-0.06	0.96	0.71	1.00									
(5) TN	-0.38	0.78	0.95	0.78	1.00								
(6) TSI-CHY-*a*	0.91	-0.15	-0.57	0.07	-0.30	1.00							
(7) TSI-TP	0.15	0.93	0.46	0.97	0.60	0.10	1.00						
(8) TSI-SD	0.79	-0.51	-0.67	-0.29	-0.42	0.88	-0.28	1.00					
(9) CHY-*a*	0.78	-0.09	-0.44	0.05	-0.31	0.96	0.21	0.85	1.00				
(10) Bacillariophyta BV %	0.35	0.26	-0.24	0.43	0.01	0.44	0.45	0.26	0.49	1.00			
(11) Chlorophyta BV %	-0.60	0.78	0.70	0.55	0.50	-0.64	0.53	-0.85	-0.62	-0.14	1.00		
(12) Cryptophyta BV %	-0.54	-0.40	0.14	-0.43	0.08	-0.60	-0.50	-0.24	-0.47	-0.24	-0.13	1.00	
(13) Cyanobacteria BV %	0.54	-0.06	-0.26	-0.04	-0.28	0.57	0.02	0.40	0.41	-0.30	-0.17	-0.78	1.00

Table 2.6. Correlation index for 2019 showing correlations for chlorophyll and phytoplankton biovolume (BV) with microcyctin, dissolved phosphorus (Diss P), dissolved nitrogen (Diss N), total phosphorus (TP), total nitrogen (TN), the trophic state values for chlorophyll-*a* (TSI-CHY-*a*), total phosphorus (TSI-TP) and secchi depth (TSI-SD) (Continued).

2019 Site 4	*(1)*	*(2)*	*(3)*	*(4)*	*(5)*	*(6)*	*(7)*	*(8)*	*(9)*	*(10)*	*(11)*	*(12)*	*(13)*
(1) Microcystin	1.00												
(2) Diss_P	-0.15	1.00											
(3) Diss_N	-0.43	0.89	1.00										
(4) TP	-0.12	0.98	0.87	1.00									
(5) TN	-0.41	0.88	0.98	0.86	1.00								
(6) TSI-CHY-*a*	0.74	-0.04	-0.41	0.02	-0.40	1.00							
(7) TSI-TP	0.16	0.91	0.62	0.93	0.63	0.20	1.00						
(8) TSI-SD	0.22	-0.37	-0.63	-0.31	-0.57	0.46	-0.04	1.00					
(9) CHY-*a*	0.82	-0.11	-0.46	-0.08	-0.44	0.95	0.26	0.40	1.00				
(10) Bacillariophyta BV %	-0.31	-0.31	-0.18	-0.32	-0.15	-0.50	-0.42	0.19	-0.41	1.00			
(11) Chlorophyta BV %	-0.52	0.61	0.72	0.57	0.72	-0.63	0.54	-0.31	-0.59	-0.11	1.00		
(12) Cryptophyta BV %	-0.52	0.14	0.32	0.07	0.30	-0.84	0.03	-0.30	-0.71	0.27	0.77	1.00	
(13) Cyanobacteria BV %	0.59	-0.48	-0.63	-0.43	-0.64	0.79	-0.37	0.31	0.71	-0.14	-0.96	-0.89	1.00
2019 Site 5	*(1)*	*(2)*	*(3)*	*(4)*	*(5)*	*(6)*	*(7)*	*(8)*	*(9)*	*(10)*	*(11)*	*(12)*	*(13)*
(1) Microcystin	1.00												
(2) Diss_P	-0.16	1.00											
(3) Diss_N	-0.28	-0.09	1.00										
(4) TP	-0.13	0.99	-0.07	1.00									
(5) TN	-0.10	-0.01	0.66	-0.02	1.00								
(6) TSI-CHY-*a*	0.60	-0.23	-0.20	-0.17	0.02	1.00							
(7) TSI-TP	-0.04	0.93	-0.10	0.96	0.03	0.02	1.00						
(8) TSI-SD	0.33	-0.77	-0.10	-0.73	-0.08	0.64	-0.58	1.00					
(9) CHY-*a*	0.70	-0.37	-0.20	-0.31	0.10	0.97	-0.03	0.63	1.00				
(10) Bacillariophyta BV %	0.26	-0.64	0.10	-0.66	0.02	-0.18	-0.72	0.31	-0.03	1.00			
(11) Chlorophyta BV %	-0.07	0.08	0.08	0.00	0.41	0.14	-0.01	-0.17	0.09	-0.37	1.00		
(12) Cryptophyta BV %	-0.15	0.79	-0.22	0.72	-0.09	-0.35	0.59	-0.83	-0.37	-0.53	0.48	1.00	
(13) Cyanobacteria BV %	-0.24	0.57	-0.12	0.64	-0.24	0.13	0.73	-0.17	0.00	-0.82	-0.22	0.20	1.00

2.5. Discussion

In our findings, the levels of P and N did not drastically deviate from a previous study on DLNWR by the Wax (2006), suggesting that the surplus of nutrients in DLNWR is not a recent phenomenon. Likely, the high levels of algal productivity seen on DLNWR are not recent either. One contrasting point between the findings in 1997 and 1998 to the current study, is the community

composition of the sampled phytoplankton. Phytoplankton sampling was done on August 12, and September 7th in 1997. In their sampling, they found that the volume of diatoms disproportionally overshadowed cyanobacteria (the second largest group) by a factor of 5.6:1 and 13.4:1 on August 12 and September 7th, respectively. This contrasts starkly with our findings, which showed cyanobacteria as nearly the exclusive group of phytoplankton throughout the 2018 season and most of 2019. This suggests that cyanobacterial growth has increased drastically on DLNWR between the 1997 to 1998 sampling and our recent sampling and is likely linked to condition changes other than nutrient abundance.

Seasonal temperature changes are expected to result in a transition within phytoplankton communities that begin with diatoms at cooler temperatures, then shift to green algae, and eventually cyanobacteria, which become the most dominant at the highest temperatures (Reynolds, 1997; Yang et al., 2017). Neither the 2018 nor the 2019 seasons showed a clear transition among phytoplankton between diatoms, green algae, and cyanobacteria. The NMS results showed, that in 2019, there was a significant difference in assemblage of phytoplankton throughout the season (Figures 2.6 and 2.7). Some of the differences in assemblage in 2019 can be explained by variations within the cyanobacteria group itself which also varied throughout the season. There were no significant changes in assemblage in 2018. The lack of significance may be attributed to a lack of diversity in assemblage as well as the 2018 season including one fewer test site and fewer samples taken during the season.

The lack of seasonal transition among phytoplankton groups may partially be attributed to the high concentrations of nutrients available throughout the year. Cyanobacteria are poor competitors for N and P in nutrient replete lakes, but dominate community structures under eutrophic conditions (Graham et al., 2004). The conditions in DLNWR were consistently eutrophic to hyper eutrophic throughout the entirety of each season creating prime conditions for

cyanobacteria to flourish. The shallow nature and north to south orientation of DLNWR make it more susceptible to heavy mixing by northerly and southerly winds, which in turn increases the likelihood of release of P from the sediment during these periods. Suspension of sediment particles into the water column increases the surface area available for P exchange; with smaller particles being more likely to be resuspended due to wave action and reside in the water column for longer periods of time (Wang & Li, 2010). Søndergaard, Jensen, and Jeppesen (2003) even found that the P pool in the sediment can be 100 times higher than the pool of nutrients present in lake water.

Sediments can play a large role in promoting or potentially inhibiting bloom formation by either sequestering or releasing P and other nutrients into the water column (Zhu et al., 2012). The degradation of blooms can also impact this sediment-water column relationship. Zhu et al. (2012) demonstrated this in a study of Lake Taihu, China. They observed that decaying blooms could effectively remove nutrients from the sediment by creating areas of hypoxia as the algae decays. These areas of hypoxia facilitate the rapid release of nutrients like ammonia and phosphorous, which then in turn fuel further bloom formation (Zhu et al., 2012).

The sediments on DLNWR are rich in organic matter, presumably from years of cycling phytoplankton blooms and subsequent die offs. Sediment cores taken from DLNWR in 2019 showed that organic carbon constituted between 0.4 and 14.4 percent of soil samples taken from the top 15 cm, with an average of 5.23 percent. The warmer temperatures that coincide with the later summer months not only result in loss of N from a system due to denitrification, but warmer temperatures may also result in a release of N into the water column from the decomposition of organic matter (Wetzel, 2001). Furthermore, cyanobacteria tend to favor biologically reduced forms of N (ammonium) over oxidized forms like nitrite and nitrate (Chaffin & Bridgeman, 2013; Paerl, Gardner, Mccarthy, Peierls, & Wilhelm, 2014; Paerl & Huisman, 2009; Paerl et al., 2015). This infers

that large late summer blooms that occurred on DLNWR may have been fueled by large releases of ammonium from organic matter as temperatures rose.

Another factor that may attribute to the dominance of cyanobacteria in DLNWR, is their ability to migrate within the water column. Some cyanobacteria, like *Microcystis,* can regulate their buoyancy by forming and collapsing intracellular gas vesicles (Walsby, Hayes, Boje, & Stal, 1997). Periods of low wind that allow cyanobacteria to take advantage of their buoyancy control, and elevated optimal growing temperatures, may be a major factor controlling blooms (Huber, Wagner, Gerten, & Adrian, 2011). Sites one through four are regularly protected from mixing by wind due to the 15-40 m valley walls on the east and west sides of the lakes. These help to block the prevailing west winds for large parts of the lake. Site five is more exposed to the prevailing west winds with shallow valley sides and a northwest to southeast orientation. Site five is also considerably shallower, often with depths of no more than 0.5 m resulting in substantial mixing during wind periods. This may in part explain the NMS stark contrast of site five with sites one through four in both seasons.

Large blooms coincide with high rates of photosynthesis and consequently high CO_2 demands (Paerl et al., 2011; Paerl & Ustach, 1982). This can result in pH levels above 9, which can result in free CO_2 representing less than 1% of total dissolved inorganic carbon (Paerl et al., 2011; Paerl & Ustach, 1982). Buoyant cyanobacteria gain a large competitive advantage over phytoplankton lower in the water column as they are better able to directly intercept free CO_2 in the atmosphere (Paerl & Ustach, 1982; Visser et al., 2016). Average pH levels within DLNWR were typically near or above nine, which suggests inorganic dissolved carbon may have been severely limited during large bloom periods, creating an advantageous environment for cyanobacteria able to control their buoyancy.

In addition to being able to compete for CO_2 and sunlight at the surface, vertical migration allows for competition near the nutrient rich sediments. *Microcystis* has a high capacity to take

advantage of this, being able to sequester P both intracellularly and on its external surfaces (Carr & Whitton, 1982; Saxton, Arnold, Bourbonniere, Mckay, & Wilhelm, 2012). Being able to migrate may in part explain why cyanobacteria were disproportionately dominant in 2018. Relative to 2019, the 2018 season was generally P limited creating conditions where the ability to both migrate and store P would be a major advantage. Additionally, site five, which was almost exclusively P limited in 2018 and 2019, showed the greatest phytoplankton diversity in both years compared to sites one through four.

Numerous studies have linked algal blooms to P and or N limitation (Chaffin & Bridgeman, 2013; Dolman et al., 2012; O'Neil et al., 2012; Schindler, 1974; Schindler, 1977; Scott & McCarthy, 2010). Despite this, we were unable to find any strong correlations that linked CHY-*a* or cyanobacterial BV with either P or N. Authors hypothesize that this could be a result of nutrient levels surpassing a critical threshold where nutrients are no longer a significant limiting factor. Once this point is surpassed, nutrient abundance may no longer be as beneficial in predicting the formation of blooms. In a study by Søndergaard et al. (2017), 817 Danish lakes were evaluated for N and P concentrations. They were able to find strong correlations to CHY-*a* between both N and P when concentrations of N and P were relatively low, but were unable to find strong correlations at higher concentrations (Søndergaard et al. 2017). This supports authors hypothesis of a potential critical threshold for cyanobacterial growth, past which nutrients are no longer a significant limiting factor.

We were also unable to link CHY-*a* or BV to any environmental factors in this study. The lack of correlations between other chemical and environmental factors may be attributed to the inherent chaotic behavior of phytoplankton communities. An eight-year experiment monitoring a closed phytoplankton community showed that the large number of interactions within phytoplankton communities make them unpredictable past a 15 to 30-day period (Benincà et al.,

2008). Once fluctuating environmental and chemical factors are added to a system like DLNWR, there is even less predictability without any single limiting factor like P or N. The strong limitations of P and N in most systems likely create a level of predictability in a system, and when those limitations are alleviated, the weaker limiting factors begin to play a stronger role in governing the outcomes of the system. Increasing the number of factors strongly influencing the structure of a system increases the difficulty of predicting future outcomes within the system.

The authors of this study predict that after a critical threshold is surpassed, in terms of nutrient availability, the system is no longer limited significantly enough to be easily predictable. In these systems, it can be assumed that the consistent availability of nutrients will always result in the formation of HCBs. However, the prediction of when and to what magnitude becomes increasingly difficult as more factors contribute to or limit the formation of blooms.

2.6. Conclusion

The historic reliance on nutrient limitations to predict and control systems is likely to become obsolete in systems like DLNWR that have become exceedingly hypereutrophic. There comes a point where other chemical and environmental factors supersede the limitations imposed by nutrients. The loss of defined nutrient limitations creates a complex system where the question of if HCBs will occur becomes redundant and instead the question of when and to what magnitude gains importance. The abundance of nutrients cause phytoplankton assemblages to lose diversity in favor of cyanobacteria that dominate in a wide range of conditions.

Based on the results of this study, HCBs are likely to be a seasonal issue in shallow hypereutrophic systems across the globe. Legacy P and the continual resuspension of sediments in shallow hypereutrophic systems can fuel HCBs for years; even if the addition of new nutrients is halted (Reddy, Newman, Osborne, White, & Fitz, 2011). Further studies are needed to explore the critical threshold idea presented in this study, looking at identifying the point at which nutrient levels

surpass a critical threshold, beyond which phytoplankton abundance and community composition becomes unpredictable, and how are these critical levels differ across nutrients and in different systems. In addition to becoming unpredictable, systems beyond this threshold become increasingly difficult to manage, with no significant limiting factor to algal growth. Future studies would likely need to include systems at varying degrees of eutrophication or nutrients would need to be artificially induced slowly over a long period of time.

Warming trends through climate change are also likely to compound issues with hypereutrophic systems. The lack of a significant limiting factor to algal growth will only make warmer seasons that favor cyanobacteria growth more difficult to manage. The knowledge that the limitations on HCBs in shallow hypereutrophic systems becomes increasingly complex with nutrient saturation will be important to land and water management globally as environmental conditions increasingly favor the growth of cyanobacteria.

Information from this study is useful to water managers across the globe who are dealing with algal blooms, cyanobacteria, and HCBs. The science shows that N and P, as well as temperature are important in blooms and their formation. However, systems with different depth, topography, location, and nutrient concentrations often react differently in the development of blooms. This study helps to contribute to the body of knowledge on shallow and hypereutrophic lakes and the formation of blooms under these conditions.

2.7. References

Anderson, M. J., Gorley, R. N., & Clarke, R. K. (2008). *PERMANOVA+ for PRIMER: guide to software and statistical methods*. PRIMER-E: Plymouth, UK

Benincà, E., Huisman, J., Heerkloss, R., Jöhnk, K. D., Branco, P., Nes, E. H. V., … Ellner, S. P. (2008). Chaos in a long-term experiment with a plankton community. *Nature*, *451*(7180), 822–825. https://doi.org/10.1038/nature06512

Boettger, W. M. (1986*). Origin and stratigraphy of Holocene sediments, Souris and Des Lacs glacial-lake spillways, north-central North Dakota* (Master's thesis). Retrieved from https://commons.und.edu/cgi/viewcontent.cgi?article=1029&context=theses

Carlson, R. E. (1977). A trophic state index for lakes[1]. *Limnology and Oceanography*, *22*(2), 361–369. https://doi.org/10.4319/lo.1977.22.2.0361

Carr N. G., & Whitton B. A. (1982). *The biology of Cyanobacteria*. Blackwell Scientific Publications.

Chaffin, J. D., & Bridgeman, T. B. (2013). Organic and inorganic nitrogen utilization by nitrogen-stressed cyanobacteria during bloom conditions. *Journal of Applied Phycology*, *26*(1), 299–309. https://doi.org/10.1007/s10811-013-0118-0

Des Lacs National Wildlife Refuge. (1999). *Des Lacs National Wildlife Refuge - Annual narrative report calendar year 1997*. Retrieved from http://ecos.fws.gov/ServCat/

Dodds, W. K., Bouska, W. W., Eitzmann, J. L., Pilger, T. J., Pitts, K. L., Riley, A. J., … Thornbrugh, D. J. (2009). Eutrophication of U.S. freshwaters: Analysis of potential economic damages. *Environmental Science and Technology*, *43*(1), 12–19. https://doi.org/10.1021/es801217q

Dolman, A. M., Rücker, J., Pick, F. R., Fastner, J., Rohrlack, T., Mischke, U., & Wiedner, C. (2012). Cyanobacteria and cyanotoxins: The influence of nitrogen versus phosphorus. *PLoS ONE*, *7*(6). https://doi.org/10.1371/journal.pone.0038757

Francis, G. (1878). Poisonous Australian lake. *Nature*, *18*(444), 11–12. https://doi.org/10.1038/018011d0

Graham, J. L., Jones, J. R., Jones, S. B., Downing, J. A., & Clevenger, T. E. (2004). Environmental factors influencing microcystin distribution and concentration in the Midwestern United States. *Water Research*, *38*(20), 4395–4404. https://doi.org/10.1016/j.watres.2004.08.004

Harke, M. J., Steffen, M. M., Gobler, C. J., Otten, T. G., Wilhelm, S. W., Wood, S. A., & Paerl, H. W. (2016). A review of the global ecology, genomics, and biogeography of the toxic cyanobacterium, *Microcystis* spp. *Harmful Algae*, *54*, 4–20. https://doi.org/10.1016/j.hal.2015.12.007

Huber, V., Wagner, C., Gerten, D., & Adrian, R. (2011). To bloom or not to bloom: contrasting responses of cyanobacteria to recent heat waves explained by critical thresholds of abiotic drivers. *Oecologia*, *169*(1), 245–256. https://doi.org/10.1007/s00442-011-2186-7

Huisman, J., Codd, G. A., Paerl, H. W., Ibelings, B. W., Verspagen, J. M. H., & Visser, P. M. (2018). Cyanobacterial blooms. *Nature Reviews Microbiology*, *16*(8), 471–483. https://doi.org/10.1038/s41579-018-0040-1

Kolars, K. A., Vecchia, A. V., & Galloway, J. M. (2019). Stochastic model for simulating Souris River Basin regulated streamflow upstream from Minot, North Dakota. *Scientific Investigations Report*. https://doi.org/10.3133/sir20185155

Kosten, S., Huszar, V. L. M., Bécares, E., Costa, L. S., Donk, E., Hansson, L.-A., … Scheffer, M. (2011). Warmer climates boost cyanobacterial dominance in shallow lakes. *Global Change Biology*, *18*(1), 118–126. https://doi.org/10.1111/j.1365-2486.2011.02488.x

Lin, Y., He, Z., Yang, Y., Stoffella, P. J., Phlips, E. J., & Powell, C. A. (2008). Nitrogen versus phosphorus limitation of phytoplankton growth in Ten Mile Creek, Florida, USA. *Hydrobiologia*, *605*(1), 247–258. https://doi.org/10.1007/s10750-008-9360-x

Lorenz, E. N. (1963). Deterministic Nonperiodic Flow. *Journal of the Atmospheric Sciences*, *20*(2), 130–141. https://doi.org/10.1175/1520-0469(1963)020<0130:dnf>2.0.co;2

Merel, S., Walker, D., Chicana, R., Snyder, S., Baurès, E., & Thomas, O. (2013). State of knowledge and concerns on cyanobacterial blooms and cyanotoxins. *Environment International*, *59*, 303–327. https://doi.org/10.1016/j.envint.2013.06.013

North Dakota Department of Environmental Quality (2020). *Standard operating procedures for the collection and preservation of lake or non-wadeable wetland water column samples for chemical analysis*. Retrieved from https://deq.nd.gov/publications/WQ/3_WM/SOPs/7.04_LakeWaterQualitySampleSOP.pdf (accessed 1 Apr. 2020)

O'Neil, J., Davis, T., Burford, M., & Gobler, C. (2012). The rise of harmful cyanobacteria blooms: The potential roles of eutrophication and climate change. *Harmful Algae*, *14*, 313–334. https://doi.org/10.1016/j.hal.2011.10.027

Paerl, H. W., Gardner, W. S., McCarthy, M. J., Peierls, B. L., & Wilhelm, S. W. (2014). Algal blooms: Noteworthy nitrogen. *Science*, *346*(6206), 175–175. https://doi.org/10.1126/science.346.6206.175-a

Paerl, H. W., Hall, N. S., & Calandrino, E. S. (2011). Controlling harmful cyanobacterial blooms in a world experiencing anthropogenic and climatic-induced change. *Science of The Total Environment*, *409*(10), 1739–1745. https://doi.org/10.1016/j.scitotenv.2011.02.001

Paerl, H. W., & Huisman, J. (2009). Climate change: a catalyst for global expansion of harmful cyanobacterial blooms. *Environmental Microbiology Reports*, *1*(1), 27–37. https://doi.org/10.1111/j.1758-2229.2008.00004.x

Paerl, H. W., & Otten, T. G. (2013). Harmful cyanobacterial Blooms: Causes, consequences, and controls. *Microbial Ecology*, *65*(4), 995–1010. https://doi.org/10.1007/s00248-012-0159-y

Paerl, H. W., & Ustach, J. F. (1982). Blue-green algal scums: An explanation for their occurrence during freshwater blooms[1]. *Limnology and Oceanography*, *27*(2), 212–217. https://doi.org/10.4319/lo.1982.27.2.0212

Paerl, H. W., Xu, H., Hall, N. S., Rossignol, K. L., Joyner, A. R., Zhu, G., & Qin, B. (2015). Nutrient limitation dynamics examined on a multi-annual scale in Lake Taihu, China: implications for

controlling eutrophication and harmful algal blooms. *Journal of Freshwater Ecology*, *30*(1), 5–24. https://doi.org/10.1080/02705060.2014.994047

Paul, V. J. (2008). Global warming and cyanobacterial harmful algal blooms. *Advances in Experimental Medicine and Biology Cyanobacterial Harmful Algal Blooms: State of the Science and Research Needs*, 239–257. https://doi.org/10.1007/978-0-387-75865-7_11

Paytan, A., & Mclaughlin, K. (2007). The oceanic phosphorus cycle. *ChemInform*, *38*(20). https://doi.org/10.1002/chin.200720268

Reddy, K. R., Newman, S., Osborne, T. Z., White, J. R., & Fitz, H. C. (2011). Phosphorous cycling in the greater everglades ecosystem: Legacy phosphorous implications for management and restoration. *Critical Reviews in Environmental Science and Technology*, *41*(sup1), 149–186. https://doi.org/10.1080/10643389.2010.530932

Resler, L. M. (2016). Edward N Lorenz's 1963 paper, "Deterministic nonperiodic flow", in Journal of the Atmospheric Sciences, Vol 20, pages 130–141: Its history and relevance to physical geography. *Progress in Physical Geography: Earth and Environment*, *40*(1), 175–180. https://doi.org/10.1177/0309133315623099

Reynolds, C. S. (1997). Successional development, energetics and diversity in planktonic communities. *Biodiversity*, 167–202. https://doi.org/10.1007/978-1-4612-1906-4_11

Saxton, M. A., Arnold, R. J., Bourbonniere, R. A., McKay, R. M. L., & Wilhelm, S. W. (2012). Plasticity of total and intracellular phosphorus quotas in *Microcystis aeruginosa* cultures and Lake Erie algal assemblages. *Frontiers in Microbiology*, *3*. https://doi.org/10.3389/fmicb.2012.00003

Schindler, D. W. (1974). Eutrophication and recovery in experimental lakes: Implications for lake management. *Science*, *184*(4139), 897–899. https://doi.org/10.1126/science.184.4139.897

Schindler, D. W. (1977). Evolution of phosphorus limitation in lakes. *Science*, *195*(4275), 260–262. https://doi.org/10.1126/science.195.4275.260

Scott, J. T., & McCarthy, M. J. (2010). Nitrogen fixation may not balance the nitrogen pool in lakes over timescales relevant to eutrophication management. *Limnology and Oceanography*, *55*(3), 1265–1270. https://doi.org/10.4319/lo.2010.55.3.1265

Søndergaard, M., Jensen, J. P., & Jeppesen, E. (2003). Role of sediment and internal loading of phosphorus in shallow lakes. *Hydrobiologia*, *506-509*(1-3), 135–145. https://doi.org/10.1023/b:hydr.0000008611.12704.dd

Søndergaard, M., Lauridsen, T. L., Johansson, L. S., & Jeppesen, E. (2017). Nitrogen or phosphorus limitation in lakes and its impact on phytoplankton biomass and submerged macrophyte cover. *Hydrobiologia*, *795*(1), 35–48. https://doi.org/10.1007/s10750-017-3110-x

Veal, C. J., Neelamraju, C., Wolff, T., Watkinson, A., Shillito, D., & Canning, A. (2017). Managing cyanobacterial toxin risks to recreational users: a case study of inland lakes in South East Queensland. *Water Supply*, *18*(5), 1719–1726. https://doi.org/10.2166/ws.2017.233

Visser, P. M., Verspagen, J. M., Sandrini, G., Stal, L. J., Matthijs, H. C., Davis, T. W., … Huisman, J. (2016). How rising CO2 and global warming may stimulate harmful cyanobacterial blooms. *Harmful Algae*, *54*, 145–159. https://doi.org/10.1016/j.hal.2015.12.006

Walsby, A. E., Hayes, P. K., Boje, R., & Stal, L. J. (1997). The selective advantage of buoyancy provided by gas vesicles for planktonic cyanobacteria in the Baltic Sea. *New Phytologist*, *136*(3), 407–417. https://doi.org/10.1046/j.1469-8137.1997.00754.x

Wang, Q., & Li, Y. (2010). Phosphorus adsorption and desorption behavior on sediments of different origins. *Journal of Soils and Sediments*, *10*(6), 1159–1173. https://doi.org/10.1007/s11368-010-0211-9

Wax P. (2006). *Lake water quality assessment for Upper Des Lacs Lake Ward and Burke Counties North Dakota.* Retrieved from https://deq.nd.gov/publications/WQ/3_WM/Lakes/DesLacs/DesLacs_Final.pdf

Wang, M., Shi, W., Chen, Q., Zhang, J., Yi, Q., & Hu, L. (2018). Effects of nutrient temporal variations on toxic genotype and microcystin concentration in two eutrophic lakes. *Ecotoxicology and Environmental Safety*, *166*, 192–199. https://doi.org/10.1016/j.ecoenv.2018.09.095

Wetzel, R. G. (2015). *Limnology: Lake and river ecosystems.* Academic Press, an imprint of Elsevier.

Wu, B., Jin, H., Gao, S., Xu, J., & Chen, J. (2019). Nutrient budgets and recent decadal variations in a highly eutrophic estuary: Hangzhou Bay, China. *Journal of Coastal Research*, *36*(1), 63. https://doi.org/10.2112/jcoastres-d-18-00071.1

Xu, H., Paerl, H. W., Qin, B., Zhu, G., & Gaoa, G. (2009). Nitrogen and phosphorus inputs control phytoplankton growth in eutrophic Lake Taihu, China. *Limnology and Oceanography*, *55*(1), 420–432. https://doi.org/10.4319/lo.2010.55.1.0420

Yang, H., Zhao, Y., Wang, J., Xiao, W., Jarsjö, J., Huang, Y., . . . Wang, H. (2020). Urban closed lakes: Nutrient sources, assimilative capacity and pollutant reduction under different precipitation frequencies. *Science of the Total Environment,* 700, 134531. doi:10.1016/j.scitotenv.2019.134531

Yang, J., Tang, H., Zhang, X., Zhu, X., Huang, Y., & Yang, Z. (2017). High temperature and pH favor *Microcystis aeruginosa* to outcompete *Scenedesmus obliquus*. *Environmental Science and Pollution Research*, *25*(5), 4794–4802. https://doi.org/10.1007/s11356-017-0887-0

Zhu, M., Zhu, G., Zhao, L., Yao, X., Zhang, Y., Gao, G., & Qin, B. (2012). Influence of algal bloom degradation on nutrient release at the sediment–water interface in Lake Taihu, China.

Environmental Science and Pollution Research, *20*(3), 1803–1811. https://doi.org/10.1007/s11356-012-1084-9

CHAPTER 3. UNDERSTANDING PHOSPHORUS SATURATION IN SEDIMENT AND IMPACT ON HARMFUL CYANOBACTERIAL BLOOMS

3.1. Abstract

Anthropogenic loading of nutrients is thought to be one of the largest factors in the abundance of Harmful cyanobacterial blooms (HCBs). Traditionally, research has focused on phosphorus (P), in the water column, within systems affected HCBs. Few studies have assessed the role P saturation in sediment has on HCBs. This study sought to assess the effects of sediment P saturation on the abundance of HCBs within a large inland freshwater riverine system divided into lakes. These lakes are shallow and prone to periodic mixing by wind, which results in frequent resuspension of sediments. Five sites were chosen within the lakes and across the channel at each site five transect locations were sampled for sediment at 0-15 cm and 15-30 cm. Phosphorus saturation levels in conjunction with soil texture, organic matter, and carbon content was tested. Additionally, four years of water sampling data was collected observing water eutrophication and HCBs. Analysis of the data showed that sediment within the lakes are near or at full P saturation. This results in the sediments being unable to sequester P, and instead are a prominent source of P, fueling the formation of HCBs throughout the season. Paired with periodic mixing of the sediments, HCBs create conditions favorable to the release of P from the sediment, further fueling their formation and increasing their severity. The results of this study are important to scientists and water managers worldwide seeking to understand the factors that cause and exacerbate HCBs, knowing that we may need to look beyond the water to get a clearer picture of what is influencing HCBs.

3.2. Introduction

Globally, the occurrence and impacts of harmful cyanobacterial blooms (HCBs) is increasing (Dodds et al., 2009; Harke et al., 2016; O'Neil, Davis, Burford, & Gobler, 2012;). Climate change and anthropogenic nutrient loading are creating favorable conditions for cyanobacteria in the

world's rivers, lakes, and oceans (Paerl, Hall, & Calandrino, 2011). The introduction of phosphorus (P) and nitrogen (N) to aquatic ecosystems is thought to be the largest contributor to the increasing abundance of HCBs (O'Neal et al., 2012). Loading of N is often offset by denitrification, which primarily occurs in the sediment (Saunders & Kalff, 2000). Phosphorus, however, is less mobile and tends to remain in aquatic systems for long periods of time by binding to the sediment (Wang & Li, 2010).

The sediment in aquatic ecosystems act as a reservoir for P, and suspended particles in the water column have a strong affinity for dissolved phosphorus (DP) (Lebo, 1991; Wu, Jin, Gao, xu, & Chen, 2019). The rate at which P is adsorbed and desorbed is dependent on sediment particle size, with an exponential increase in adsorption with decreasing particle size (Walter & Morse, 1984; Zhang & Huang, 2007). Aerobic conditions typically favor adsorption of P, while anaerobic conditions typically favor desorption (Hietanen & Lukkari, 2007). Even though P in the sediment can greatly influence P available for algal blooms, little to no research exists correlating HCBs and P saturation in the sediment. Most of the literature on HCB's to date focuses strictly on P and N in the water column (Chaffin & Bridgeman, 2013; Dolman et al., 2012; O'Neil et al., 2012; Schindler, 1974; Schindler, 1977; Scott & McCarthy, 2010).

Phosphorus exchange across the sediment–water interface, via adsorption and desorption, plays a crucial role in governing the availability of water-soluble P (Froelich, 1988). Wind-induced and maintained resuspension of sediment particles is more likely to occur in shallow lakes (Jeppesen et al., 1997). Consequently, suspension of sediment particles into the water column increase the surface area available for P exchange; with smaller particles being more likely to be re-suspended due to wave action and reside in the water column for larger periods of time (Wang & Li, 2010). Thus, greater amounts of fine particles are likely to increase adsorption and desorption of P into and out of the water column.

These sediments can play a large role in promoting or potentially inhibiting algal bloom formation, by either sequestering or releasing P and other nutrients into the water column (Zhu et al., 2012). The degradation of blooms can also impact the sediment-water column relationship by creating areas of hypoxia, which then facilitate the rapid release of nutrients like ammonia and phosphorous, and in turn fuel further bloom formation (Zhu et al., 2012). Despite the large role sediment can play in promoting or inhibiting HCBs, limited research to date has assessed the relationship between sediment and HCBs.

Sediments capable of sequestering additional P act as a sink under the right environmental conditions, and can limit the amount of P available for algal consumption (Christophoridis & Fytianos, 2006). Conversely, under different environmental conditions, sediments can act as a source of P for algal blooms (Christophoridis & Fytianos, 2006). These dynamics between P adsorption and release in sediments have been studied extensively (Zhang & Huang, 2007; Zhu et al., 2012); however, little work has been done assessing P saturation in eutrophic aquatic sediment and the implications highly saturated sediment may have on HCBs.

When sediments near saturation they become limited in their capacity to further sequester P. Thus, highly saturated sediment would not sequester new P entering a system, and could act as a source of P under the right conditions. To the authors' knowledge, this study is the first of its kind to assess the saturation of P in the sediments of a shallow lake system prone to HCBs. Specifically, this study seeks to assess: 1) the saturation levels of sediments in a highly eutrophic system; and 2) the effect of sediment saturation on the formation of HCBs.

3.3. Methods and Materials

3.3.1. Study area and site selection

The study took place in the Des Lac National Wildlife Refuge (DLNWR) near Kenmare, North Dakota, USA. The DLNWR is comprised of three naturally formed lakes that span a 45 km

long river valley that eventually feeds into the Souris River. The refuge is in the northwest corner of North Dakota, borders the Canadian province of Saskatchewan to the north, and is approximately 145 km east of Montana, USA (Figure 3.1).

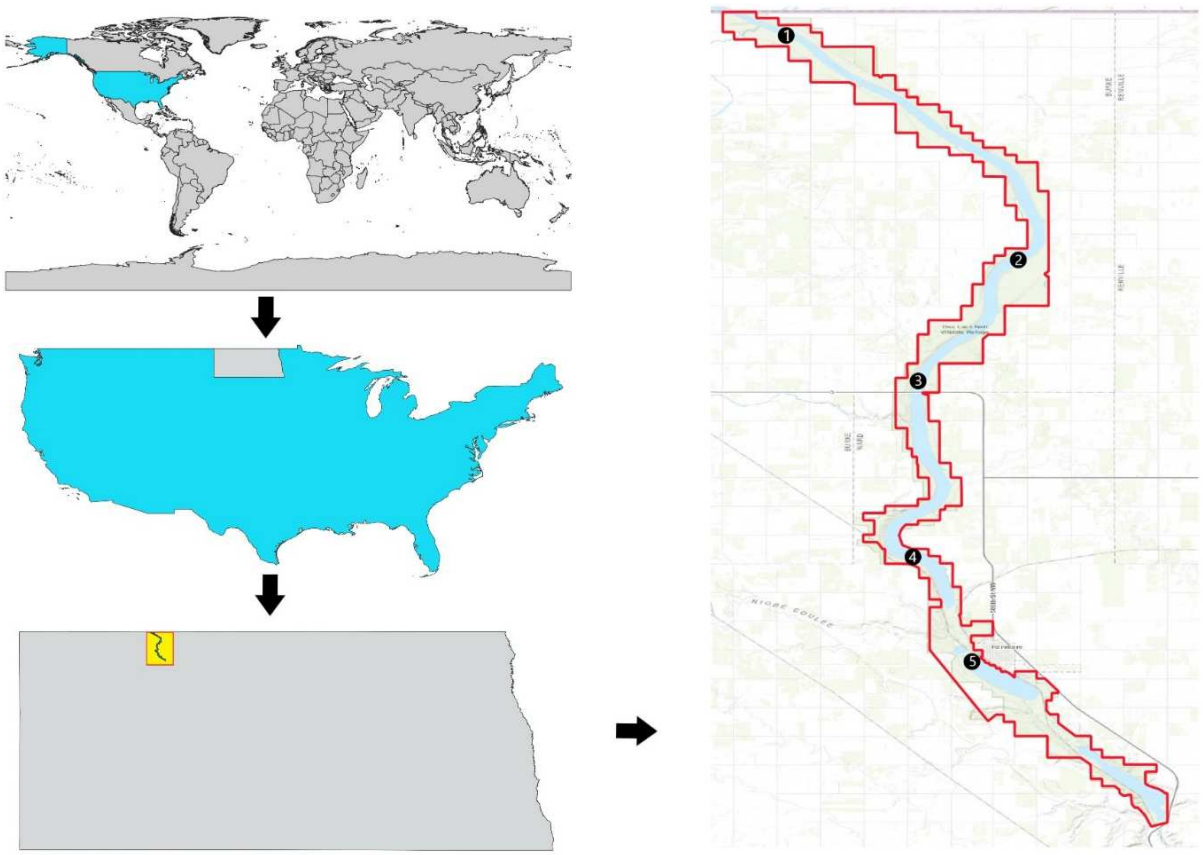

Figure 3.1. Map showing sites one through five where samples were collected on Des Lacs National Wildlife Refuge in North Dakota, USA.

The Des Lacs River Valley was initially formed from a sudden and catastrophic drainage of Glacial Lake Regina, resulting in a steep and narrow valley (Boettger, 1986). Slumping, and the formation of ephemeral streams, eventually widened the valley and deposited coarse alluvial sediments along the valley sides with finer materials in the valleys center (Boettger, 1986). The area around the Des Lacs Valley is dictated by smooth drift plains that transition to steep slopes descending 15-40 m to the river (Des Lacs National Wildlife Refuge, 1999). Soils in the river valley are mapped as Zahl-Williams Association (Zhal: Fine-loamy, mixed, superactive, frigid Typic

Calciustolls; Williams: Fine-loamy, mixed, superactive, frigid Typic Argiustoll) formed from medium to moderately-fine textured glacial till (NRCS, 2013).

A total of eight water control structures create the series of lakes and wetlands that comprise the refuge today. A total of five sites, site one (48°59'24.1"N 102°11'33.4"W), site two (48°52'25.2"N 102°04'16.8"W), site three (48°48'37.2"N 102°07'11.7"W), site four (48°43'37.8"N 102°07'49.4"W), and site five (48°40'19.6"N 102°05'37.0"W) were selected in areas that represent individual pools of water. These pools are separated throughout the refuge water area by distance, water control structures, or both. Each site included five points in which sediment cores were collected, forming a cross section across the lake (Figure 3.2). The cross section included cores on the east and west shores, a core from the middle of the river, and a core between the middle and east shore and middle and west shore.

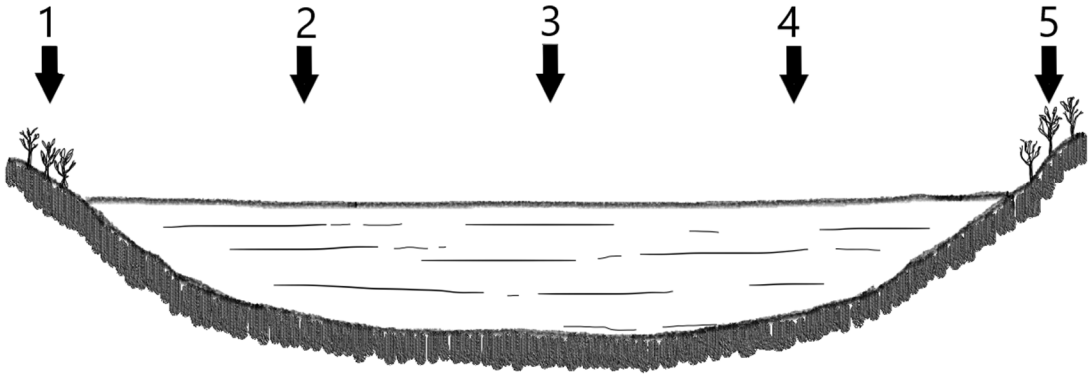

Figure 3.2. Example cross section of site where a transect of five cores were collected across the lake.

3.3.2. Soil sampling

Soil samples were collected in June and July of 2019. Soil cores taken within the lake were collected using a universal percussion corer (Aquatic Research Instruments, Hope, Idaho, USA). Shore samples were taken using a 10 cm diameter bucket auger. The top 30 cm at each site was collected and split into 0 to 15 cm and 15 to 30 cm samples. Cores were stored in glass jars, kept on

ice, and shipped to the North Dakota Department of Environmental Quality (NDDEQ) lab (Bismarck, North Dakota, USA) to be analyzed for total phosphorus (TP). A second set of samples was collected using the same protocol mentioned above, but air dried after collection. Dried samples were stored in paper bags before being ground to pass through a 2 mm sieve and then stored at 20° C in plastic zip-lock bags. These samples were analyzed for soil pH, organic and inorganic carbon content, P sorption rates, and particle size.

Particle size analysis was conducted using the pipette method (Gee & Bauder, 1986). Due to the difficulty of removing the high organic content, half the suggested amount of soil was used for each sample taken within the lake. Total carbon (TC) and soil inorganic carbon (IC) were evaluated using a Primacs SLC TOC Analyzer (Skalar Analytical B.V., Breda, The Netherlands); soil organic carbon (OC) was calculated as the difference between TC and IC.

3.3.3. Phosphorus sorption

Phosphorus sorption was measured using the SERA-IEG 17 standard procedure (Graetz & Nair, 2009). A total of 1.2 grams was taken from each sample and weighed into 50 mL polyethylene centrifuge tubes with 30 mL of the corresponding concentrations of P: 0, 0.01, 0.1, 0.5, 10, 25, 50 and 100 mg P L^{-1} as potassium phosphate (KH_2PO_4) prepared using 0.01 M $CaCl_2$. Samples were shaken on a horizontal shaker for 24 hours at room temperature (approximately 20°C) then centrifuged at a relative centrifugal force of 650 x g for 10 min. The supernatant was filtered through 2.5 μm No. 42 Whatman glass fiber filters (GE Healthcare Life Sciences, Marlborough, Massachusetts, USA) and given to the North Dakota State University Soils Testing Lab (Fargo, North Dakota, USA) for total P analysis.

Phosphorus sorption parameter estimates were obtained utilizing Langmuir and Freundlich isotherm models. In these models, P not detected in solution is assumed to be adsorbed by sample soils (Graetz & Nair, 2009). In the Langmuir equation:

$$\frac{C}{S} = \frac{1}{kS_{max}} + \frac{C}{S_{max}}$$

S (mg lg^{-1}) is the soil-bound P concentration after equilibrium, C (mg L^{-1}) is the aqueous P concentration after equilibrium, S_{max} (mg kg^{-1}) is the maximum capacity of soil to bind P, and k (L mg^{-1}) is the sorption coefficient related to the affinity or binding energy P has for soil.

In the Freundlich equation:

$$S = K_F C^{1/n}$$

S (mg lg^{-1}) is the soil-bound P concentration after equilibrium, C (mg L^{-1}) is the aqueous P concentration after equilibrium, K_F (L mg^{-1}) is a constant value relating the bonding energy of soil and P, and 1/n (unitless) is an empirical fitting parameter related to the shape or linearity of the isotherm. Phosphorus removed from solution is assumed to be sorbed by the soil (Graetz & Nair, 2009). Langmuir and Freundlich Isotherm models were utilized to fit the sorption data.

Freundlich (K_F and 1/n) and Langmuir (k and S_{max}) parameters were estimated by inversely fitting the respective equations to the measures S (dependent) and C (independent) experimental data. The Solver Add-in for Microsoft Excel (Microsoft Corporation) was utilized to optimize the Freundlich and Langmuir isotherm parameters to achieve best fits for the respective equations using the measured data. The generalized reduced gradient method was used to find best fit parameters.

3.3.4. Water sampling

Water sampling was conducted weekly at all five sites in 2019 to test for ammonia, nitrate+nitrite, total nitrogen, and total phosphorus. Samples were collected using a Wildco 1.2 L Kemmerer sampler (Yulee, Florida, USA) according to North Dakota Department of Environmental Quality (NDDEQ) protocol (North Dakota Department of Environmental Quality 2020). Sites one, two, four, and five were also tested for dissolved phosphorus (DP) and dissolved

nitrogen (DN). Samples for DP and DN were filtered through a 0.45-micron filter (Geotech, Denver, Colorado, USA) with a peristaltic pump (Cole-Parmer (Model 7533-50), Vernon Hills, Illinois, USA). All samples were preserved and placed on ice before shipping to the NDDEQ lab in Bismarck, North Dakota, USA, for analysis.

A PVC column sampler (two-meter length, six cm diameter) was used to collect a sample from the top two meters, or only the pelagic zone where depths did not permit two meters of sampling. A Wildco 8 L churn splitter (Yulee, Florida, USA) was used to thoroughly mix the sample before a minimum of 50 and a maximum of 1,000 mL of water (high CHY-*a* levels made it difficult to filter more than 50 mL of water at times) was filtered through a 0.65 μm Whatman glass fiber filters (GE Healthcare Life Sciences, Marlborough, Massachusetts, USA). Filters were placed in sealed plastic tubes with aluminum wrapping before being stored on ice prior to shipping to the NDDEQ lab for analysis. Secchi disc (SD) measurements were made in conjunction to all water sampling as well as site specific water temperature and pH. Water temperature and pH were measured with a YSI PRODSS sonde (Yellow Springs, Ohio, USA).

3.3.5. Statistical analysis

Statistical tests were performed in Microsoft Excel version 1908 (Microsoft Corporation). Coefficient of determination was run to assess the goodness of fit between Freundlich and Langmuir predicted values and the observed soil values. The Analysis Toolpak in Excel (Microsoft Corporation) was used to create a correlation matrix for all tested soil parameters. Clay amounts, percent P, iron, and calcium were tested using block design ANOVA where site and transect position are a fixed factor, depth is nested under position. Because depth was not replicated it was included as a factor in the ANOVA, but it was not directly tested. A t-test was run to determine if the two depths were different for the various response variables.

3.4. Results

When the coefficient of determination was used to compare predicted and observed P sorption values in the soil, the Freundlich equation was selected as the best predictive representation. Phosphorus sorption estimates obtained from Freundlich isotherm modeling showed that the sediments on DLNWR are between 95 and 100 percent saturated with P (Table 3.1). While modeling sorption rates, no tested concentration of P resulted in a plateau, indicating a concentration at which the soils capacity to adsorb P is reached. However, full sorption capacity was modeled at realistic water column P concentrations. The highest recorded P concentration within the water column on DLNWR was 1.08 ppm (Table 3.2), and full P soil saturation was found in tested concentrations as high as 50 ppm (Table 3.1). Nested ANOVA showed that sorption was different by site, but not by transect location (Table 3.3). It should be noted that analysis of sorption values was limited due to the limited range of the variables. At realistic in-lake P levels, saturation was at or above 100 percent saturation following Freundlich predicted values.

The standard pipette method (Gee & Bauder, 1986) for classifying soil textures was used with slight modifications. Due to an abundance of organic matter in the sediment samples, averaging 19.9 percent across sights, chemical burn off with the standard amount of test soil was not feasible. As such, only half the amount of suggested soil was used in our analysis, which resulted in a more thorough chemical burn off. Soils on DLNWR were dominated primarily by loams (Figure 3.3). The majority of silty sediments were within the lake itself (west middle, middle, and east middle) and the majority of sandy sediments were on the east shore (east) (Table 3.4). The nested ANOVA showed that clay percentages were significantly different by both transect location and by site (Table 3.3). As would be expected, t-tests showed IC and OC were significantly different ($p=0.039$ for IC, $p=0.003$ for OC) by depth with higher concentrations of both in the upper 1-15 cm.

Table 3.1. Freundlich predicted soil saturation in the corresponding concentrations of phosphorus (P): 0, 0.01, 0.1, 0.5, 10, 25, 50 and 100 mg P L^{-1} as potassium phosphate (KH_2PO_4) prepared using 0.01 M $CaCl_2$. Values above 100 percent indicate leaching of P into the water column.

Concentration of P as KH_2PO_4	Mean % Saturation	Median % Saturation	Min. % Saturation	Max % Saturation
0 ppm	100	100	99	100
0.01 ppm	100	100	100	101
0.1 ppm	100	100	99	100
0.5 ppm	100	100	100	100
10 ppm	99	99	97	100
25 ppm	98	98	95	100
50 ppm	98	98	95	100
100 ppm	98	98	95	99

Table 3.2. Water column phosphorus averages (in mg/L) at each site during the sampling season (May through October) between the years 2016 and 2019.

Water Column Phosphorus Averages at all Sites and all Years (mg/L)					
Year	2016	2017	2018	2019	Average Across All Years
Site 1					
Average	0.13	0.23	0.11	0.20	0.17
Min	0.07	0.07	0.04	0.07	0.06
Max	0.27	0.74	0.27	0.51	0.45
Site2					
Average	0.13	0.21	0.10	0.21	0.16
Min	0.08	0.08	0.05	0.06	0.07
Max	0.23	0.48	0.33	0.47	0.38
Site 3					
Average	0.13	0.21	0.11	0.24	0.17
Min	0.07	0.06	0.06	0.05	0.06
Max	0.30	0.45	0.22	0.52	0.37
Site 4					
Average	0.14	0.20	0.10	0.30	0.19
Min	0.08	0.06	0.05	0.05	0.06
Max	0.26	0.55	0.17	0.68	0.42
Site 5					
Average	0.51	0.33	0.23	0.39	0.37
Min	0.20	0.05	0.07	0.12	0.11
Max	1.08	0.60	0.53	0.93	0.79
All Sites Combined					
Average	0.21	0.24	0.13	0.27	0.21
Min	0.10	0.06	0.05	0.07	0.07
Max	0.43	0.56	0.30	0.62	0.48

Table 3.3. Nested ANOVA results showing significance of difference between transect location and site location between tested variables. Phosphorus uptake was Freundlich predicted phosphorus sorption percentage, phosphorus percent was the amount of recorded phosphorus in the native sediment samples. Variables marked with * were significant at $p<0.05$.

Variable	Factor	P-value
Phosphorus Sorption	Site*	0.0387
	Transect	0.0844
Clay Percentage	Site*	0.0094
	Transect*	<.0001
Phosphorus Percent In Soil	Site*	0.0203
	Transect	0.0597
Fe Amount In Soil	Site*	0.0178
	Transect*	<.0001
Ca Amount In Soil	Site	0.6763
	Transect*	0.0268
Inorganic Carbon In Soil	Site	0.3395
	Transect*	0.0031
Organic Carbon In Soil	Site	0.0992
	Transect*	0.0001

Total carbon constituted between 0.7 and 15.6 percent of soil samples with the highest concentrations within the lakes. Organic carbon constituted the greater majority of TC. The nested ANOVA showed that there were no significant differences in IC or OC content by site, but they were significantly different by transect location (Table 3.3). Transect locations within the lake, especially the center, tended to be the richest in TC (Table 3.5).

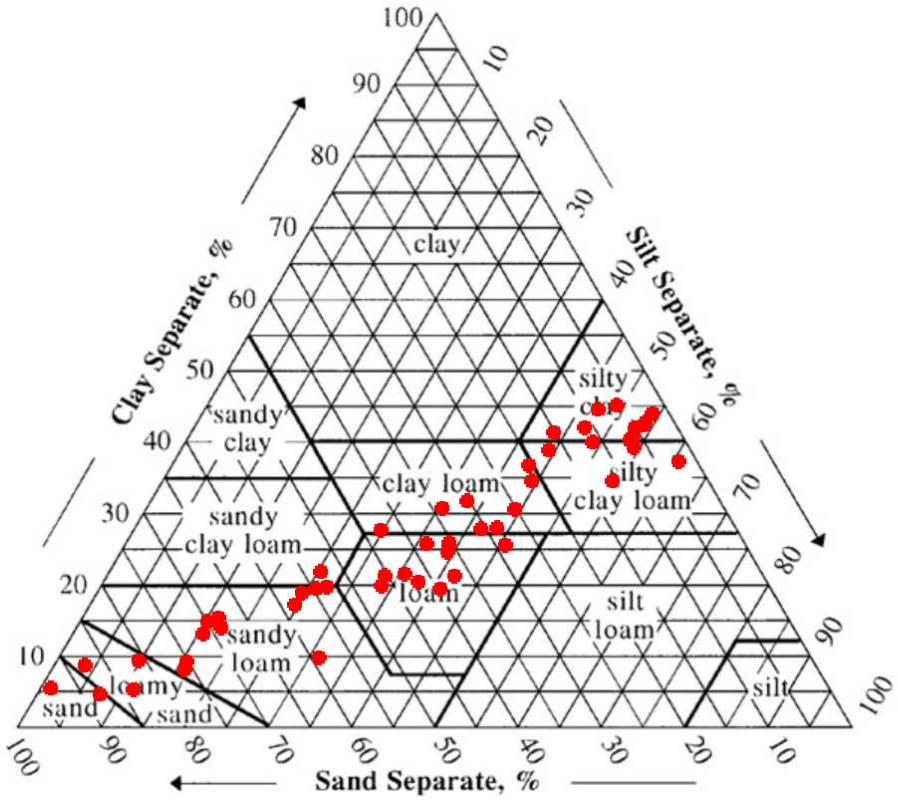

Figure 3.3. Soil texture chart depicting the range of soil textures of all samples collected on Des Lacs National Wildlife Refuge.

Table 3.4. Sediment types by site, transect, and depth. East, East-Middle, Middle, West-Middle, and West refer to transect points across the lake. Each transect included a 0 to 15 cm and a 15 to 30 cm sample. West and East sides were collected from shore and all others were collected by boat.

Site	Depth	West	West Mid	Middle	East Mid	East
1	0-15cm	Sandy Loam	Sandy Loam	Clay Loam	Sandy Loam	Sand
	15-30cm	Sandy Clay Loam	Sandy Loam	Sandy Loam	Loamy Sand	Loamy Sand
2	0-15cm	Clay Loam	Sand	Silty Clay	Silty Clay Loam	Loam
	15-30cm	Clay Loam	Loamy Sand	Silty Clay Loam	Silty Clay	Sandy Loam
3	0-15cm	Loam	Silty Clay	Silty Clay	Clay Loam	Loam
	15-30cm	Loam	Clay Loam	Silty Clay loam	Clay Loam	Sandy Loam
4	0-15cm	Loam	Silty Clay	Silty Clay Loam	Silty Clay Loam	Silty Clay
	15-30cm	Loam	Silty Clay	Silty Clay	Silty Clay	Silty Clay Loam
5	0-15cm	Loam	Sandy Loam	Clay loam	Clay Loam	Sandy Loam
	15-30cm	Loam	Sandy Loam	Loam	Loam	Sandy Loam

Soil texture strongly correlated to most tested parameters (percent P, Fe, Ca, pH, TC, OC, IC) with silt and clay tending to correlate positively, while sand correlated negatively (Table 3.6). Silt and clay had a strong positive correlation to Fe (0.86 each), and sand had a strong negative correlation to Fe (-0.88). Opposed to this, Ca was moderate to weakly correlated to silt, clay, and sand. Iron likely binds more strongly to P in this system. Additionally, carbon was also strongly correlated to soil texture. Total carbon correlated to sand negatively (-0.76), and to silt and clay positively with a correlation of 0.76 and 0.72 respectively, suggesting carbon is a driving factor of P retention.

Table 3.5. Total carbon, inorganic carbon and organic carbon present represented as percent. East, East-Middle, Middle, West-Middle, and West refer to transect points across the lake. Each transect included a 0 to 15 cm and a 15 to 30 cm sample.

0-15 cm Percent Total Carbon					
	East	East-Middle	Middle	West-Middle	West
Site 1	3.2	3.8	8.4	3.5	1.5
Site 2	2.0	0.7	10.6	10.5	15.6
Site 3	4.1	9.9	10.5	8.2	5.1
Site 4	7.5	9.8	10.1	9.7	2.6
Site 5	3.3	3.4	4.5	4.4	2.2
Mean	4.0	5.5	8.8	7.3	5.4
15-30 cm Percent Total Carbon					
	East	East-Middle	Middle	West-Middle	West
Site 1	2.0	2.3	3.0	1.7	1.3
Site 2	1.6	1.1	10.1	9.8	3.4
Site 3	3.2	8.2	9.7	5.3	2.8
Site 4	5.2	9.9	10.2	8.5	1.7
Site 5	1.7	1.7	3.3	3.9	1.3
Mean	2.7	4.6	7.2	5.8	2.1

Table 3.5. Total carbon, inorganic carbon and organic carbon present represented as percent (Continued). East, East-Middle, Middle, West-Middle, and West refer to transect points across the lake. Each transect included a 0 to 15 cm and a 15 to 30 cm sample.

0-15 cm Percent Inorganic Carbon					
	East	East-Middle	Middle	West-Middle	West
Site 1	0.8	0.6	1.5	0.6	0.3
Site 2	1.2	0.3	1.4	0.8	1.2
Site 3	1.6	1.7	1.7	1.1	0.0
Site 4	0.0	1.3	1.5	1.2	1.4
Site 5	1.2	0.9	0.9	1.1	0.0
Mean	1.0	1.0	1.4	0.9	0.6
15-30 cm Percent Inorganic Carbon					
	East	East-Middle	Middle	West-Middle	West
Site 1	0.0	0.3	0.4	0.2	0.8
Site 2	1.1	0.3	0.9	0.7	0.1
Site 3	2.2	1.2	1.3	0.8	0.0
Site 4	0.1	1.1	1.2	1.0	1.4
Site 5	1.4	0.4	0.0	0.9	1.0
Mean	1.0	0.7	0.7	0.7	0.7
0-15 cm Percent Organic carbon					
	East	East-Middle	Middle	West-Middle	West
Site 1	2.4	3.2	6.9	3.0	1.2
Site 2	0.7	0.4	9.3	9.7	14.4
Site 3	2.5	8.2	8.8	7.1	5.0
Site 4	7.5	8.5	8.7	8.5	1.3
Site 5	2.1	2.5	3.6	3.4	2.2
Mean	3.0	4.6	7.4	6.3	4.8
15-30 cm Percent Organic carbon					
	East	East-Middle	Middle	West-Middle	West
Site 1	2.0	1.9	2.6	1.5	0.5
Site 2	0.5	0.8	9.1	9.1	3.4
Site 3	1.0	7.0	8.4	4.4	2.8
Site 4	5.1	8.8	9.0	7.4	0.3
Site 5	0.3	1.3	3.3	3.0	0.3
Mean	1.8	3.9	6.5	5.1	1.5

Table 3.6. Correlation matrix for sediments sampled at Des Lacs National Wildlife Refuge, where sediment saturation values of phosphorus (P) in varying concentrations of KH_2PO_4 are referred to as "n" ppm P. Percent P refers to percent concentration of P in the soil, and TC, IC, and OC refer to total carbon, inorganic carbon, and organic carbon respectively. Numbers in parenthesis on the horizontal axis refer to the parentheses numbered indices on the vertical axis.

	(1)	(2)	(3)	(4)	(5)	(6)	(7)	(8)	(9)	(10)	(11)	(12)	(13)	(14)	(15)	(16)	(17)	(18)
(1) 0 ppm P	1.00																	
(2) 0.01 ppm P	-0.32	1.00																
(3) 0.1 ppm P	-0.10	-0.33	1.00															
(4) 0.5 ppm P	0.14	0.03	-0.56	1.00														
(5) 10 ppm P	-0.05	-0.50	0.31	-0.54	1.00													
(6) 25 ppm P	-0.10	-0.53	0.30	-0.57	0.99	1.00												
(7) 50 ppm P	-0.13	-0.54	0.28	-0.57	0.97	1.00	1.00											
(8) 100 ppm P	-0.13	-0.56	0.25	-0.55	0.95	0.99	1.00	1.00										
(9) % Sand	-0.26	-0.39	0.22	-0.45	0.44	0.55	0.58	0.62	1.00									
(10) % Silt	0.27	0.38	-0.20	0.41	-0.42	-0.53	-0.57	-0.60	-0.98	1.00								
(11) % Clay	0.24	0.38	-0.24	0.49	-0.45	-0.54	-0.58	-0.60	-0.97	0.91	1.00							
(12) % P	0.22	0.18	-0.12	0.17	0.15	0.04	0.00	-0.04	-0.61	0.63	0.55	1.00						
(13) Fe	0.26	0.17	-0.32	0.60	-0.40	-0.47	-0.49	-0.49	-0.88	0.86	0.86	0.54	1.00					
(14) Ca	-0.06	0.31	0.11	0.16	-0.33	-0.37	-0.38	-0.40	-0.40	0.42	0.37	0.25	0.32	1.00				
(15) pH	-0.17	0.11	-0.03	0.32	-0.51	-0.48	-0.47	-0.46	-0.17	0.17	0.16	-0.17	0.23	0.54	1.00			
(16) TC	0.34	0.38	-0.08	0.16	-0.17	-0.30	-0.35	-0.41	-0.76	0.76	0.72	0.61	0.50	0.15	-0.21	1.00		
(17) IC	0.05	0.48	-0.13	0.34	-0.49	-0.55	-0.58	-0.60	-0.66	0.65	0.64	0.34	0.52	0.72	0.58	0.40	1.00	
(18) OC	0.35	0.33	-0.07	0.12	-0.11	-0.23	-0.28	-0.34	-0.70	0.70	0.66	0.59	0.45	0.05	-0.30	0.99	0.27	1.00

The lakes on DLNWR were characterized as eutrophic to hypereutrophic throughout the sampling season by use of a Trophic State Index (TSI) (Carlson, 1977; Yang et al., 2020) (Table 3.7). The TSI was determined by independently using CHY-*a*, SD, and P readings to obtain a trophic

level value for each parameter. Of the three parameters, P was consistently the highest indicator of eutrophication. Eutrophication values were similar across all years (2016-2019), but only sampling from the 2019 season is included. While a TSI has no upper or lower bounds, values less than 30 indicate an oligotrophic system, values between 30 and 50 indicate a mesotrophic system, values between 50 and 70 indicate a eutrophic system, and values greater than 70 indicate a hypereutrophic system.

Table 3.7. Trophic State Index for Des Lacs National Wildlife Refuge. Parameters used were chlorophyll-*a* (C-*a*), total phosphorus (TP), and Secchi disk depth (SD).

Date	Site 1			Site 2			Site 3		
	TSI (C-*a*)	TSI (TP)	TSI (SD)	TSI (C-*a*)	TSI (TP)	TSI (SD)	TSI (C-*a*)	TSI (TP)	TSI (SD)
5/16	69.29	68.88	69.99	73.60	68.38	73.20	76.44	76.69	73.20
5/31	69.21	67.69	75.13	72.19	71.53	77.35	74.05	72.06	77.35
6/5	59.99	74.56	79.98	69.62	73.06		73.60	74.12	83.19
6/13	68.60	73.31	79.98	76.07	75.20	83.19	77.97	78.87	83.19
6/19	68.98	79.74	83.19				74.00	82.50	77.35
6/25	64.48	92.02	75.13	64.99	82.25	77.35	63.97	84.93	73.20
7/1	57.17	93.18	66.21	59.38	90.44	69.99			
7/8	71.82	92.56	75.13	63.90	90.26	68.61	54.21	90.90	65.14
7/16	60.79	94.05	73.20	62.18	92.05	52.78	65.25	94.33	64.15
7/22	73.76	92.08	73.20	70.99	91.25	57.37	67.05	92.75	61.52
7/29	82.77	86.11	75.13	73.26	89.77	62.34	73.69	93.76	62.34
8/5	85.70	88.41	71.51	80.20	92.75	65.14	76.26	91.66	62.34
8/14	79.49	81.99	60.00	78.79	84.93	61.52	82.07	89.69	55.15
8/21	73.72	79.43	65.14	65.53	84.77	54.16	72.65	88.08	58.63
8/28	81.76	76.88	73.20	77.40	82.69	57.37	81.15	87.01	66.21
9/4	82.38	72.94	73.20	76.53	74.78	66.21	77.40	84.83	66.21
9/10	77.65	69.82	69.99	74.30	75.20	64.15	79.15	76.69	67.36
9/16	80.63	67.16	71.51	76.16	65.21	65.14	73.10	68.04	62.34
9/23	77.32	67.34	69.99	73.87	68.04	65.14	73.98	70.12	62.34
10/1	79.01	66.97	69.99	71.41	70.12	60.00			
10/8	67.75	65.41	68.61	62.82	65.62	55.68	60.28	65.62	57.37
10/16	69.62	66.21	67.36	64.03	62.70	59.30	61.27	62.20	56.78
10/22	64.22	64.56	64.15	58.16	67.16	56.22	59.33	60.56	54.16

Table 3.7. Trophic State Index for Des Lacs National Wildlife Refuge (Continued). Parameters used were chlorophyll-*a* (C-*a*), total phosphorus (TP), and Secchi disk depth (SD).

Date	Site 4			Site 5		
	TSI (C-*a*)	TSI (TP)	TSI (SD)	TSI (C-*a*)	TSI (TP)	TSI (SD)
5/16	72.81	78.04	69.99	63.97	72.57	77.35
5/31	66.79	76.50	79.98	58.22	75.20	73.20
6/5	63.97	79.96	77.35	62.18	87.86	69.99
6/13	63.04	89.11	67.36	62.18	88.08	73.20
6/19	55.38	88.37	60.74	63.97	90.40	73.20
6/25	57.17	97.41	60.74	61.01	95.24	71.51
7/1	44.89	94.33	50.38	61.14	98.72	71.51
7/8	59.74	97.55	53.23	75.35	96.49	77.35
7/16	64.06	98.20	52.78	77.32	102.76	73.20
7/22	68.70	91.46	57.99	78.12	101.37	77.35
7/29	76.62	91.08	62.34	80.69	99.38	87.34
8/5	77.81	93.71	64.15	85.04	95.78	83.19
8/14	75.28	89.65	55.15	82.53	94.30	73.20
8/21	77.65	85.09	68.61	81.76	86.54	83.19
8/28	74.46	84.77	68.61	86.15	83.12	87.34
9/4	75.97	81.26	67.36	89.03	80.91	87.34
9/10	74.50	79.35	65.14	86.52	83.71	87.34
9/16	69.47	72.82	59.30	83.56	78.71	83.19
9/23	73.60	77.51	68.61	82.91	86.78	83.19
10/1	71.49	65.00	62.34	83.56	80.33	83.19
10/8	55.69	64.78	57.99	79.88	78.04	83.19
10/16	64.60	61.67	62.34	79.15	77.51	87.34
10/22	55.22	60.85	54.65	74.14	74.00	79.98

3.5. Discussion

While ANOVA testing showed that P sorption was significantly different at each site, the differences were unlikely to be significant enough to strongly affect the formation of HCBs. Additionally, the results of P sorption modeling showed that the sediments throughout all of DLNWR are at or near saturation. The lack of variation in the data does not allow us to accurately compare the affects saturation has on HCBs at varying levels of saturation. However, it does allow us to observe the results of a system where the sediments act primarily as a source of P and sequester little to no new P. In a typical system, the sediments act as a sink for ambient P with Ca,

Fe, and Al forming less soluble cations, which in turn reduces the amount of soluble P available for uptake by phytoplankton (Lebo, 1991; Wu, Jin, Gao, Xu, & Chen, 2019). When the sediments are unable to sequester further P, all new P entering the system remains available for uptake and use by phytoplankton, likely increasing the frequency and severity of HCBs. Additionally, the P that is already sequestered in the system becomes a source of P and can be as high as 100 times greater than the P in the water column (Søndergaard, Jensen, & Jeppesen, 2003). This internal loading of P can be as much as 80 percent of a lakes total P input (Penn et al., 2000). Once it is known that a lake is near or at full P saturation, the next course of action is identifying the factors that attribute to the release of stored P to the water column. Experiments on lakes sediments by Wu, Wen, Zhou, & Wu (2013) showed that, in order of magnitude, dissolved oxygen supply, temperature, and pH were the primary drivers of P release from the sediments. Both temperature and pH were high on DLNWR during peak bloom times.

The sediments on DLNWR are, for practical purposes, fully saturated with P throughout the summer and fall. During modeling, concentrations nearly ten times greater than the highest recorded value of P in the water column resulted in saturation values ranging from 97 to 100 percent. These soils, once saturated, will be unable to sequester further P. Phosphorus entering the system will therefore remain in the water column and available for uptake by phytoplankton. With the sediments fully saturated, P will build up over time in the water column resulting in high levels of eutrophication. The effects of high P saturation in the sediments on DLNWR may have been seen as early as 1997, where a previous study by Wax (2006) found the lakes on DLNWR were eutrophic to hypereutrophic. Furthermore, a TSI created from the results of CHY-a, P, and SD sampling between 2016 and 2019 showed that the water column on DLNWR was eutrophic to hypereutrophic nearly the entirety of each sampling season. This is likely largely influenced by the sediments no longer being able to sequester new sources of P, implying that eutrophication on

DLWNR is not a recent phenomenon and the sediments may have been heavily to fully saturated for a long time.

The amount of P a system can sequester is largely dependent on suspended particulate matter in the water column and on the sediments (Zhang & Huang, 2007). While sands on DLNWR constituted a sizeable portion of samples, the majority were in cores taken on the shoreline, outside of the lake itself. Within the lake, smaller particle sized sediments like silts, loams, and clays predominated, creating a prime environment for P sequestration. In a study by Shrestha and Lin (1996), sediments comprised of sand, subsurface farm soil, and commercial bentonite were mixed at varying ratios and tested for P saturation capacity. In their study, treatments with higher clay content showed markedly higher P saturation capacity (Shrestha & Lin, 1996). The rates at which P is adsorbed and desorbed is dependent on sediment particle size with an exponential increase in adsorption with decreasing particle size (Walter & Morse, 1984; Zhang & Huang, 2007). This suggests the large amount of fine particle sediments, like clays, in DLNWR substantially increase the lakes capacity to sequester P. The importance of clays in the binding of P is further supported by our correlation r value of 0.91 between percent P and clay (Table 3).

One of the reasons soil texture and particle size is so important is the susceptibility of shallow lakes, like those on DLNWR, to mixing by wind resulting in the resuspension of sediments. Suspension of sediment particles into the water column increases the surface area available for P exchange; with smaller particles being more likely to be resuspended due to wave action and reside in the water column for larger periods of time (Wang & Li, 2010). Phosphorus exchange across the sediment–water interface, via adsorption and desorption, plays a crucial role in governing the availability of water-soluble P (Froelich, 1988). Even small amounts of resuspended fine particles can greatly increase the total surface area in sediments. As shown by Walter and Morse (1984), where sediments were divided by particle size greater than and less than 62 microns. The smaller

particle group accounted for only 16 percent of total weight; however, the smaller particle group accounted for an adsorption rate ten times higher than all particles greater than 62-microns (Walter & Morse, 1984).

The lakes on DLNWR are primarily oriented in a north to south direction with valley walls that protect them from the prevailing west winds. They are however susceptible to heavy mixing in times of a northern or southern wind where the long length, or fetch, of the lakes can result in the formation of large waves (Sverdrup, Duxbury, & Duxbury, 2006). The heavy mixing during these wind events has two major implications. First, the sediments become suspended in the water column creating prime conditions for sorption; and secondly, they heavily aerate the water column which in a typical system would favor adsorption of P onto the sediments (Hietanen & Lukkari, 2007; Lasater & Haggard, 2017).

The aerobic conditions created by wind driven mixing typically favor P adsorption, as opposed to anaerobic conditions, which typically favor desorption (Hietanen & Lukkari, 2007; Lasater & Haggard, 2017). This would suggest that the shallow nature of the DLNWR lakes would result in little release of stored P, however pH also plays a major role in the sorption of P onto the sediments (Wu et al., 2013). The pH levels in a lake heavily affect the solubility of P in relation to the bonds it forms with cations, primarily Al^{3+}, Fe^{3+}, and Ca^{2+} (Shrestha & Lin, 1996). In acidic sediments, $Al^{3+}$and Fe^{3+} rapidly precipitate phosphates, and in basic sediments, Ca^{2+} more rapidly precipitate phosphates (Hepher, 1958; Shrestha & Lin, 1996). Shrestha and Lin (1996) also examined the ratios of loosely bound P, Al-P, Fe-P and Ca-P, and showed in treatments of increased clay content, Al-P and Ca-P increased appreciably, but Fe-P decreased with increasing clay content (Shrestha & Lin, 1996). Although wind induced mixing has an aerating effect on the water column, the high pH levels of the water found on DLNWR will likely still induce the release of P from Fe that is resuspended into the water column.

The abundance of P in the water column helps to fuel the formation of HCBs, which also in turn affects the conditions in the water column and sediments, through their growth and decay. The degradation of blooms can also impact this sediment-water column relationship creating areas of hypoxia and increasing pH. In addition to increasing pH levels in the water column through high levels of primary production, Zhu et al. (2012) observed that decaying blooms could effectively release nutrients from sediment into the water column by creating areas of hypoxia as the algae decays. These areas of hypoxia facilitate the rapid release of nutrients like ammonia and phosphorous, which in turn fuels further bloom formation (Zhu et al., 2012). In relation to the sediments at DLNWR, observations showed that OC was greater in samples collected from within the lake than outside of it, which suggest that processes within the lake are likely increasing OC concentrations. Additionally, the ANOVA test showed that OC and IC were significantly different by transect, but not by site, which suggests that the pattern was likely lake wide and most probably caused by decaying algal blooms. The decay of HCBs likely creates large hypoxic zones within the lake which in turn fuel the formation of more HCBs.

Shallow lakes, like those on DLNWR, have increased susceptibility to higher temperatures which further enhance the effect HCBs have on conditions within the lake. Increased temperatures decrease the capacity of sediments to adsorb P, as well as increasing biological activity and accelerating the decay of blooms (Perkins & Underwood, 2001). Increasing temperatures also increase the mineralization of organic matter which in turn releases increased amounts of CO_2 in the water column, and facilitates the precipitation of $CaCO_3$ (Wu et al., 2013) further increasing pH levels and enhancing release of Ca-bound P.

3.6. Conclusion

High levels of P saturation, like those seen on DLNWR, decrease a systems capacity to sequester P, which in turn increases the P available for consumption by phytoplankton. Greater

amounts of fine sediments like clays and silts greatly increase a lakes capacity to adsorb P, but also increase the likelihood of re-release through resuspension. Additionally, increased phytoplankton productivity further compounds the issues of P release into the system by: 1) increasing pH levels through primary production; and 2) the eventual decay of blooms. These blooms result in large amounts of decaying organic matter in the sediment creating large areas of hypoxia that induce further P releases from the sediment. A cycle of P uptake and release is created that continuously fuels HCBs each season.

The DLNWR sediment lacked variability in P saturation, and therefore we were unable to correlate the degree to which factors within the system may have led to saturation. We were however able to observe the results of a system that is at full p saturation. With the sediments unable to further sequester P, as well as being a potential source of P, HCBs had an abundance of P available to them. This was evident by the high levels of eutrophication observed as well as the abundance of organic matter in the sediments. High levels of primary production created conditions of elevated pH, which in turn allowed for the release of P from Ca-P cations further increasing HCBs primary production. The abundance of fine particle clays and silts within the lake further this cycle through the ease in which they are resuspended. Due to all of these factors, an ever-perpetuating cycle is formed where P is continually recycled within the lake. This cycle is brought about by the sediments inability to further sequester P.

Remediation to shallow highly saturated systems like DLNWR would require aggressive measures to see short term results. Draining the system and removing the saturated sediments would likely alleviate excess P available to HCBs. Dredging could also assist in the removal of P from the system but could also result in a temporary increased release of dissolved reactive P which is more biologically available to HCBs (Ni, Yuan, & Liu, 2020). Due to the difficulty of remediation, the authors suggest that these systems be heavily monitored for the formation of HCBs. After which,

access to areas affected by HCBs should be heavily restricted to reduce potentially harmful exposure to cyanobacterial toxins.

While we were unable to observe gradients of sediment saturation, this study serves as a bookend showing the effects of full saturation of P in sediments. Showing that the full saturation of P in a system has the potential to create a cycle in which HCBs accelerate the availability of P through their own growth and decay. Further research assessing the role of P in sediments should focus on systems in varying degrees of saturation, and investigating the degree to which these levels of saturation create a cycle of P release and availability to fuel HCBs. The information from this study is useful to water managers across the globe dealing with HCBs in shallow water systems.

3.7. References

Boettger, W. M. (1986*). Origin and stratigraphy of Holocene sediments, Souris and Des Lacs glacial-lake spillways, north-central North Dakota* (Master's thesis). Retrieved from https://commons.und.edu/cgi/viewcontent.cgi?article=1029&context=theses

Carlson, R. E. (1977). A trophic state index for lakes[1]. *Limnology and Oceanography*, *22*(2), 361–369. https://doi.org/10.4319/lo.1977.22.2.0361

Chaffin, J. D., & Bridgeman, T. B. (2013). Organic and inorganic nitrogen utilization by nitrogen-stressed cyanobacteria during bloom conditions. *Journal of Applied Phycology*, *26*(1), 299–309. https://doi.org/10.1007/s10811-013-0118-0

Christophoridis, C., & Fytianos, K. (2006). Conditions affecting the release of phosphorus from surface lake sediments. *Journal of Environmental Quality*, *35*(4), 1181–1192. https://doi.org/10.2134/jeq2005.0213

Des Lacs National Wildlife Refuge. (1999). *Des Lacs National Wildlife Refuge - Annual narrative report calendar year 1997*. Retrieved from https://ecos.fws.gov/ServCat/DownloadFile/40996?Reference=41203

Dodds, W. K., Bouska, W. W., Eitzmann, J. L., Pilger, T. J., Pitts, K. L., Riley, A. J., … Thornbrugh, D. J. (2009). Eutrophication of U.S. freshwaters: Analysis of potential economic damages. *Environmental Science and Technology*, *43*(1), 12–19. https://doi.org/10.1021/es801217q

Dolman, A. M., Rücker, J., Pick, F. R., Fastner, J., Rohrlack, T., Mischke, U., & Wiedner, C. (2012). Cyanobacteria and cyanotoxins: The influence of nitrogen versus phosphorus. *PLoS ONE*, *7*(6). https://doi.org/10.1371/journal.pone.0038757

Froelich, P. N. (1988). Kinetic control of dissolved phosphate in natural rivers and estuaries: A primer on the phosphate buffer mechanism. *Limnology and Oceanography*, *33(4 part 2)*, 649–668. https://doi.org/10.4319/lo.1988.33.4_part_2.0649

Gee, G.W. & Bauder, J.W. (1986). Particle-size analysis. In: Klute, A.(Ed.), *Methods of Soil Analysis*, *Part I,* (2nd ed., pp. 383-411). Madison, WI: ASA and SSSA.

Graetz, D. A. & Nair, V. D. (2009). Phosphorus sorption isotherm determination. InJ.L. Kovar and G.M. Pierzynski (eds.) *Methods of phosphorus analysis for soils, sediments, residuals, and waters* (pp. 33-37). Southern Coop. Ser. Bull. 408. Virginia Tech Univ., Blacksburg.

Harke, M. J., Steffen, M. M., Gobler, C. J., Otten, T. G., Wilhelm, S. W., Wood, S. A., & Paerl, H. W. (2016). A review of the global ecology, genomics, and biogeography of the toxic cyanobacterium, *Microcystis* spp. *Harmful Algae*, *54*, 4–20. https://doi.org/10.1016/j.hal.2015.12.007

Hepher, B. (1958). On the dynamics of phosphorus added to fishponds in Israel1. *Limnology and Oceanography*, *3*(1), 84–100. https://doi.org/10.4319/lo.1958.3.1.0084

Hietanen, S., & Lukkari, K. (2007). Effects of short-term anoxia on benthic denitrification, nutrient fluxes and phosphorus forms in coastal Baltic sediment. *Aquatic Microbial Ecology*, *49*, 293–302. https://doi.org/10.3354/ame01146

Jeppesen, E., Jensen, J. P., Søndergaard, M., Lauridsen, T., Pedersen, L. J., & Jensen, L. (1997). Top-down control in freshwater lakes: The role of nutrient state, submerged macrophytes and water depth. *Hydrobiologia*, *342/343*, 151–164. https://doi.org/10.1023/a:1017046130329

Lasater, A. L., & Haggard, B. E. (2017). Sediment phosphorus flux at Lake Tenkiller, Oklahoma: How important are internal sources? *Agricultural and Environmental Letters*, *2*(1), 1-5. https://doi.org/10.2134/ael2017.06.0017

Lebo, M. E. (1991). Particle-bound phosphorus along an urbanized coastal plain estuary. *Marine Chemistry*, *34*(3-4), 225–246. https://doi.org/10.1016/0304-4203(91)90005-h

Ni, X., Yuan, Y., & Liu, W. (2020). Impact factors and mechanisms of dissolved reactive phosphorus (DRP) losses from agricultural fields: A review and synthesis study in the Lake Erie basin. *Science of The Total Environment*, *714*, 136624. https://doi.org/10.1016/j.scitotenv.2020.136624

North Dakota Department of Environmental Quality (2020). *Standard operating procedures for the collection and preservation of lake or non-wadeable wetland water column samples for chemical analysis*. Retrieved from https://deq.nd.gov/publications/WQ/3_WM/SOPs/7.04_LakeWaterQualitySampleSOP.pdf (accessed 1 Apr. 2020)

NRCS – Soil survey staff. (2013). Natural Resources Conservation Service, United States Department of Agriculture. Web Soil Survey. http://websoilsurvey.nrcs.usda.gov/ (accessed 1 Apr. 2020)

O'Neil, J., Davis, T., Burford, M., & Gobler, C. (2012). The rise of harmful cyanobacteria blooms: The potential roles of eutrophication and climate change. *Harmful Algae*, *14*, 313–334. https://doi.org/10.1016/j.hal.2011.10.027

Paerl, H. W., Hall, N. S., & Calandrino, E. S. (2011). Controlling harmful cyanobacterial blooms in a world experiencing anthropogenic and climatic-induced change. *Science of The Total Environment*, *409*(10), 1739–1745. https://doi.org/10.1016/j.scitotenv.2011.02.001

Penn, M. R., Auer, M. T., Doerr, S. M., Driscoll, C. T., Brooks, C. M., & Effler, S. W. (2000). Seasonality in phosphorus release rates from the sediments of a hypereutrophic lake under a matrix of pH and redox conditions. *Canadian Journal of Fisheries and Aquatic Sciences*, *57*(5), 1033–1041. https://doi.org/10.1139/f00-035

Perkins, R., & Underwood, G. (2001). The potential for phosphorus release across the sediment–water interface in an eutrophic reservoir dosed with ferric sulphate. *Water Research*, *35*(6), 1399–1406. https://doi.org/10.1016/s0043-1354(00)00413-9

Saunders, D., & Kalff, J. (2001). Denitrification rates in the sediments of Lake Memphremagog, Canada–USA. *Water Research*, *35*(8), 1897–1904. https://doi.org/10.1016/s0043-1354(00)00479-6

Schindler, D. W. (1974). Eutrophication and recovery in experimental lakes: Implications for lake management. *Science*, *184*(4139), 897–899. https://doi.org/10.1126/science.184.4139.897

Schindler, D. W. (1977). Evolution of phosphorus limitation in lakes. *Science*, *195*(4275), 260–262. https://doi.org/10.1126/science.195.4275.260

Scott, J. T., & McCarthy, M. J. (2010). Nitrogen fixation may not balance the nitrogen pool in lakes over timescales relevant to eutrophication management. *Limnology and Oceanography*, *55*(3), 1265–1270. https://doi.org/10.4319/lo.2010.55.3.1265

Shrestha, M. K., & Lin, C. (1996). Determination of phosphorus saturation level in relation to clay content in formulated pond muds. *Aquacultural Engineering*, *15*(6), 441–459. https://doi.org/10.1016/s0144-8609(96)01007-2

Søndergaard, M., Jensen, J. P., & Jeppesen, E. (2003). Role of sediment and internal loading of phosphorus in shallow lakes. *Hydrobiologia*, *506-509*(1-3), 135–145. https://doi.org/10.1023/b:hydr.0000008611.12704.dd

Sverdrup, K. A., Duxbury, A. B., & Duxbury, A. C. (2006). *Fundamentals of oceanography* (5th ed.), McGraw Hill, New York (2006)

Walter, L. M., & Morse, J. W. (1984). Reactive surface area of skeletal carbonates during dissolution: Effect of grain size. *Journal of Sedimentary Research*, *54*(4), 1081–1090. https://doi.org/10.1306/212f8562-2b24-11d7-8648000102c1865d

Wang, Q., & Li, Y. (2010). Phosphorus adsorption and desorption behavior on sediments of different origins. *Journal of Soils and Sediments*, *10*(6), 1159–1173. https://doi.org/10.1007/s11368-010-0211-9

Wax P. (2006). *Lake water quality assessment for Upper Des Lacs Lake Ward and Burke Counties North Dakota.* Retrieved from https://deq.nd.gov/publications/WQ/3_WM/Lakes/DesLacs/DesLacs_Final.pdf

Wu, B., Jin, H., Gao, S., Xu, J., & Chen, J. (2019). Nutrient budgets and recent decadal variations in a highly eutrophic estuary: Hangzhou Bay, China. *Journal of Coastal Research*, *36*(1), 63. https://doi.org/10.2112/jcoastres-d-18-00071.1

Wu, Y., Wen, Y., Zhou, J., & Wu, Y. (2013). Phosphorus release from lake sediments: Effects of pH, temperature and dissolved oxygen. *KSCE Journal of Civil Engineering*, *18*(1), 323–329. https://doi.org/10.1007/s12205-014-0192-0

Yang, H., Zhao, Y., Wang, J.-H., Xiao, W.-H., Jarsjö, J., Huang, Y., … Wang, H.-J. (2020). Urban closed lakes: Nutrient sources, assimilative capacity and pollutant reduction under different precipitation frequencies. *Science of The Total Environment*, *700*, 134531. https://doi.org/10.1016/j.scitotenv.2019.134531

Zhang, J.-Z., & Huang, X.-L. (2007). Relative importance of solid-phase phosphorus and iron on the sorption behavior of sediments. *Environmental Science & Technology*, *41*(8), 2789–2795. https://doi.org/10.1021/es061836q

Zhu, M., Zhu G., Zhao, L., Yao, X., Zhang, Y., Gao, G., & Qin, B. (2012). Influence of algal bloom degradation on nutrient release at the sediment–water interface in Lake Taihu, China. *Environmental Science and Pollution Research*, *20*(3), 1803–1811. https://doi.org/10.1007/s11356-012-1084-9